



**Characterization of Physiological Biomarkers in Long-Term
Kratom (*Mitragyna speciosa* Korth.) Users: A Preliminary Study**

Wanumaidah Saengmolee

**A Thesis Submitted in Partial Fulfillment of the Requirements for
the Degree of Doctor of Philosophy in Physiology**

Prince of Songkla University

2022

Copyright of Prince of Songkla University



**Characterization of Physiological Biomarkers in Long-Term
Kratom (*Mitragyna speciosa* Korth.) Users: A Preliminary Study**

Wanumaidah Saengmolee

**A Thesis Submitted in Partial Fulfillment of the Requirements for
the Degree of Doctor of Philosophy in Physiology**

Prince of Songkla University

2022

Copyright of Prince of Songkla University

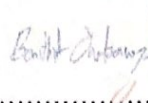
Thesis Title Characterization of physiological biomarkers in long-term
kratom (*Mitragyna speciosa* Korth.) users: a preliminary study

Author Miss Wanumaidah Saengmolee

Major Program Physiology

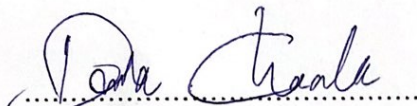
Major Advisor


(Assoc. Prof. Dr. Ekkasit Kumarnsit)

Examining Committee:


Digitally signed by
Banthit Chetsawang
Date: 2022.07.08
14:50:06 +07'00'

.....Chairperson
(Prof. Dr. Banthit Chetsawang)

Co-advisor


(Asst. Prof. Dr. Dania Cheaha)

.....Committee
(Asst. Prof. Dr. Theerawit Wilaiprasitporn)

.....Committee
(Assoc. Prof. Dr. Ekkasit Kumarnsit)

.....Committee
(Asst. Prof. Dr. Dania Cheaha)

.....Committee
(Dr. Nifareeda Samerphob)

The Graduate School, Prince of Songkla University, has approved this thesis as partial fulfillment of the requirements for the Doctor of Philosophy Degree in Physiology

.....
(Prof. Dr. Damrongsak Faroongsarng)

Dean of Graduate School

This is to certify that the work here submitted is the result of the candidate's own investigations. Due acknowledgement has been made of any assistance received.

.....Signature

(Assoc. Prof. Dr. Ekkasit Kumarnsit)

Major Advisor

.....Signature

(Asst. Prof. Dr. Dania Cheaha)

Co-advisor

.....Signature

(Wanumaidah Saengmolee)

Candidate

I hereby certify that this work has not been accepted in substance for any degree, and is not being currently submitted in candidature for any degree.

.....Signature

(Wanumaidah Saengmolee)

Candidate

ชื่อวิทยานิพนธ์	การศึกษานำร่องลักษณะจำเพาะของตัวชี้วัดทางสรีรวิทยาในผู้บริโภคน้ำผึ้ง กระท่อมเป็นระยะเวลา 14 วันติดต่อกัน
ผู้เขียน	นางสาววันอุไม๊ะหะห์ แสงโมลี
สาขาวิชา	สรีรวิทยา
ปีการศึกษา	2565

บทคัดย่อ

ในปัจจุบันการศึกษาผลตอบสนองต่อการบริโภคน้ำผึ้งกระท่อมระยะเวลานานทางสรีรวิทยา ระบบประสาทที่ยังไม่ทราบเป็นที่แน่ชัด การศึกษานี้จึงมีวัตถุประสงค์เพื่อหาตัวบ่งชี้ทางชีวภาพของการตอบสนองดังกล่าวจากอาสาสมัครจำนวน 52 คน ประกอบไปด้วย ผู้ใช้กระท่อมเป็นระยะเวลานานจำนวน 28 คน และกลุ่มควบคุมจำนวน 24 คน ทำการบันทึกสัญญาณ 1) คลื่นไฟฟ้าสมองด้วยอุปกรณ์พกพาอย่างง่ายเพื่อสกัดอัตราส่วนคลื่นพลังงานริต้า/อัลฟา และความแปรปรวนของพลังงานคลื่นความถี่ และ 2) คลื่นไฟฟ้าหัวใจเพื่อสกัดความแปรปรวนของอัตราการเต้นของหัวใจ นอกจากนี้ยังทำการทดสอบเชิงประสาทพฤติกรรม เช่น ความสามารถทางการรู้คิด(ความจำเพื่อใช้งาน) และ อาการติดกระท่อม จากนั้นทำการทดสอบทางสถิติเพื่อเปรียบเทียบผู้ใช้น้ำผึ้งกระท่อม และกลุ่มควบคุม และศึกษาในด้านปัจจัยต่างๆ (อายุ ระยะเวลาที่บริโภค และ ปริมาณบริโภคน้ำผึ้งกระท่อมต่อวัน) ตัวชี้วัดที่มีนัยสำคัญทางสถิติจะถูกนำไปทดสอบด้วย 1) การวิเคราะห์เส้นทางเพื่อดูความสัมพันธ์เชิงเหตุผลระหว่างตัวชี้วัดดังกล่าวกับปัจจัยต่างๆ และ ตัวชี้วัดทางประสาทพฤติกรรม และ 2) การจำแนกกลุ่มแบบไบนารีด้วยแมชชีนเลิร์นนิงทั่วไป ผลการทดลองพบว่าตัวชี้วัดทางคลื่นไฟฟ้าสมองเท่านั้นที่พบความแตกต่างอย่างมีนัยสำคัญระหว่างกลุ่ม โดยระดับอัตราส่วนคลื่นพลังงานริต้า/อัลฟาเพิ่มขึ้นอย่างมีนัยสำคัญในกลุ่มผู้บริโภคน้ำผึ้งกระท่อมเทียบกับกลุ่มควบคุมเมื่อพิจารณาในช่วงอายุ > 50 ปี และเพิ่มขึ้นอย่างเห็นได้ชัดในกลุ่มบริโภคน้ำผึ้งกระท่อมในปริมาณมาก นอกจากนี้ความแปรปรวนของพลังงานคลื่นความถี่ของอัลฟายังลดลงในกลุ่มดังกล่าวอีกด้วย และมีความสัมพันธ์กับคะแนนที่ทำการประเมินอาการติดกระท่อม ผลการเปลี่ยนแปลงดังกล่าวเป็นผลโดยตรงจากปริมาณการใช้น้ำผึ้งกระท่อมวัดจากการวิเคราะห์ด้วยเส้นทาง อีกทั้งการรวมคุณลักษณะของตัวชี้วัดทางคลื่นสมองดังกล่าวยังสามารถใช้จำแนกกลุ่มผู้บริโภคน้ำผึ้งในขนาดต่างกันโดยใช้ อัลกอริทึมของซัพพอร์ตเวกเตอร์แมชชีนในการประเมิน ดังนั้นการศึกษาเบื้องต้นนี้แสดงถึงความไวของตัวชี้วัดชีวภาพด้วยคลื่นไฟฟ้าสมองและในอนาคตอาจมีความเป็นไปได้ที่จะใช้แมชชีนเลิร์นนิงจำแนกผู้บริโภคน้ำผึ้งกระท่อมเกินขนาดที่อาจจะพัฒนาไปสู่การติดกระท่อม โดยด้วยคุณลักษณะของคลื่นไฟฟ้าสมองดังกล่าว

คำสำคัญ: คลื่นไฟฟ้าสมอง, อัตราการผันแปรของการเต้นของหัวใจ, การบริโภคน้ำผึ้งกระท่อม

Thesis Title	Characterization of physiological biomarkers in long-term kratom (<i>Mitragyna speciosa</i> Korth.) users: a preliminary study
Author	Wanumaidah Saengmolee
Major Program	Physiology
Academic Year	2022

ABSTRACT

A neurophysiological outcome associated with long-term kratom chewing in traditional use context is still unknown. Thus, the primary aim of this study was to investigate biomarkers of neurological response to the long-term kratom chewing. The fifty-two participants (controls; n=24 and long-term kratom users (LKU) who chewed kratom leaves; n = 28) were recruited with background-matched control group. Neurophysiological parameters with the proposed EEG (Theta/alpha ratio (TAR) and power function variance (PVFA), and all domains of ultra-short heart rate variability (HRV) heart rate variability were assessed during resting-state. Cognitive performance (Working memory) and kratom dependence score rating were also examined. All the proposed features were compared between the controls and long-term kratom chewers and determined in the relevant factors (age, duration, and daily quantity of kratom use). The statistically significant proposed features were proved by 1) path analysis for evaluating the causal relationship, and 2) the recognized machine-learning algorithms (Random Forest, Support vector machine, k -Nearest neighbor, and Logistic regression) for binary classification. The results showed that only the proposed EEG feature (TAR) was significantly increased, compared to the control in the same age range of 50 years. The increased TAR and decreased PVF in the alpha band (PVFA) were direct effects of kratom leaves use and were significantly observed in LKU with a very high dose use. In addition, PVFA was a negative correlation with Kratom dependence. The results were also confirmed by the support vector machine achieved the highest performance to classify LKU with different doses of Kratom consuming by using the combination features TAR (both electrodes and average) and PVF in the alpha band. These preliminary results first highlighted the sensitive EEG biomarkers to characterize the LKU with a large effect size. These findings may lead to effective machine learning approaches based on EEG biomarkers for screening excessive Kratom users that might eventually develop Kratom dependence.

Keywords: Electroencephalogram (EEG), Heart rate variability (HRV) and Kratom

ACKNOWLEDGEMENT

I would like to thank my supervisor Assoc Prof. Dr. Ekkasit Kumarnsit who gives me a chance for Ph.D. research transition from molecular into EEG signal processing laboratory. This chance made me learn new things and found myself in what I am good at. I will unforgettable this important opportunity and his good wish. He also supports and helps me in all the time of research and writing of this thesis.

Besides my supervisors, I would like to express my sincere gratitude to Asst. Prof. Dr. Theerawit Wilaiprasitporn and his team (Interface), for their advice, encouragement, and insightful comments. All of them stand behind the scenes looking at the successful process of my first engineering publication.

My sincere thank also goes to my co-adviser Asst. Prof. Dr. Dania Cheaha attempted to advise and see beyond our research problems, making me obtain the opportunity to collaborate with Interface.

Lastly, I would like to thank the Physiological program, Division of Health and Applied Sciences. The financial supported by grants from Graduate School Dissertation Funding for Thesis and Revenue Budget Fund, and Educational Institutions Scholarship for Outstanding GPA, Prince of Songkla University, Hatyai, Songkhla.

Wanumiadah Saengmolee

TABLE OF CONTENTS

CONTENTS	PAGE
Abstract (Thai)	v
Abstract	vi
Acknowledgement	vii
Contents	viii
List of Tables	xi
List of Figures	xiii
List of Abbreviations and Symbols	xvi
List of Original Publication	xvii
CHAPTER 1 GENERAL INTRODUCTION	1-42
1.1 Background and Rational	1
1.2 Literature Review	4
1.2.1 Kratom	4
1.2.2 Electroencephalography (EEG)	11
1.2.3 Hear rate variability (HRV)	20
1.2.4 Supervised Machine-learning algorithms	28
1.2.5 Path analysis	36
1.3 Research Objectives	39
1.4 Conceptual Framework	40
1.5 Hypotheses	42
1.6 Expected benefits	42
CHAPTER 2 RESEARCH METHODOLOGY	42-57
2.1 Materials	43
2.2 Subjects recruitments	45

TABLE OF CONTENTS (Continue)

CONTENTS	PAGE
2.3 Procedure	46
2.4 EEG recording and preprocessing	47
2.5 EEG analysis	47
2.6 ECG recording and preprocessing	49
2.7 Ultra-short HRV analysis	49
2.8 Neurobehavioral testing	50
2.9 Statistical analysis	54
2.10 Path analysis	56
2.11 Classification	57
 CHAPTER 3 RESULTS	 63-81
3.1 Statistical results	64
3.1.1 Socio-demographic characteristics and kratom use history	64
3.1.2 The comparison of EEG power and their variability between the controls and LKU	65
3.1.3 The correlation between the proposed EEG features and age	66
3.1.4 The comparison of TAR between groups in different age ranges	67
3.1.5 TAR and PVF were involved in the daily dose-dependent manner of kratom consumption	71
3.1.6 The comparison of neurological behaviors in different doses of kratom use.	73
3.1.7 The correlation between the proposed EEG and neurological behaviors	74
3.1.8 The EEG features represented a more sensitive biomarker over than the HRV in LKU	75
3.2 The result of path analysis	78

TABLE OF CONTENTS (Continue)

CONTENTS	PAGE
3.3 The results of classification	79
3.3.1 The classification between the control and LKU group in various age ranges	79
3.3.2 The classification between the low to high doses and very high doses of kratom consumption	81
CHAPTER 4 DISCUSSION	84-87
CHAPTER 5 CONCLUSION	88
CHAPTER 6 APPLICATION	89
REFERENCES	90
APENDIX	103
VITAE	105

LIST OF TABLES

TABLES	PAGE
CHAPTER 1 GENERAL INTRODUCTION	
1.1 The pharmacokinetics of mitragynine in human and animal study	6
1.2 The definition and implication of different HRV indices	20
1.3 The list of common kernel functions	30
 CHAPTER 2 RESEARCH METHODOLOGY	
2.1 HRV indices in different domains with Nuerokit function	50
2.2 The proposed features and working memory performances for MANOVA testing	55
2.3 The indicators of model fitness and their recommended best fit value	57
2.4 Hyperparameter tuning	60
 CHAPTER 3 RESULTS	
3.1 Participant's demographic characteristics	64
3.2 Kratom use history	65
3.3 The ANOVAs results for the group comparison between control and LKU in the same age range > 50 years old on individual EEG features	68
3.4 The ANOVAs results for the group comparison between LKU for those with LTH and those with VH on individual EEG features	72
3.5 The comparison between the control and LKU groups based on age (> 50 years old) across multiple features in domains of HRV and EEG tested by MANOVA	77
3.6 The comparison based on daily doses of Kratom use between the LKU those with low to high doses (LTH) and very high dose (VH) across multiple features in domains of HRV and EEG tested by MANOVA	77

LIST OF TABLES (Continue)

TABLES	PAGE
CHAPTER 3 RESULTS (continue)	80
3.7 The classification results for LKU classifying from the controls in different age ranges	
3.8 The classification results for LKU classifying between low to high dose and very high dose consumption	82

LIST OF FIGURES

FIGURES	PAGE
CHAPTER 1 GENERAL INTRODUCTION	
1.1 Kratom trees and their leaves	4
1.2 The chemical structure of alkaloid compound extracted from Kratom leaves	5
1.3 Muse portable device and Muse electrodes	12
1.4 Mind monitor application; raw signal and absolute power	12
1.5 Signal in time-series is converted into the frequency domain using FFT technique	15
1.6 The PSD in FFT and Welch methods	16
1.7 The differences among time domain, Fourier transform (FT), short-time Fourier transform (STFT), and continuous wavelet transform (CWT).	17
1.8 Generating continuous wavelet transform	18
1.9 The variability of EEG power across frequencies at each electrode	19
1.10 The continuous RR-intervals signal and interpolated RR signal	24
1.11 The continuous RR-intervals signals in time series are transformed in PSD using a welch periodogram	24
1.12 RR intervals and their proceeding	25
1.13 The visualized RR-intervals with Poincaré plot	25
1.14 The Illustration of SVM to classify two classes using the optimal hyperplane in linear separable data	28
1.15 The classification of K-NN algorithm	31
1.16 Logistic regression classifier	32
1.17 The structure of Random Forest	35
1.18 The possible path model.	37
1.19 The possible model and the output of the multiple regression	38
1.20 The schematic diagram of the conceptual frame work in the present study	41

LIST OF FIGURES

FIGURES	PAGE
CHAPTER 2 RESEARCH METHODOLOGY	
2.1 The overview of the subject recruitment and the inclusion/ exclusion criteria.	45
2.2 The overview of the procedures in this study	46
2.3 Schematic representation of 2-back working memory block structure	51
2.4 Signal detection theory shows the possible consequences of the responses to the present and absent signal	52
2.5 The distributions of response to a signal (present signal) and noise (absent signal) are separated by the distance of Dprime	52
2.6 The ROC curve plots the hit rate against the false alarm rate on different d' (Dprime) values.	52
2.7 The expected model of path analysis in LKU	56
2.8 The procedure of feature extractions	58
2.9 The procedure of cross-validation and evaluation models	62
CHAPTER 3 RESULTS	
3.1 The overview of the results description in different parts.	63
3.2 The comparison of PSD and PVF during resting-state (eyes-closed) between groups	66
3.3 The correlation between PSD, PVF, and age in sub-frequency bands; theta and alpha	67
3.4 The broad PSD and TAR in the different age range between the control and LKU group	69
3.5 The effect of TAR levels on smoking and alcohol drinking between groups	70
3.6 The correlation between average TAR and the relevant factors (quantity of Kratom leaves consumption, duration, and age)	70
3.7 The effect of TAR (A) and PVF (B) in low to moderate doses (LTH), moderate to high doses (MTH), and very high (VH)	72

LIST OF FIGURES (Continue)

FIGURES	PAGE
CHAPTER 3 RESULTS (Continue)	
3.8 The neurological behaviors	74
3.9 The correlation between the proposed EEG and neurological behaviors in cognitive tasks with working memory and Kratom dependent score	75
3.10 The comparison of ultra-short HRV in time, frequency, and non-linear domains between the control (n=19) and LKU group (n=19)	76
3.11 The illustration of path analysis for causal relationship in LKU (n = 24) among relevant factors	78
3.12 The ROC curve and the confusion matrix with SVM by using features combination to classify LKU (n = 12) from the controls (n = 19) in the age range of 50 years old	81
3.13 The ROC curve and the confusion matrix with SVM by using features combination to classify LKU those with VH (n = 14) from those with LTH (n = 14)	83

LIST OF ABBREVIATIONS AND SYMBOLS

LKU	Long-term Kratom users
PSD	Power spectrum density
TAR	Theta/Alpha ratio
PVF	Power variance function
PVFA	Power variance function in alpha band
PVFT	Power variance function in theta band
HRV	Heart rate variability
RMSSD	Root mean square of successive RR intervals differences
SDNN	The standard deviation of the normal-to-normal RR intervals
LFn	Normalized low frequency to total power
HFn	Normalized high frequency to total power
SD1	Standard deviation of the RR intervals on the width of the fitted ellipse in Poincaré plot
SD2	Standard deviation of the RR intervals on the length of the fitted ellipse in Poincaré plot
RF	Random Forest
SVM	Support vector machines
LR	Logistic regression
kNN	<i>k</i> -Nearest neighbors
WM	Working memory
KDS	Kratom dependence score
MANOVA	Multiple analysis of variance

LIST OF ORIGINAL PUBLICATION

This thesis contains some of the research outputs published in the international refereed journals.

Saengmolee, W., Chaisaen, R., Autthasan, P., Rungsilp, C., Sa-ih, N., Cheaha, D., ... & Wilaiprasitporn, T. (2022). Consumer-Grade Brain Measuring Sensor in People with Long-Term Kratom Consumption. *IEEE Sensors Journal*

CHAPTER 1

GENERAL INTRODUCTION

1.1 Background and Rationale

Kratom or *Mitragyna speciosa* (Korth.), an ethnomedicinal plant, has been widely used as a traditional remedy and energy-boosting to hard work among laborers and farmers, particularly in Thailand and Malaysia (Hassan et al., 2013). Kratom consumption was concerned about the long-time period of use, high dose ingestion and, age-related to kratom consumption. Prolonged high dose kratom use among people can increase the risk for developing kratom dependence and withdrawal symptoms (D. Singh et al., 2017). However, its withdrawal symptoms were lower in intensity than that of classical opioid (D. Singh, Narayanan, et al., 2018). Old adults also intensively ingested kratom for a long-time (Charoenratana et al., 2021) and they were expected to have greater risks of chronic kratom use due to their pharmacokinetic changing (Graves et al., 2021). All these concerns, the neurological biology in response to long-term kratom consumption is important for a better understanding of how prolonged and high dose kratom use contributed to the neurological oscillation. It would be more beneficial if there are biomarkers for identifying the LKUs who are sensitive to risks-related to kratom consumption.

Kratom contains various psychoactive alkaloids that mitragynine and 7-hydroxy mitragynine are the most common alkaloids. Their targets are primarily μ -opioid receptors located in the brain (Larsen et al., 2022). Interestingly, the peripheral nervous system also expressed the local opioid receptors such as a heart (Sobanski et al., 2014). Recently, long-term kratom users have been limited for investigation on the neurological assessment in that organ activity. Although there were a few pieces of evidence of electrocardiogram (Leong Abdullah et al., 2020), and the brain structure with brain magnetic resonance imaging (D. Singh et al., 2018) that did not show the abnormality in regular kratom users those who brewed kratom tea, they need to be confirmed with alternatively physiological methods, such as EEG and heart rate variability activity, and different form of kratom consumption with chewing the whole leaves that have been never explored.

Electroencephalography (EEG) is a non-invasive method to evaluate brain activity (Biasiucci et al., 2019). Since LKU were rural dwellers, MUSE (InteraXon Inc., Toronto) (*Muse*, n.d.), a few electrodes based on EEG consumer-grade device, has practical advantages and is convenient to record brain activity in a field setting more than a clinical EEG system (Mehreen et al., 2019). With its potential application (ease of use, low-cost, quick preparation), it can quickly and easily collect EEG data from participants (Krigolson, Williams, & Colino, 2017).

A power spectrum density is commonly analyzed to convert the time-series of the EEG signals into sub-band frequencies: delta, theta, alpha, beta, and gamma (Petroff et al., 2016). Theta/Alpha ratio (TAR) was found in both normal aging (Trammell et al., 2017) and age-related diseases, such as Alzheimer's (Fahimi et al., 2017; Meghdadi et al., 2021) and Parkinson's diseases (Orso et al., 2020). Moreover, power variance function (PVF) is one of the EEG features that was also evaluated well in neurodegenerative disease (Ueda et al., 2010) and mild cognitive impairment, even though used a few electrodes for assessment (Ueda et al., 2016). Interestingly, LKUs were typically found in older people and those who ingested a high dose consumption (Charoenratana et al., 2021). There was evidence to indicate that the high dose of mitragynine induced human neuronal cell death by enhancing the levels of Reactive oxygen species (ROS) (Saidin et al., 2015), implicating in neurodegenerative disease (Simpson & Oliver, 2020). Accordingly, it was possible that the TAR and PVF may be observed in LKU. However, only those features could not imply that LKU will promote neurodegenerative disease. These EEG features should investigate coupled with the neurobehavioral tests as well.

It was reported that regular kratom users showed no prevalence of abnormalities in electrocardiogram (ECG) (Leong Abdullah et al., 2020). However, they need further confirmation with other methods. Heart rate variability (HRV) reflects the fluctuation in the interval heartbeats called RR intervals (Hayano, 2016). It is a well-known method to assess the activity and the modulation of the autonomic nervous system (ANS) responsible for regulating cardiac activity (Ho et al., 2020). The HRV analysis is typically evaluated by time, frequency, and nonlinear domains (Shaffer & Ginsberg, 2017). The ultra-short-term HRV (< 5-minutes for ECG recording) has more practical in the limited-time requirement and its validity was not different from those of short-standard measurements (Castaldo et al., 2019; Chen et al., 2020; Munoz et al., 2015). Thus, we analyzed all HRV domains over a time period of 3-minutes in the present study.

Therefore, this pilot study aims to primarily focus on the resting-state neurological biomarkers measured by the proposed EEG extracted from consumer-grade EEG device recording and ultra-short HRV features in LKU consuming it in the form of chewing the whole leaves. We hypothesized that the proposed EEG (TAR and PVF) are more sensitive to represent a potential biomarker for LKU than ultra-short HRV features, and the quantity of kratom use might be the major effect related to the neurological response and could be able to accurately classify LKU those for at different daily doses. Our four principal contributions are presented as follows:

- The current study was the first to propose EEG extracted from a portable EEG device and ultra-short HRV features to investigate the resting-state biomarkers in LKU for those who chewed kratom leaves.
- The proposed EEG, HRV features were compared between-group differences (LKU vs. controls) and also determined by several factors (age, duration, quantity, and daily dose of kratom use).
- The neurobehavioral testing (working memory and kratom dependence score rating) were also investigated whether they corresponded to the proposed neurophysiological biomarkers.
- The statistical significance-based proposed features were proved by path analysis and binary classification using the recognized machine-learning technique.
- The future applications of machine learning-based neurological biomarkers are feasible to detect LKUs who are at risk for kratom consumption.

1.2 Review of literature

1.2.1 Kratom

Kratom or *Mitragyna specioca* (Korth.), the Rubiaceae family, is a tropical medical plant of Southeast Asia (**Figure 1.1**), particularly in Thailand and Malaysia (Hassan et al., 2013). In Thailand, kratom has been currently considered partial legalization for traditional use and medical purpose (Charoenratana et al., 2021). It is commonly used as an indigenous medicinal plant to treat pain, diarrhea, diabetes, and hypertension (Hassan et al., 2017). The consumption of the kratom plant is mostly in form of chewing of raw leaves in Southern Thailand (Tanguay & Drug Policy Consortium, 2012) while drinking as a tea was observed in North Malaysia (D. Singh, Narayanan, et al., 2018).



Figure 1.1 Kratom trees and their leaves (D. Singh et al., 2017)

1.2.1.1 Chemistry

Kratom leaves contain over 25 alkaloids isolated from kratom leaves consisting of 66% mitragynine, 10% paynantheine, 9% speciociliatine, 7% speciogynine, 2% 7-hydroxymitragynine, and less than 1% of the remaining alkaloid (**Figure 1.2**) (Warner et al., 2016). Mitragynine exhibits a morphine-like chemical component and is 13 times more potent than morphine in its opioid-like effect while 7-HMG show having 4 times more potent than mitragynine in its stimulant and depressant effects (Warner et al., 2016). It shows dose-dependent (Matsumoto et al., 2006; Yusoff et al., 2017). Low to moderate doses (1-5 g of raw leaves) of the leaves produce mild stimulant effects while moderate to high doses (5-15 g of raw leaves) promote opioid-like effects and very high doses (> 15g of raw leaves) exhibits the sedative effect (Prozialeck et al., 2012).

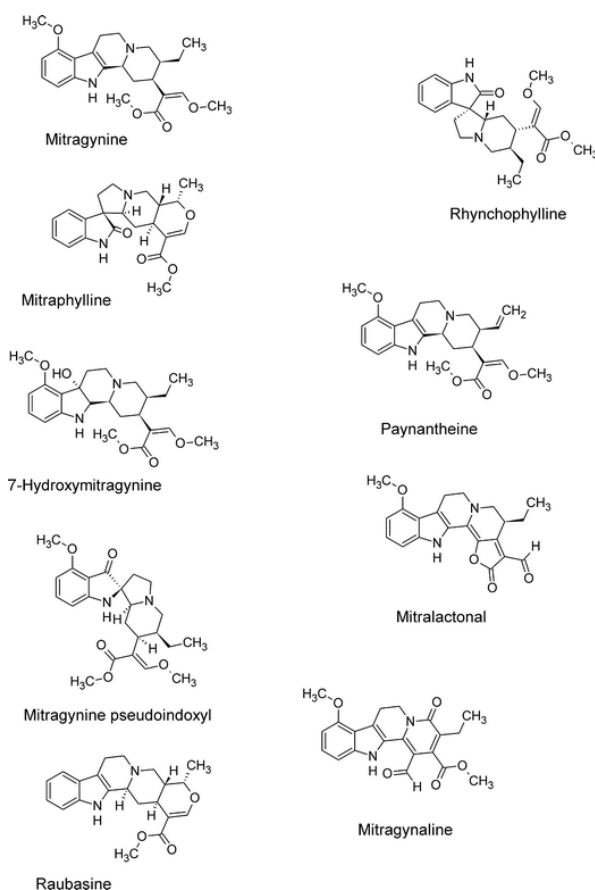


Figure 1.2 The chemical structure of alkaloid compound extracted from kratom leaves (Warner et al., 2016)

1.2.1.2 Pharmacokinetics

The metabolism of kratom alkaloid is occurred primarily in hepatocyte. It is metabolized through phase I and phase II mechanisms. In phase I, the mitragynine is hydrolyzed at the side-chain methyl ester in position 16. Then, the 9-and 17-methoxy were replaced by O-demethylation. The intermediate aldehydes from the oxidative and reductive transformation proceed to be the carboxylic and alcohol, respectively. Subsequently, the formation of glucuronide and sulfate conjugate is a final product in phase II metabolism which is eliminated from the body with the urine. The pharmacokinetics of kratom with oral administration in humans is different from the animal studies (**Table 1.1**).

Table 1.1 The pharmacokinetics of mitragynine in human and animal study. All data are expressed with mean \pm SD (Warner et al., 2016)

Pharmacokinetic parameters	Human (N = 10)	Animal (N=6)
Terminal half-life (t 1/2, h)	23.24 \pm 16.07	9.43 \pm 1.74
Apparent volume of distribution (V d, L/kg)	38.04 \pm 24.32	89.50 \pm 30.30
Time point of maximum concentration (t max, h)	0.83 \pm 0.35	1.83 \pm 1.25
Clearance (CL, L/h)	1.40 \pm 0.73	1.60 \pm 0.58

1.2.1.3 Pharmacology

The pharmacological effects of kratom have been observed in both the central nervous system (CNS) and peripheral nervous system (PNS).

1.2.1.3.1 Pharmacological CNS effect

The onset effect of kratom starts to appear about 10 minutes, and the full effect is experienced within 30-60 minutes after ingestion, lasting 5-6 hours (Stieglitz & Cotten, 2020). It inhibits the reuptake of norepinephrine, serotonin, and dopamine at a low dose, promoting the stimulant effect and mood enhancement while a high dose provides an analgesic and calming

effect through the mechanism of the activation of opioid and alpha-2 receptors (Anand, A., & Hosanagar, 2022).

- **The pharmacological CNS effect of alkaloid kratom acts on both opioid and non-opioid receptors:**

Opioid receptors: mitragynine and its related indole alkaloids, 7- showed a significant central analgesic activity via opioid receptors with different binding affinity. The affinity of mitragynine for opioid receptors is less than that of morphine, while 7-OH-mitragynine produced a more potent affinity than either which is approximately 46-times that of mitragynine (Kenjiro Matsumoto et al., 2005) and 13-times that of morphine (Kinzo Matsumoto et al., 1996). The mitragynine acts primarily on subtype opioid receptors with μ - and δ -receptors while 7-OH-mitragynine is more selective for μ - and κ -receptors (Hassan et al., 2013). Indole alkaloids in kratom bind to opioid receptors and activate the G-protein-coupled receptor (GPCR) signaling, but do not initiate the β -arrestin pathway involved in negative side effects from opioid use, such as respiratory depression, sedation, constipation. Its biased selective binding provides less intense side effects than those traditional opioids, such as morphine (Eastlack et al., 2020).

Non-opioid receptors

- **Adrenergic receptor**

Besides its opioid-like analgesic effects, mitragynine seems to block pain signaling via activating the α -2 adrenergic postsynaptic receptors which are expressed in the modulatory “descending” pain pathway. (Hanapi et al., 2021).

- **Serotonin Receptors**

Serotonin (5-HT) receptors are GPCRs and ligand-gate ion channels, involved in mood, through their natural ligand serotonin. Mitragynine acts as an agonist for the 5-HT_{1A} receptor which promotes mood improvement. (Hanapi et al., 2021).

- **Dopamine Receptors**

Dopamine receptors are a class of GPCRs that regulate the level of dopamine neurotransmitters in the brain. The mitragynine exhibits an anxiolytic effect through stimulating the dopamine receptor, particularly the D1 and D2 receptor, while Kratom leaves extract produces that effect via the suppression of D2 receptors. The controversy caused by Kratom leaves extract provides the border ranges of CNS receptors from crude extract, leading to different effects from pure mitragynine (Hanapi et al., 2021).

- **Putative addictive properties**

Rat administrated chronic mitragynine at the doses of ≥ 10 mg/kg and 15 mg/kg (i.p.) exhibited addiction-like behavior and discriminative stimulus properties, respectively. Mitragynine produced the complexity of pharmacological effects with a stimulant to opioid effect. The dual effect was confirmed with that mitragynine can completely replace the morphine at dose of 5 mg/kg and partially substitute for cocaine (10 mg/kg, ip). The rodent received mitragynine at doses ≥ 10 mg/kg (i.p.) exerted the rewarding tested by conditioned place preference. The reward effect can be blocked by opioid antagonist (naloxone) (Yusoff et al., 2017). However, the doses of mitragynine in animal studies were higher than the daily traditional kratom consuming in human which typically ingested in the range of less than 3 mg/kg (p.o), providing that regular kratom user produced less intense compared to animal studies. (Hassan et al., 2017).

- **Cognitive effect of Kratom use**

Mitragynine caused memory impairment in rats. The cognitive deficit might be through the suppression of calcium efflux and the disruption of hippocampal synaptic transmission and long-term potentiation induction (Hassan et al., 2019). On the other hand, chronic Kratom users had no impairment in cognition in motor, memory, and attention compared to control participants (D. Singh et al., 2019).

1.2.1.3.2 Pharmacological PNS effect of Kratom use

- **Gastrointestinal effects**

Subcutaneous injection of 7-HMG injection inhibited a gastrointestinal transition in mice (Matsumoto et al., 2006). Its indole alkaloid (paynantheine and speciogynine) acted a muscarinic antagonist in ileal smooth muscle, causing constipation (White, 2018). Kratom leaf extract exhibited its anti-diarrheal effect by inhibiting the gastric transition in rats. The effect might occur through opioid receptor (Chittrakarn et al., 2008) . In addition, the mitragynine produced the inhibitory effect on gastric secretion via opioid receptor which speculated the mechanism of the side effects of kratom, such anorexia and weight loss (Tsuchiya et al., 2002).

- **Cardiac effect**

Human-induced pluripotent stem cell-derived cardiomyocytes exposure to mitragynine (10 mM) exerted potential QT prolongation and produced arrhythmia. The mitragynine might cause potentiate Torsade de Pointes which inhibited the rapid delayed rectifier potassium current (IKr). However, regular Kratom users who daily drunk Kratom tea with higher mitragynine of 434.28 mg did not show electrocardiographic abnormalities (Leong Abdullah et al., 2020).

1.2.1.4 Side effects or withdrawal symptoms

Logn-term Kratom use produced mild withdrawal symptoms, such as fatigue, constipation, dehydration, weight loss, and hyperpigmentation over the cheek (Abdullah et al., 2019), and psychological symptoms such as Kratom dependence, mood swings, and nervousness (Domnic et al., 2022).

1.2.1.5 Toxicology of Kratom

Administered Kratom methanol extract at 100, 500, and 1,000 mg/kg in rats for 14-day showed mild nephrotoxicity and moderate hepatotoxicity, but no significant change in hematology, organ weights, body weights. In the same way, 28-day exposure to methanol extract also promoted liver and kidney toxicity but did not alter hematology (Kruegel & Grundmann, 2018).

In human studies, toxicology is poorly reported in the literature. However, there is a case report in two women who presented hepatic toxicity in form of intrahepatic evaluated by the increased glutathione-S-transferase after Kratom powder intake at overdose for two weeks (Kapp et al., 2011).

1.2.2 Electroencephalogram (EEG)

Electroencephalography is a recording and interpretation of the electroencephalogram. EEG is a record of the electrical signals produced by the collaborative action of neurons in the brain. The time course of extracellular field potentials produced by their synchronous action. EEG is measured by means of electrodes attached to the scalp directly on the cortex (Pampiglione, 1980).

1.2.2.1 EEG recording

The conventional EEG system based on 10-20 electrodes placement is the gold standard for EEG recording. However, a dozen electrodes are not practical for use in the real world in terms of long-time spending for preparation. On the other hand, a consumer-grade EEG system offers potential solutions to that problem. These EEG systems usually have fewer electrodes and lower price than medical-grade EEG systems providing them easily accessible (LaRocco et al., 2020).

1.2.2.2 InterAxon Muse

Muse portable device is one of EEG consumer-grade system that records brain activity via 4 EEG sensors at AF7, AF8, TP9, and TP10, all reference to Fpz based on the standard 10-20 system. Each electrode is made of a different material. AF7, AF8, and Fpz are dry silver contacts whereas TP9 and TP10 comprise conductive silicon (**Figure 1.3**) (Mansi et al., 2021).

Raw EEG signals are recorded and collected using Mind monitor Application (**Figure 1.4**) (*Mind Monitor*, n.d.) connected to MUSE through Bluetooth. This application collects the data in the CSV format consisting of the absolute power of each frequency, raw signal, and the information of head movement detected by the accelerometer and gyroscope sensor. The EEG data are recorded with a sampling rate of 256 Hz (Teo & Chia, 2019).

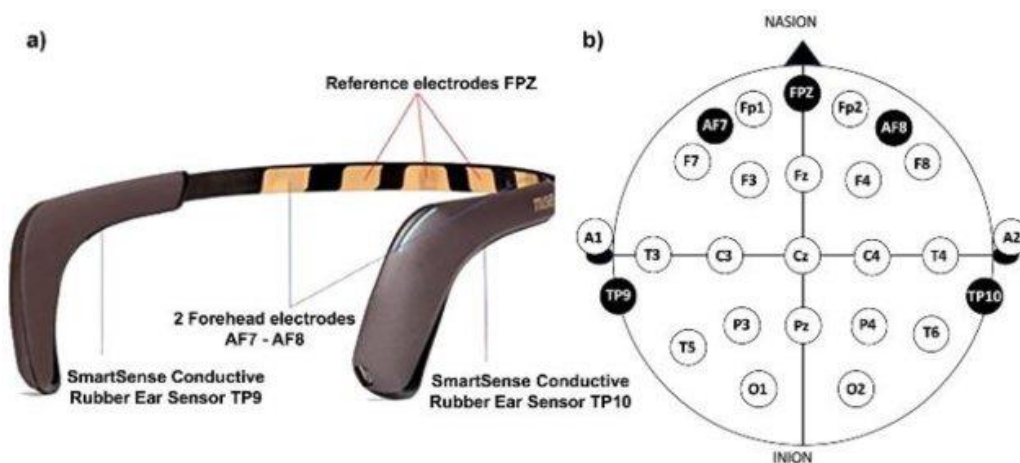


Figure 1.3 Muse portable device (a) and Muse electrodes (b) (Mansi et al., 2021)

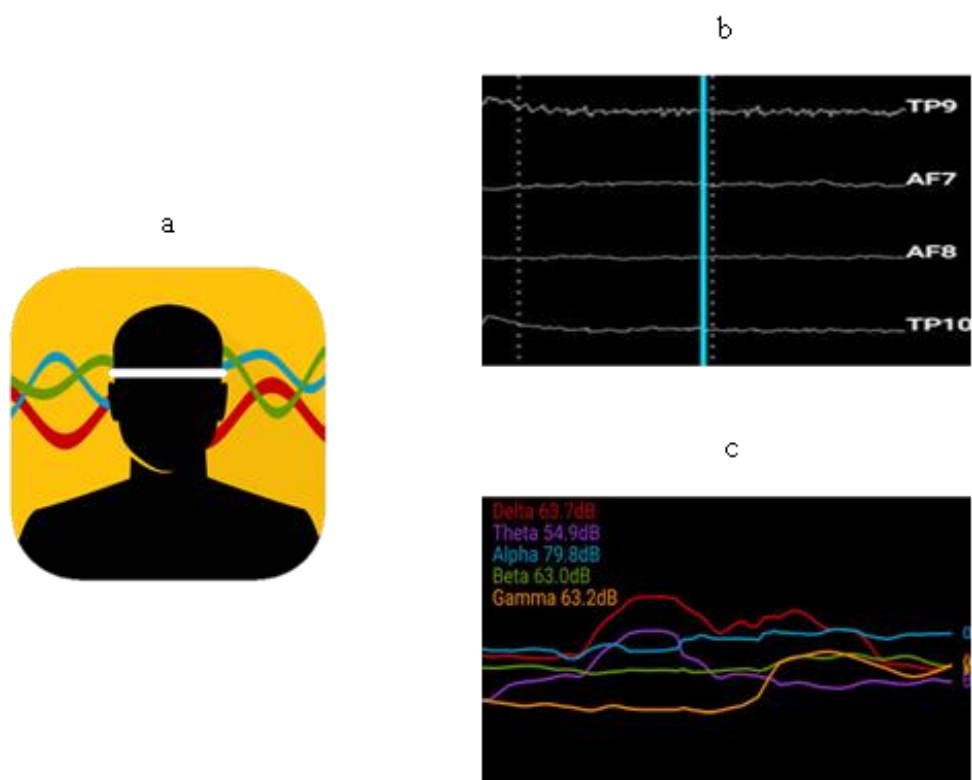


Figure 1.4 Mind monitor application (a), raw signal (b) and absolute power (c) (*Mind Monitor*, n.d.)

1.2.2.3 Muse validation

Muse portable device was initially designed as meditation training related to changes in alpha waves (Przegalinska et al., 2018). It was concerned whether the MUSE device could be used in clinical trial research as AF7 and AF8 electrodes are closely located at eyes movement artifacts that can disrupt the measurement of brain waves, and their dry electrodes are likely in poor contact with the head surface over time, resulting in reduced signal accuracy. In addition, certain head sizes and head shapes made it difficult for data collection (Przegalinska et al., 2018). However, several studies showed that its ability could be used in a study experimental setting:

- MUSE can be conducted successfully for Event-Related Potential (ERP) research. The reliability of ERP data collected from MUSE was examined by N200 and P300 ERP components in the visual oddball task even if the experiment was observed in a small number of participants (Krigolson, Williams, Norton, et al., 2017).
- The quantitative EEG signal and test-retest reliability of MUSE device were compared with the EEG medical grade. The study illustrated that the PSD of MUSE device was similar to the medical system, but it had a higher variation of PSD in broadband at the frontal area with the ratios between 1.125 and 1.225 during the eyes-closed conditions and up to 1.2 in eyes-opened condition. The increased variation in broadband may reflect the artifacts in data recorded by dry electrodes (Ratti et al., 2017). However, this problem was solved by signal processing for cleaning and removing the artifacts (Mansi et al., 2021).

1.2.2.4 The EEG characteristic in Kratom exposure

Most studies on the effect of mitragynine on brain activity were widely investigated in animals. Chronic mitragynine administration in rats delayed response specified frequency band in cortical region (increase in delta and decrease in the alpha band). The mechanism of action of chronic mitragynine exposure changes in independent neighboring frequency caused by the high dose of mitragynine suppressing dopaminergic activity represented by a decrease in alpha band followed by the change in cholinergic activity reflected in the increase in delta activity. The result

showed the delayed response of the neuronal system between dopaminergic and cholinergic activity (Farah et al., 2021).

In a human study, although the brain structures measured by Brain Magnetic Resonance Imaging of regular Kratom users were reported no change in regular Kratom users compared to the non-Kratom users (D. Singh et al., 2018), the brain activity with EEG patterns in chronic Kratom users has never been reported. There was evidence that a high dosage of mitragynine caused human neuronal cell death by increasing reactive oxygen species levels (ROS) (Saidin et al., 2015). ROS can cause neuronal cell damage and accumulated in the brain, leading to the development of neurodegenerative diseases (A. Singh et al., 2019). Thus, EEG features involved in neurodegenerative disorders need to be observed.

- Theta/Alpha ratio (TAR): TAR was an indicator of cognitive ability in older adults. It can be used to discriminate Alzheimer's disease from healthy older controls (Trammell et al., 2017).
- Power variance function (PVF): PVF is the variability of EEG power at a frequency and it is also related to neurodegenerative diseases, such as Alzheimer's disease (Ueda et al., 2010) and mild cognitive disorder (MCI) (Ueda et al., 2013). It can well differentiate MCI from the normal subjects although used a few electrodes for detection (Ueda et al., 2016).

1.2.2.5 EEG analysis

- **Power spectrum density (PSD)**

One of the most widely used methods to analyze EEG data is to convert signal in time-series into frequency component computed by Fast Fourier Transform (FFT) for the estimation of PSD, the distribution of signal power across frequency (**Figure 1.5**). However, the FFT method produces a higher variance and their frequency resolution is limited by the available data record duration, resulting in a poor spectral estimator (Übeyli et al., 2008).

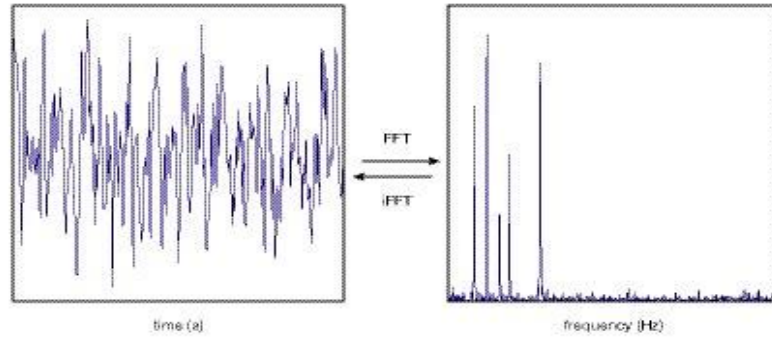


Figure 1.5 Signal in time-series is converted into the frequency domain using FFT technique (Sundling et al., 2006)

Welch, a modified periodogram method, is widely used to evaluate the PSD (**Figure 1.6**). This method firstly divides the signals in the window into overlapping segments. Then, the periodograms calculated by discrete Fourier transform (DFT) are computed in each segment followed by averaging these spectra. The Welch spectral estimator is mathematically according to (Saidatul et al., 2011) and formed in equation (1.1) :

$$P_d(f) = \frac{1}{MU} \left| \sum_{n=0}^{M-1} x_d(n) w(n) e^{-j2\pi f n} \right|^2 \quad (1.1)$$

Where $P_d(f)$ is the periodogram estimate of segment (d), L is the signal segment, and each segment length is M . U is the normalization for the power in the window function $w(n)$ and can be expressed by equation (1.2):

$$U = \frac{1}{M} \sum_{n=0}^{M-1} |w(n)|^2 \quad (1.2)$$

Finally, Welch Power Spectrum (PSD), which is the averaging of the periodogram for each segment, can be represented in equation (1.3):

$$P_d^w(f) = \frac{1}{L} \sum_{i=0}^{L-1} P_d(f) \quad (1.3)$$

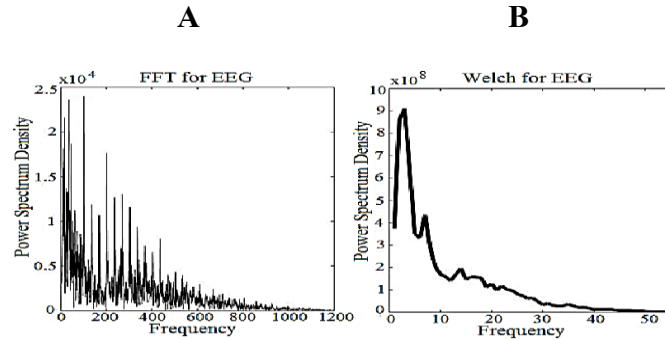


Figure 1.6 The PSD in FFT (A) and Welch methods (B) (Yucelbas et al., 2013)

- **Power variance function (PVF)**

PVF is the variability of EEG power at each frequency. The PVF is an index for mild cognitive impairment (MIC) diagnosis. It was achieved to classify the MCI patient among healthy subjects even though it used only four electrodes for recording. The MCI patient showed a higher PVF in theta, and Alzheimer's disease (AD) patient showed a lower PVF in the alpha band than the healthy subject. PVF was quantified by using the wavelet transform method (Ueda et al., 2010).

Wavelet transform (WT) is an approach to measure time-frequency analysis for non-stationary signals. This method is developed from a short-time Fourier transform (STFT), a time-frequency analysis that improves the standard Fourier transform (FT). The STFT provides time-localized frequency information, while FT only provides frequency information by averaging throughout the signal time interval. The STFT segment the signal in a small segmentation by applying the window function where the window is equal to the segment of the signal assumed to be stationary. However, this method is limited to using a fixed window size at all times and for all frequencies (Dadu & Deka, 2016). In fact, EEG signal is a non-stationary signal that changes over time (Yucelbas et al., 2013). Thus, WT is a better method to represent the time-frequency analysis than the STFT (**Figure 1.7**).

The WT applies the varying window using the mother wavelet function to segment the signal into its wavelets (small wave) which are scaled and shifted of the original signal. The WT consists of two types that are continuous and discrete wavelet transform.

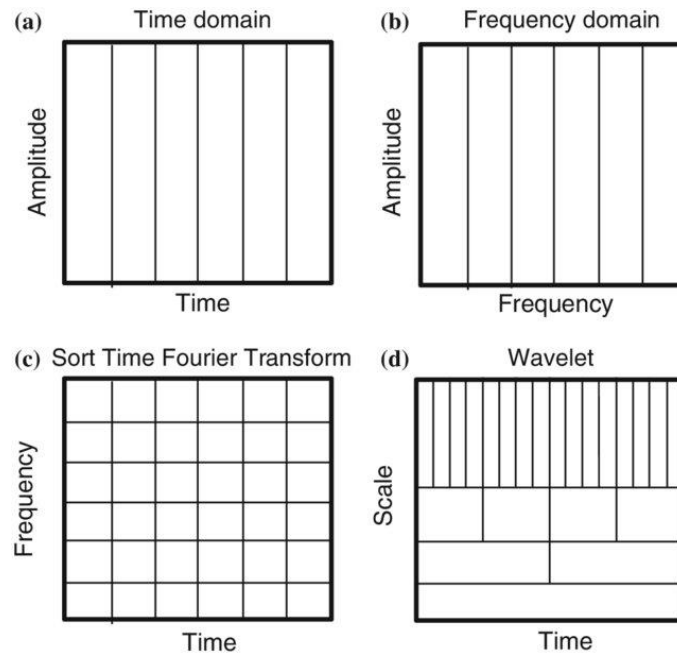


Figure 1.7 The differences among time domain, Fourier transform (FT), short-time Fourier transform (STFT), and continuous wavelet transform (CWT). The CWT provides more accuracy in either time or frequency resolution. The long-time time interval produces more precise low-frequency information whereas short-time interval provides the high frequency information (Kuyuk, 2015).

The PVF uses the continuous wavelet transform (CWT) to find the variability of EEG power according to a previous study (Ueda et al., 2010) , as given in equation (1.4).

$$\begin{aligned}
 C(a, t) &= CWT[x(t)] \\
 &= \frac{1}{\sqrt{a}} \int_{-\infty}^{\infty} x(\tau) \psi\left(\frac{t-\tau}{a}\right) d\tau
 \end{aligned}
 \tag{1.4}$$

$CWT[x(t)]$ is the transformed signal in which the signal is multiplied with the mother function $\psi(t)$ using the changing of two variables that are scale (a) and translation factor (t), respectively, over time (**Figure 1.8**).

The scale parameter (a) is defined as $1/\text{frequency}$. The translation (t) refers to the window's location as the window is shifted over the signal. This term provides the time information in the transform domain. Low frequencies (high scales) provide the global information of a signal, whereas high frequencies (low scales) provide detailed information about a hidden pattern in the short time of the signal (Dadu & Deka, 2016).

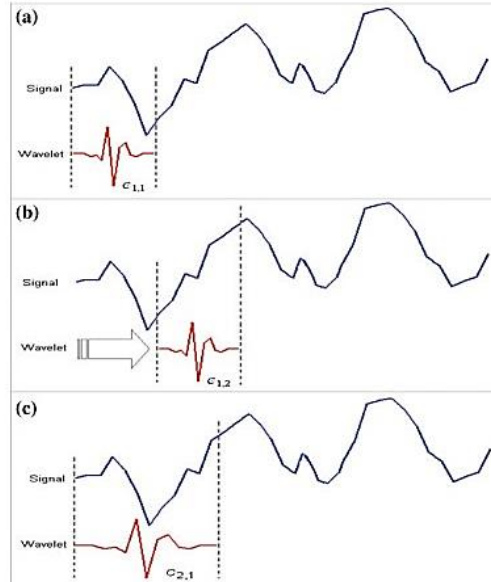


Figure 1.8 Generating continuous wavelet transform (Dadu & Deka, 2016)

The output of $CWT[x(t)]$ returns the variability characteristics of $x(t)$ at frequency. Then, the normalized variability is normalized to eliminate the fluctuation of the signal/noise given equation (1.5):

$$P_i(f, t) = \left\| \left\| CWT \left[\frac{x_i(t)}{\sqrt{\langle x_i^2(t) \rangle}} \right] \right\| \right\|^2 \quad (1.5)$$

The equation (1.6) refers to PVF, which $\sigma_i^2(f)$ indicates how the EEG variability at the frequency (**Figure 1.9**)

$$\sigma_i^2(f) = \langle (P_i(f, t) - \langle P_i(f, t) \rangle)^2 \rangle \quad (1.6)$$

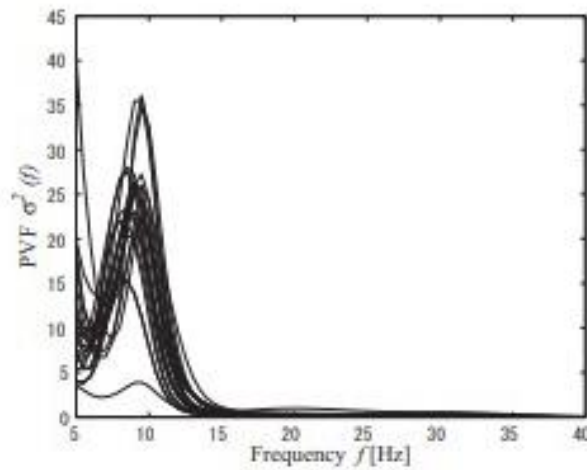


Figure 1.9 The variability of EEG power across frequencies at each electrode (Ueda et al., 2010).

1.2.3 Heart rate variability (HRV)

The electrocardiogram (ECG) in regular kratom users did not show the ECG abnormality (Leong Abdullah et al., 2020). However, they need to be confirmed with other methods, such as HRV activity.

HRV is the oscillation in the time intervals between adjacent heartbeats, which is widely used to evaluate the cardiac autonomic nervous system (ANS) (Mejía-Mejía et al., 2020). The HRV can measure the changing in cardiac sympathetic and parasympathetic branches of the ANS in different domain analyses; time, frequency, and nonlinear domain described in (Table 1.2). The HRV evaluation typically uses a standard duration for short-term measurements (5-minutes) (Kinnunen et al., 2020). However, the ultra-short-term HRV (< 5 min) is also examined in several studies (Shaffer & Ginsberg, 2017).

Table 1.2 The definition and implication of different HRV indices

HRV indices	Description	Implication
Time domain		
RMSSD (ms)	Root mean square of successive RR intervals differences	Vagal activity (Shaffer & Ginsberg, 2017)
MeanNN (ms)	The mean value of all RR intervals	The variation in time of beat to beat (Shaffer & Ginsberg, 2017)
SDNN (ms)	The standard deviation of the normal-to-normal RR intervals	Mostly vagal but also partially sympathetic activity (Mol et al., 2021)

Frequency domain

LF(ms ²)	LF power	Sympathetic and parasympathetic modulation (Shaffer & Ginsberg, 2017)
HF(ms ²)	HF power	Vagal activity (Shaffer & Ginsberg, 2017)
LFn (n.u)	Normalized LF to total power	Marker of sympathetic modulation when LF is normalized to total power (Unoki et al., 2009)
HFn (n.u)	Normalized HF to total power	Marker of vagal or parasympathetic activity
LFn/HFn	The ratio between LFn and HFn	(Shaffer & Ginsberg, 2017) Sympatho-vagal balance (Shaffer & Ginsberg, 2017)

Nonlinear measures

SD1 (ms)	Standard deviation of the RR intervals on the width of the fitted ellipse in Poincaré plot	Marker of parasympathetic activity (Shaffer & Ginsberg, 2017)
SD2 (ms)	Standard deviation of the RR intervals on the length of the fitted ellipse in Poincaré plot	Marker of sympathetic activity (Vanderlei et al., 2010)

SD1/SD2	The ratio between SD1 and SD2	The ratio between sympathetic and parasympathetic activity (Shaffer & Ginsberg, 2017)
---------	-------------------------------	---

The detail of different methods for HRV analysis as described below:

1.2.3.1 Time-domain

The time domain analysis directly measures RR intervals for the root mean square of successive RR interval differences (RMSSD), the standard deviation of all normal-to-normal RR intervals (SDNN), and mean NN intervals. The mentioned time-domain indices are defined according to a previous study (Bartels et al., 2017) and expressed by equation (1.7-1.9).

$$RMSSD = \sqrt{\frac{1}{N-1} \sum_{j=1}^{N-1} (RRi_{j+1} - RRi_j)^2} \quad (1.7)$$

Where N is the total number of RRi intervals, $RRij$ is the j th RRi value.

$$SDNN = \sqrt{\frac{1}{N-1} \sum_{j=1}^N (RRi_j - \bar{RRi})^2} \quad (1.8)$$

N is the total number of RRi intervals. $RRij$ is the j th RRi value.

$$MeanNN = \frac{1}{N} \sum_{j=1}^N (RRij) \quad (1.9)$$

1.2.3.2 Frequency domain

The transformation of HRV in time-series to frequency component is used to separate the parasympathetic and sympathetic activity (Vishwajeet et al., 2020). There are three main frequency components as referred to:

- Very low frequency (VLF) - 0.003-0.04 Hz
- Low frequency (LF) - 0.04-0.15 Hz
- High frequency (HF) - 0.15-0.4 Hz

The magnitude of the HF component indicates vagal activity, whereas the magnitude of the LF component indicates the combination of sympathetic activity with vagal regulation. The LF/HF ratio is used to measure the sympathovagal balance. VLF, LF, and HF power components are often measured in absolute power (ms²). Furthermore, LF and HF can be measured in normalized units (n.u.), which show the relative value of each power component infraction to total power, excluding the VLF components. The advantage of the relative power is that normalization tends to reduce the fluctuation in total power on the LF and HF components (Vishwajeet et al., 2020).

The HRV in frequency component is performed with a welch periodogram. Before quantifying in this method, unevenly sampled RR interval signals (**Figure 1.10A**) are firstly transformed into a continuous signal using an interpolation technique. Then, the interpolated signals are resampled to obtain an evenly sampled RRI signal (**Figure 1.10B**) and converted into power spectrum density (PSD) (**Figure 1.11**) (Cao et al., 2020). The computation of the PSD using the welch periodogram of the RR series is defined according to a previous study (Estévez et al., 2016), and can be expressed by the equation (10.1).

$$\text{PSD}(f) = \frac{1}{F_s * N} \left| \sum_{n=1}^N \text{RR}_n e^{j\left(\frac{2\pi f}{F_s}\right)n} \right|^2 \quad (10.1)$$

Where f is discrete spectral frequency, F_s and N are the sampling frequency and number of samples in the series, respectively. The number of samples ordered in the RR series is represented with n .

The normalized values of power spectrum band frequencies are computed using the given expression (11.1).

$$\text{nuBand} = \frac{\text{AbsVal}(\text{Band})}{\text{TotalPSD}} \quad (11.1)$$

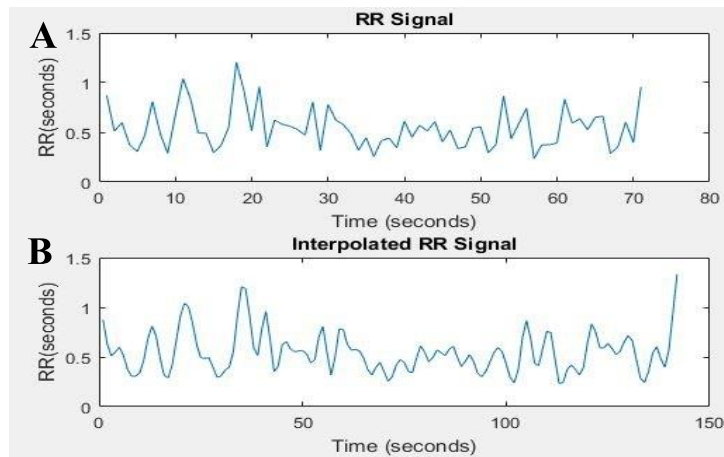


Figure 1.10 The continuous RR-intervals signal (A) and interpolated RR signal (B)

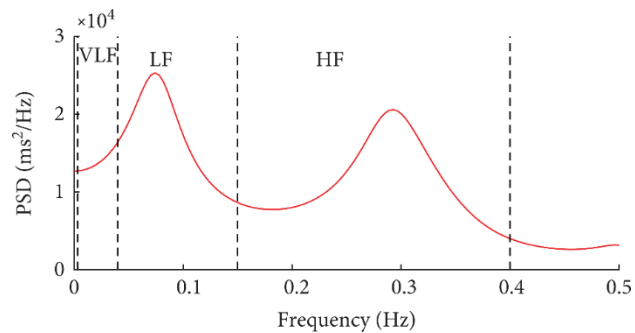


Figure 1.11 The continuous RR-intervals signals in time series are transformed in PSD using a welch periodogram (Naranjo-Hernández et al., 2017)

1.2.3.3 Non-linear analysis

The Poincaré plot analysis is used to visualize the morphological RR-interval in time series into phase space. The plot shows the correlation between the current RR-interval and (RR_i) the preceding RR-interval (RR_{i+1}) (**Figure 1.12**). These adjacent RR intervals represent one point in the scatters plot (**Figure 1.13**) (Tayel, M., & AlSaba, 2015). However, assessing these quality classifications is challenging due to their subjectivity. Therefore, the quantitative analysis of the HRV has adjusted it to an ellipse. The method is quantified by standard deviation1, Standard deviation 2, and the ellipse area to visually fit the data onto the 45° imaginary diagonal line (the normal axis). The points falling on the imaginary line are considered as $RR_n = RR_{n+1}$ (Tayel, M., & AlSaba, 2015).

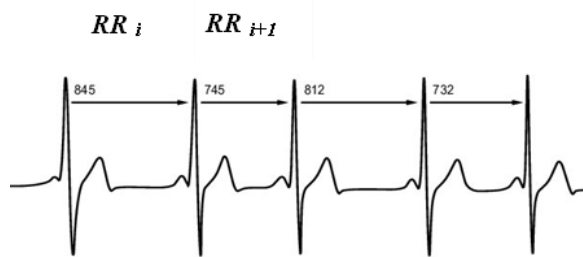


Figure 1.12 RR intervals and their preceding (Rubin et al., 2016)

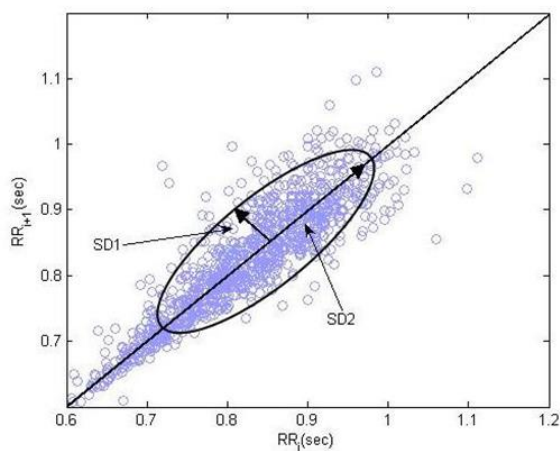


Figure 1.13 The visualized RR-intervals with Poincaré plot (Karmakar et al., 2009)

The parameters in nonlinear analysis with Poincaré plot are described according to a previous study (Tayel, M., & AlSaba, 2015) as follows:

- **Standard Deviation 1 (SD1)** is the standard deviation of the instantaneous (short-term) RR interval variability (the width of the ellipse), which is determined by equation (1.12).

$$SD1 = \sqrt{var(x1)} \quad (1.12)$$

- **Standard Deviation 1 (SD2)** is the standard deviation of the long-term RR interval variability (the length of the ellipse), which is calculated by equation (1.13).

$$SD2 = \sqrt{var(x2)} \quad (1.13)$$

Where $var(x)$ is the variance of variable x , x_1 and x_2 are defined in equation (1.14-1.5).

$$x_1 = \frac{\overrightarrow{RR_l} - \overrightarrow{RR_{l+1}}}{\sqrt{2}} \quad (14)$$

$$x_2 = \frac{\overrightarrow{RR_l} + \overrightarrow{RR_{l+1}}}{\sqrt{2}} \quad (15)$$

$\overrightarrow{RR_l}$ and $\overrightarrow{RR_{l+1}}$ represent vector of RR-intervals according to the equation (1.16-1.17)

$$\overrightarrow{RR_l} = (RR_1, RR_2, \dots, RR_{N-1}) \quad (1.16)$$

$$\overrightarrow{RR_{l+1}} = (RR_2, RR_3, \dots, RR_N) \quad (1.17)$$

Then, $\overrightarrow{RR_l}$ and $\overrightarrow{RR_{l+1}}$ are performed in an angle $\frac{\pi}{4}$ transformation to get a new axis x_1 and x_2 , as shown in equation (1.18).

$$\begin{bmatrix} x_1 \\ x_2 \end{bmatrix} = \begin{bmatrix} \cos \frac{\pi}{4} & -\sin \frac{\pi}{4} \\ \sin \frac{\pi}{4} & \cos \frac{\pi}{4} \end{bmatrix} \cdot \begin{bmatrix} RR_l \\ RR_{l+1} \end{bmatrix} \quad (1.18)$$

- **Area of the ellipse (S)** is the amount of area covered by the ellipse, which is quantified by equation (1.19).

$$S = \pi \cdot SD1 \cdot SD2 \quad (1.19)$$

1.2.4 Classification in Machine Learning

Supervised machine learning is a discipline of computer science used to classify the new data set observations on the training data set by learning a function based on input-output pairs to enhance performance on various tasks (Jiang et al., 2020). Supervised machine learning is broadly used as follows:

1.2.4.1 Support Vector Machine (SVM)

SVM aims to obtain the optimal hyperplane via the maximal margin and minimal misclassification error between labeled classes from the input features or x-dimensions (Figure 1.14). Defining the separating Hyperplane can be determined according to the previous study (Nanda et al., 2018), as the given equation (1.20).

$$w \cdot x_i + b = 0 \quad (1.20)$$

Where w is the weight vector, x_i and b represent the input feature vector and bias, respectively.

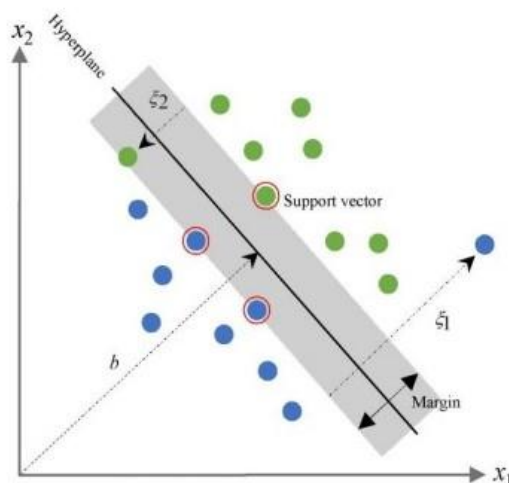


Figure 1.14 The Illustration of SVM to classify two classes using the optimal hyperplane in linear separable data (Nanda et al., 2018)

The equation (1.21) shows how to convert the optimization of the margin of its support vector into a constrained quadratic programming problem (Nanda et al., 2018).

$$\left\{ \begin{array}{l} \min \frac{1}{2} \| w \|^2 + C \sum_{i=1}^n \xi_i \\ \text{s.t. } y_i(w^T x_i + b) \geq 1 - \xi_i \\ \xi_i \geq 0 \end{array} \right. \quad (1.21)$$

Where, ξ_i is the misclassified sample of the corresponding margin hyperplane, C represents the optimum parameters of cost. The larger values of C show a higher error minimization, whereas lower values of C emphasize the margin maximization.

When the dispersion of data provides a difficult linear classification, the kernel function can be used to solve the obstacles in the classification. The kernel function is expressed by equation (1.22).

$$K(x_n, x_i) = \phi(x_n)\phi(x_i) \quad (1.22)$$

Where $K(x_n, x_i)$ is the kernel function that transforms the original data space into a new space in a higher dimension with dot production ϕ , the transformation function. Finally, the hyperplane can be defined by the equation (1.23).

$$f(x_i) = \sum_{n=1}^N \alpha_n y_n K(x_n, x_i) + b \quad (1.23)$$

Where x_n is the support vector data and α_n is a lagrange multiplier, y_n is the labeled classes $\in \{+1, -1\}$ of $n = 1, 2, 3, 4, \dots, N$. There are certain kernel functions as listed in **(Table 1.3)**. To achieve the highest result performance, each function has a certain parameter that must be optimized by grid- search method.

Table 1.3 The list of common kernel functions (Nanda et al., 2018)

Kernel function	Formula	Optimization Parameter
Linear	$K(x_n, x_i) = (x_n, x_i)$	C , and γ
Radial basis function (RBF)	$K(x_n, x_i) = \exp(-\gamma \ x_n - x_i\ ^2 + C)$	C , and γ
Sigmoid	$K(x_n, x_i) = \tanh(\gamma(x_n, x_i) + r)$	C , γ , and r

Note: C : cost; γ : gamma; r : coefficient

1.2.4.2 K -nearest neighbors (KNN)

KNN is a supervised machine learning algorithm that proposes the nearest distance approach for group classification of new data mapping in the training set. During the training phase, the number of neighbors (k values) is required to find the feature space through the training sample. Then, the testing data are categorized into a feature space based on the minimum distance from the majority vote of its neighbor's class **(Figure 1.15)**. The classification results will be influenced by the parameter of the value of k and the distance matrix, a method to find the distance between the new dataset and the existing training dataset (Md Isa et al., 2017). The Euclidean and Manhattan distance are commonly used for model optimization. These methods can be explained as follows:

- Manhattan distance is calculated from the sum of the absolute difference between two points (x, y) , as shown in equation (1.24).

$$d(x, y) = \sum_{i=1}^k |x_i - y_i| \quad (1.24)$$

- Euclidean Distance is calculated between two points (x, y) in k-space. Then, the distance between both of them is quantified by Pythagoras's formula, as shown in equation (1.25).

$$d(x, y) = \sqrt{\sum_{i=1}^k (x_i - y_i)^2} \quad (1.25)$$



Figure 1.15 The classification of K-NN algorithm (Hasan et al., 2020)

1.2.4.3 Logistic regression

Logistic regression (LR) is a popular binary classification method based on statistical modeling in which the probability (P) of an outcome is highly related to the input features (Siuly et al., 2014) (**Figure 1.16**). The goals of the LR model are:

- To estimate hyperplane with a linear function and transform to sigmoid function for prediction of the class label of a new example (Ryali et al., 2010).

- To find a subset of the features that are most informative about the class differentiation (Ryali et al., 2010).

For example, x_1, x_2, \dots, x_n are the input features that are independent variables while y is the dependent variable or labeled class of its input features in both 0 and 1. When $D = \{(x_i, y_i)\}$, $i = 1, 2, \dots, N$ is a number of training examples, the probability of the y that the i -th example belongs to class-1 is expressed in equation (1.26) according to the previous study (Ryali et al., 2010):

$$P(y^i = 1 | x^i, \theta) = h_{\theta}(x^i) \quad (1.26)$$

Where $h_{\theta}(x)$ is a logistic or sigmoid function given by $\frac{1}{\exp(-\theta^t x)}$, θ is a vector of weights related to each input feature and is estimated by using maximum likelihood estimation (MLE), as given in the equation (1.27).

$$L(\theta) = \sum_{i=1}^N \log P(y^i | x^i, \theta) \quad (1.27)$$

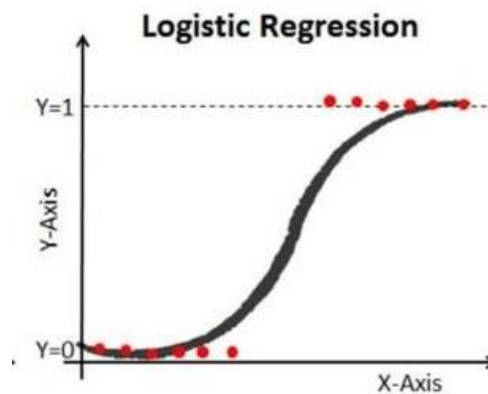


Figure 1.16 Logistic regression classifier (Lim, 2020)

If the number of training examples is smaller than the number of features, there is a possibility of overfitting the model. To handle this problem, the regularization parameters are applied (Ryali et al., 2010), as given in equations (1.28-1.29).

- **L2 Regularization**

$$L_g(\theta) = \sum_{i=1}^N \log P(y^i | x^i, \theta) - \gamma \theta^t \theta \quad (1.28)$$

Where γ regulates the degree of regularization. Maximizing the cost function is solved by decreasing the magnitudes of weight corresponding to irrelevant features in the small value but not in exactly zero.

- **L1 Regularization (*Gauss*)**

$$L_L(\theta) = \sum_{i=1}^N \log P(y^i | x^i, \theta) - \gamma |\theta|_1 \quad (1.29)$$

The cost function needs to be maximized before making the weights related to irrelevant features to be zero. When the features are uncorrelated, optimizing this cost function yields a sparse solution.

1.2.4.4 Random Forest (RF)

RF utilizes many individual classification trees, and each tree is built on the bootstrap sample of the data. The whole feature set is split randomly into a feature candidate set at each split. Every tree is a classifier by itself that provides a certain weight for its classification output which is used to determine the overall classification output voted by all the decision trees (Fraivan et al., 2012).

RF acquires many individual classification trees, and each tree is classified by itself. Its classification output is derived from the overall classification voted by all the decision trees (Figure 1.17).

The steps for building the RF classifier are briefly described in a previous study (Fraiwan et al., 2012) as follows:

- Suppose that the number of label classes in the training set is represented with N . Next, the N sample or in-bag data set is formed by sampling the training set using bootstrapping technique (sampling with replacement).
- Suppose that the dimension of input features denotes Y . The subset feature of Y is represented with Y_i which is randomly selected out of the Y features. These Y_i -dimensional features with the highest information gain (IG) are used to construct the root node. The IG of splitting the training data set (Y) into subsets (Y_i) can be expressed in the equation (1.30).

$$IG = - \sum_i \frac{|Y_i|}{|Y|} E(Y_i) \quad (1.30)$$

The operator $|\cdot|$ is the vector of the set and $E(Y_i)$ is the entropy of the set (Y_i) is shown as given equation (1.31).

$$E(Y_i) = - \sum_{j=1}^N p_j \log_2 (p_j) \quad (1.31)$$

N is the number of label classes and p_j is the proportion of each label class in the set (Y_i)

- Then splitting the training data (Y) into subsets of the feature (Y_i) makes a branch for each possible value of the feature until the branch cannot prune.
- The procedure is repeated until all of the trees have been constructed.
- The out-of-bag data is then used to test each tree as well as the overall forest. The average misclassification error, also known as out-of-bag error, can be used to adjust the weights of each decision tree's vote.

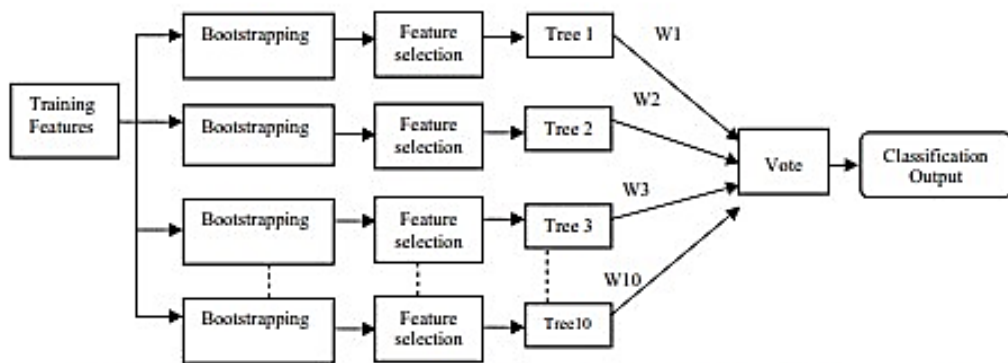


Figure 1.17 The structure of random forest (Fraivan et al., 2012)

1.2.5 Path analysis

Path analysis (PA) is a potential statistical technique that allows us to analyze more sophisticated and realistic relationships between variables than multiple regression, in which the numerous independent variables predict only the dependent variables (Streiner, 2005). The highlights of path analysis are:

It can analyze the various independent variable and their covariance (relationship) to predict several final dependent variables in which there are ‘path’ of influence among them.

- It can compare different models to find which one best fits the data.
- It can determine the direct effect of the independent variables on the dependent variables.
- It can examine the indirect effect of the independent variables on the dependent variables via a mediator.

The terminology and drawing of the possible path analysis are defined according to a previous study (Streiner, 2005), described below and illustrated (**Figure 1.18**).

- **Exogenous variables:** The single-headed arrows exit from them. There are no single-headed arrows pointing at them (except error terms).
- **Covariance:** Double-headed arrow indicates covariance between two variables (when they affect each other) and no causal relations are assumed.
- **Mediate or indirect variable:** The box is between exogenous and endogenous variables.
- **Endogenous variables:** There is at least one headed straight arrow pointing to them.

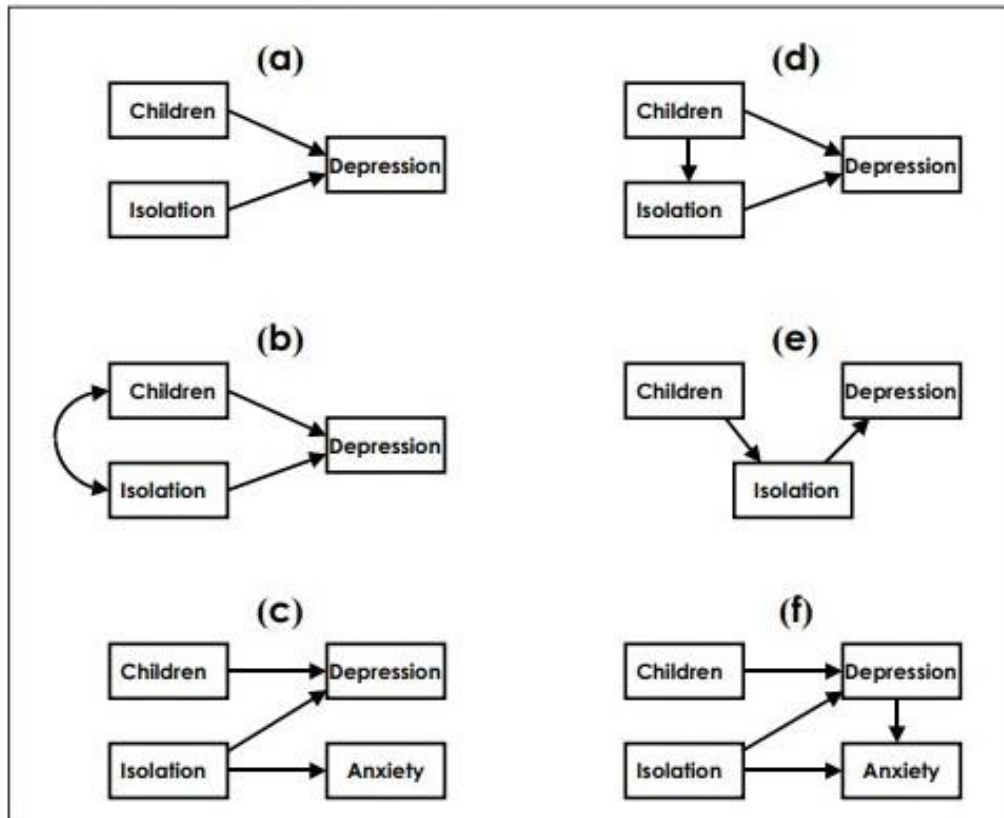


Figure 1.18 The possible path model. The left panel shows the direct path model. Children and isolation are exogenous variables while depression is an endogenous variable. The right panel indicates the indirect path model in which isolation and anxiety are mediators (Streiner, 2005).

For example, it is hypothesized that photonumerophobia (PNP) is predicted by anxiety (ANX), high school math grade (HSM), and income tax returns (TAX) levels (**Figure 1.19**).

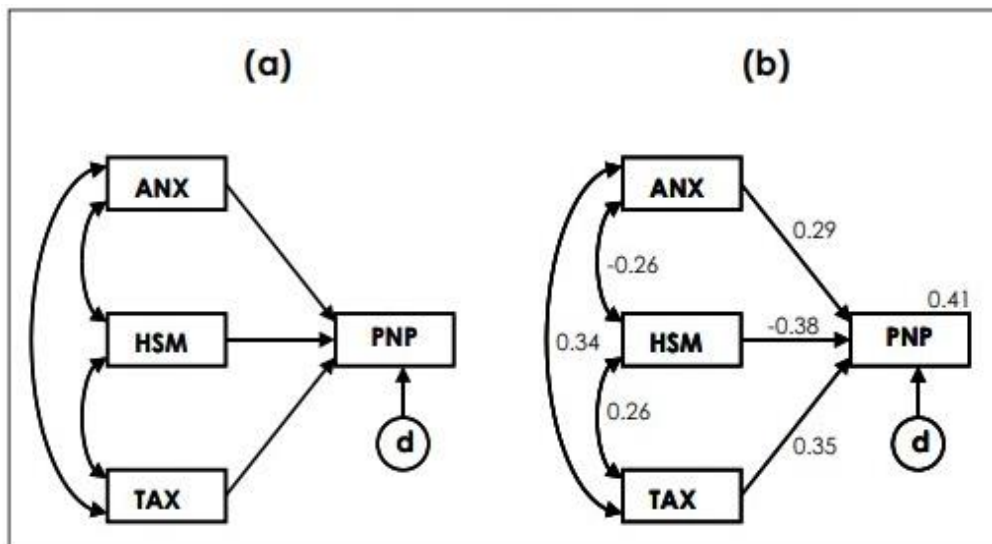


Figure 1.19 The possible model (a) and the output of the regression (b) (Streiner, 2005)

The path analysis frames it first in multiple regression (**Figure1.19**) which can be expressed as the equation (1.32).

$$PNP = b_0 + b_1ANX + b_2HSM + b_3TAX + d \text{ (Error)} \quad (1.32)$$

Where b_0 is intercept, b_1 , b_2 and b_3 are the weights of each exogenous variable. d is the error term of regression. However, the only significant path coefficients or weights (b) themselves cannot tell us whether the overall model is significant or not (Streiner, 2005). Therefore, the fitting model of path analysis is further determined by structural equation modeling to examine multivariate causal relationships (Fan et al., 2016).

1.3 Objectives

The main objective of this study is to mainly investigate the neurological biomarkers with the proposed EEG and HRV in LKU during resting-state. The specific objectives are described in the following:

- To examine the proposed EEG and HRV in LKU, compared to the controls, and also investigate in different factors (age, duration, the quantity and daily doses of kratom use).
- To determine whether the proposed biomarkers are corresponded and related to neurobehavioral testing, evaluated by cognitive task (working memory), and kratom dependence rating score.
- To investigate the causal relationship between the relevant factors/ neurobehavioral testing and the significant-based proposed biomarkers in LKU using path analysis.
- To perform the binary classification using the recognized machine-learning algorithms with the significant-based proposed features corresponding to the important factors.

1.5 Conceptual framework

Based on the literature review, Kratom users were concerned about possible Kratom dependence (D. Singh et al., 2017) and cognitive deficit (Ismail et al., 2017; D. Singh et al., 2019; Yusoff et al., 2016). Prolonged and high dose of Kratom consumption was normally found in older adults (Charoenratana et al., 2021). Nowadays, scientific research is limited on how the neurophysiological signals from the brain and heart respond to long-term Kratom consumption. There is little evidence of the neurological assessment with electrocardiogram (Leong Abdullah et al., 2020), and the brain structure evaluated by brain magnetic resonance imaging (D. Singh, et al., 2018) in regular Kratom users did not show differences from non-Kratom users. However, they need to further investigate with alternative methods, such as brain activity with EEG recording and heart rate variability activity. These introduced methods are feasible to represent the biomarker for LKU, and possible to apply that neurological biomarker for screening LKU who are sensitive to risks related to kratom consumption. Thus, the objective of this study is to investigate the biomarkers in LKU consuming it in the form of chewing the whole leaves measured by the proposed EEG features (TAR and PVF) and ultra-short HRV during resting state (eyes-closed condition). Moreover, the neurological behavior testing with working memory task and their score rating for Kratom dependent were also assessed. The proposed EEG and HRV, including the neurological behavior, were compared between LKU and controls and also examined in different factors. Subsequently, the statistical significance-based biomarkers were further as the input features to perform path analysis for exploring the casual relationship and machine-learning technique for binary classification. As mentioned above, our conceptual framework is illustrated (**Figure 1.20**).

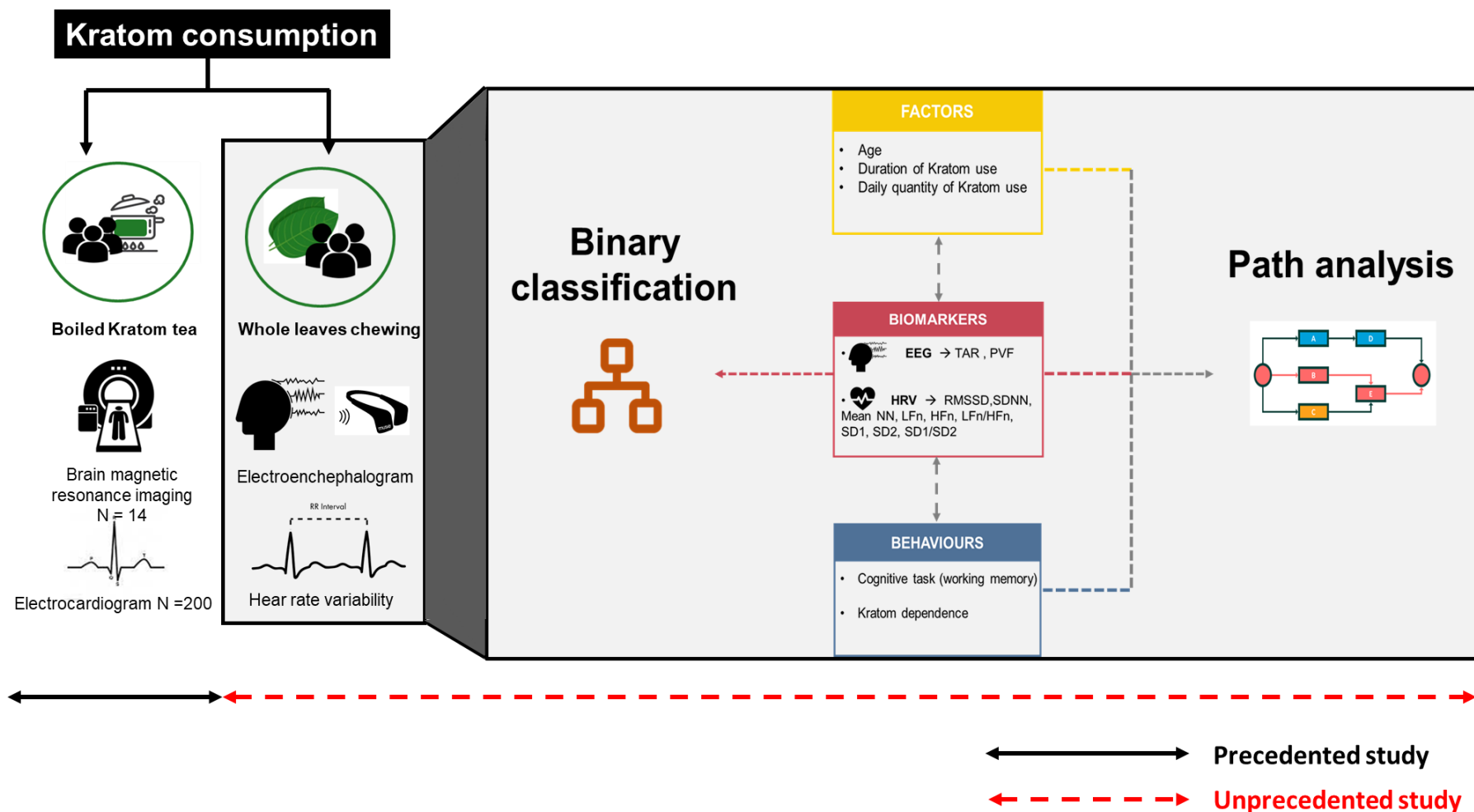


Figure 1.20 The schematic diagram of the conceptual framework in the present study

1.6 Hypotheses

- 1) The proposed EEG (TAR and PVF) cloud is more effective than HRV to be a surrogate biomarker in LKU.
- 2) The proposed EEG features would be different between LKU and control groups when age increase.
- 3) The quantity of Kratom use might be the direct effect related to the proposed EEG biomarkers.
- 4) The proposed EEG features would also show differences in different daily doses of Kratom consumption and could be related to the Kratom dependence.
- 5) The binary classification cloud be able to differentiate 1) the LKU from the control with age increase, and 2) LKU who those consumed Kratom in different daily doses.

1.7 Expected benefits

- 1) This study provides the first physiological evidence about long-term Kratom consumption with chewing the whole leaves.
- 2) It makes helps us understand how prolonged Kratom use responds to neurological oscillation.
- 3) It would be more beneficial to detect the LKU for those with a larger amount of kratom consumption that might develop toward Kratom dependence by using neurological biomarkers-based machine-learning classification.

CHAPTER 2

RESEARCH METHODOLOGY

2.1 Materials

2.1.1 EEG equipment

2.1.1.1 EEG recording

- Muse head band (*Muse*, n.d.)
- Mind monitor application (*Mind Monitor*, n.d.)
- Tablet

2.1.1.2 EEG analysis

- EEGLAB (EEG MATLAB toolbox) (Delorme & Makeig, 2004)
- SciPy (open-source Python library) (*Scipy*, n.d.)

2.1.2 ECG recording equipment

2.1.2.1 ECG recording

- LabChart
- Power lab
- Bio Amp
- ECG electrodes
- ECG Switch box
- ECG electrode patch

2.1.2.2 ECG analysis

- Neurokits (Python Toolbox for Neurophysiological Signal Processing)
(Makowski et al., 2021)

2.1.3 Cognitive testing

- PsychoPy (Open source software package written in the Python programming to create experiments in behavioral science) (*Psychopy*, n.d.)

2.1.4 Machine learning for classification

- Scikit-learn (Python library for machine learning) (*Scikit-Learn*, n.d.)

2.1.5 Path analysis

- Lavaan (R package to evaluate structural equation modeling) (*R Programming*, n.d.)

2.2 Subjects

Seventy-four male subjects were a total sample (36 controls and 38 long-term Kratom users (LKU)) collected from Ban Nasarn district, Surat Thani province, and Natavee district, Songkhla province. To match the background factors of LKU, the LKU were recruited at first followed by the controls. The inclusion and exclusion criteria are shown (**Figure 2.1**). The subject recruitments along with the inclusion and exclusion criteria. Finally, 52 male subjects (24 controls and 28 LKU) for EEG evaluation and 38 subjects (19 controls and 19 LKU) for ECG assessment met inclusion criteria. The experimental procedure was conducted according to the Declaration of Helsinki and was approved by the Ethics Committee of Prince of Songkla University, Thailand (HSc-HREC-63-017-1-1).

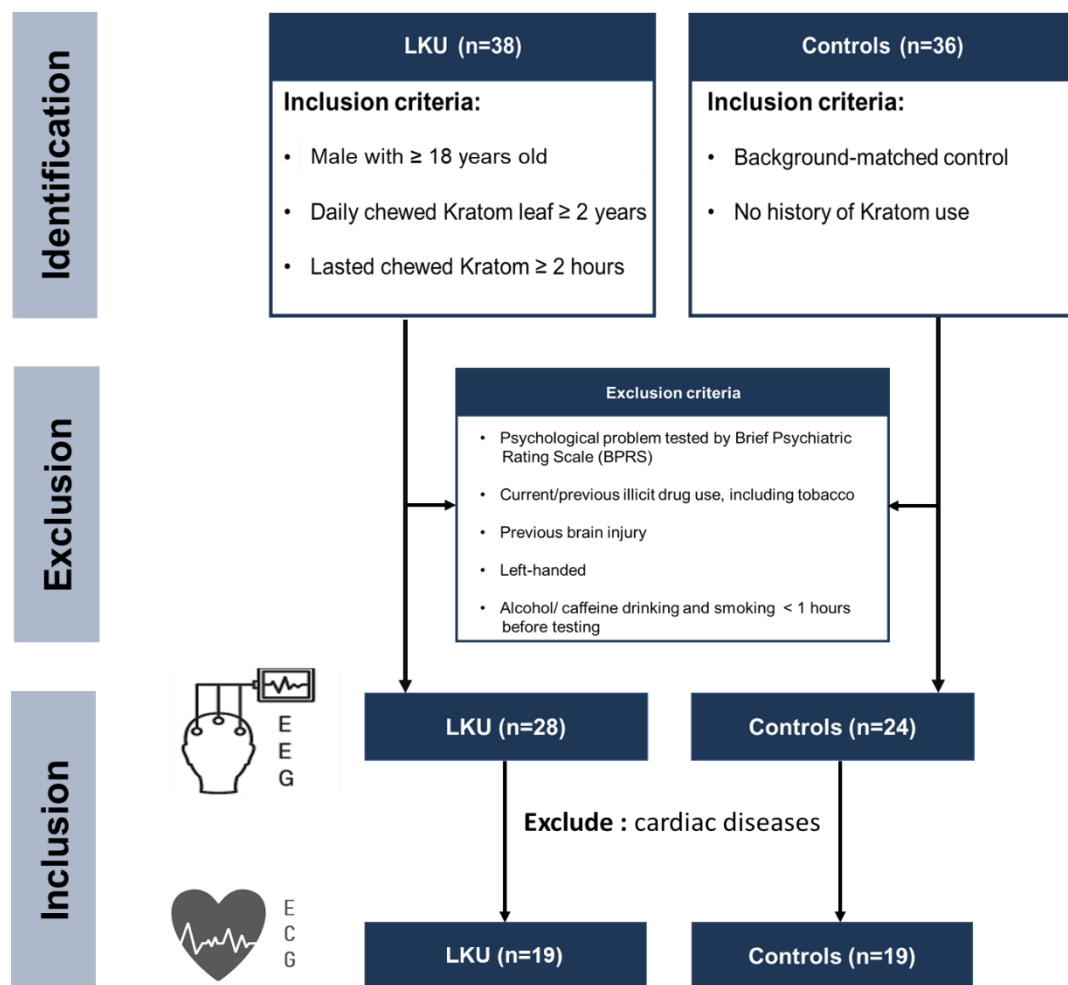


Figure 2.1 The overview of the subject recruitment and the inclusion/ exclusion criteria.

2.3 Procedure

Initially, the subjects were instructed to inform their demographic characteristics. Then, the physiological signals from EEG and ECG were recorded for 3 minutes at rest with an eyes-closed condition. After physiological recording, the subjects were instructed to perform cognitive testing with working memory and rate their Kratom dependence.

The proposed EEG features and HRV from ECG recording in LKU were compared to the control group and also examined in the different factors, such as age, duration, and the daily quantity of Kratom consumption. The statistical significances based on the proposed biomarkers were proved by 1) a supervised machine learning technique for binary classification and 2) path analysis for evaluating the causal relationship between the proposed features and the relevant factors. The overview of the procedures in this study was illustrated (**Figure 2.2**).

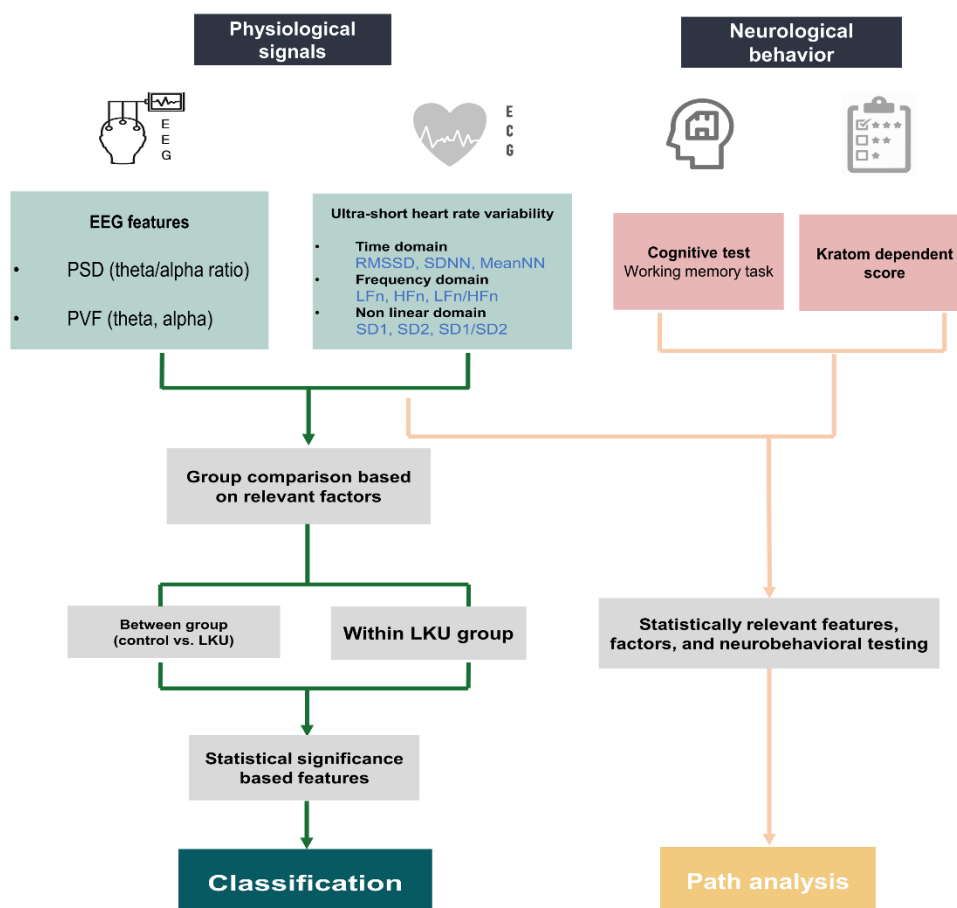


Figure 2.2 The overview of the procedures in this study

2.4 EEG recording and preprocessing

The continuous EEG data were collected by MUSE device that recorded EEG data via Mind monitor application. The data were recorded with a sampling rate of 256 Hz for 180 seconds (3 minutes) with subjects in the eyes-closed condition in order to avoid the artifacts caused by eyes-blink. The recorded EEG from both sides of AF (prefrontal) located nearly eyes-movement during eyes-closed were removed. Thus, the only temporal electrodes at TP9 (Left temporal) and TP10 (right temporal) were chosen. As eyes-blink basically occurred before eyes-closed, the time interval of 10 seconds after the onset was cut-off. The final time of EEG data in 170 seconds was further band-pass filtered (4-25 Hz) using Finite Impulse Response. Then, the artifacts were removed by using Independent Component Analysis (ICA) implemented in EEGLAB toolbox version (2019.1) (Delorme & Makeig, 2004).

2.5 EEG analysis

- **Power spectrum density (PSD)**

The processed EEG data was computed PSD using *spectopo* function implemented in EEGLAB. The function is equal to *pwelch* function or Welch periodogram in MATLAB which applied hamming window (Dedeo & Garg, 2021). The *spectopo* function returned the output in the logarithm of PSD in the decibel (dB) as the given equation (2.1). To obtain the PSD value in absolute power (mv^2/Hz), the eliminating logarithm was quantified, as shown in equation (2.2). The PSD values were normalized to the total power (4-25 Hz) and decomposed into sub-two bands of interest: theta (4-7 Hz) and alpha bands (8-13 Hz). The theta/alpha ratio was evaluated according to the equation (2.3) in each electrode and their averaging from both electrodes.

$$X = 10 \times \log (PSD) \quad (2.1)$$

$$PSD = e^{X/10} \quad (2.2)$$

$$TAR = \frac{\text{theta power}}{\text{alpha power}} \quad (2.3)$$

- **Power variance function (PVF)**

The activity of EEG variability at each frequency (f) in the temporal direction was quantified by continuous wavelet transformation according to a previous study (Ueda et al., 2016). It is defined by the equation (2.4).

$$CWT[x(t)] = \frac{1}{\sqrt{a}} \int_{-\infty}^{\infty} x(\tau) w\left(\frac{t-\tau}{a}\right) d\tau \quad (2.4)$$

where $CWT[x(t)]$ is the continuous wavelet transform of the time series of EEG signal $x(t)$, a is the scale parameter, and $w(t)$ is the mother wavelet, as shown in the equation (2.5).

$$w(t) = \frac{1}{2\sigma\sqrt{\pi}} e^{-\frac{t^2}{\sigma^2}} e^{-i2\pi f_0 t} \quad (2.5)$$

The Gabor wavelet is used as the mother wavelet. Where σ is the bandwidth of the Gaussian window, i is the imaginary number, and f_0 is the central frequency. The central frequency of the mother wavelet values is set between 5 and 25 Hz in steps of 0.5 Hz.

As the variability characteristic of $x(t)$ at frequency derived from (1) generally produced the fluctuation in different individuals. To solve the problem, the normalized variability is used to apply in the equation (2.6).

$$(f, t) = \left\| \left\| CTW \left[\frac{X_i(t)}{\sqrt{E[x_i^2(t)]}} \right] \right\| \right\|^2, \quad (2.6)$$

Where $E[\mathcal{X}]$ is the average of the time series x , $\|\mathcal{X}\|$ is the absolute value of x after being generated by CTW. The variance of EEG power at each frequency is further quantified by the equation (2.7).

$$\sigma_i^2(f) = E[(P_i(f, t) - E[P_i(f, t)])^2] \quad (2.7)$$

Where $\sigma_i^2(f)$ shows a variance for EEG power $P_i(f, t)$ of electrode (i), PVF(f) is finally transformed to a normal distribution using natural logarithm, as expressed by the equation (2.8).

$$PVF(f) = \log \sigma_i^2(f) \quad (2.8)$$

2.6 ECG recording and preprocessing

The ECG was also recorded during a resting state for 3 minutes. The recordings were made with lead I configuration at 1000-Hz sampling frequency using LabChart 7 ECG software module (ADInstruments, Australia). To eliminate the movement artifacts, the ECG signals from Lead I was measured between the left and right side of the clavicle with positive and negative electrodes, respectively with the electrode of the right leg acting as the ground (Sarang & Telles, 2006). The ECG signals were band pass filtered between 0.3-30 Hz (Palma et al., 2013).

2.7 Ultra-short Hear rate variability (HRV) analysis

Although the gold standard of HRV measurement was 5 minutes for ECG recording, the ultrashort HRV was successfully evaluated in several studies (Castaldo et al., 2019; Chen et al., 2020; Munoz et al., 2015). The collected ECG signals for 3 minutes were cleaned by artifact correction and extracted RR intervals. Then, the time, frequency, and nonlinear domains were evaluated by the open-source Python library NeuroKit (Makowski et al., 2021). The interesting

HRV parameters in different domains were computed with the functions implemented in NeuroKit, as shown (Table 2.1).

Table 2.1 HRV indices in different domains with *Neurokit* function (Makowski et al., 2021)

HRV domain for analysis	Neurokit functions	HRV indices
Time domain	<i>hrv_time()</i>	<ul style="list-style-type: none"> • Mean_NN • SDSD • RMSSD
Frequency domain	<i>hrv_frequency()</i> using Welch method	<ul style="list-style-type: none"> • LFn (0.04-0.15 Hz) • HFn (0.15-0.4 Hz) • LFn / HFn
Nonlinear	<i>hrv_nonlinear ()</i>	<ul style="list-style-type: none"> • SD1 • SD2 • SD1/SD2

2.8 Neurobehavioral testing

- **Cognitive test with working memory (WM)**

The 2-Back WM was performed with PsychoPy, an open-source software package written in Python programming (Peirce, 2007). The procedure structure is illustrated in (Figure 2.3). The block was started with a 1 sec where participants were instructed to relax and fixate on a centrally presented back fixation cross. Subsequently, a stimulus target was presented for a 1-sec. Between the stimuli, there were interstimulus intervals (ISI) with a fixation cross for the 1-sec duration. The participants needed to hold 2 items in memory and remember their order. Participants were instructed to respond using a keyboard whenever the current stimuli matched the presented stimuli 2 trail back. The match pressed the “→” button and the mismatch pressed the “←” button.

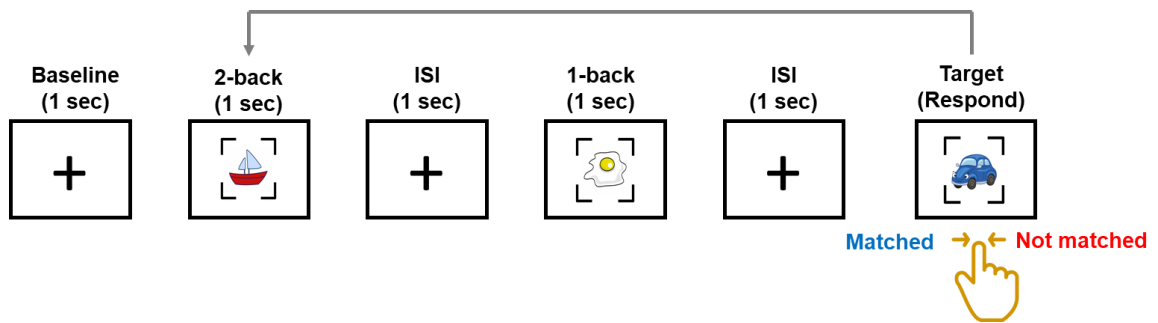


Figure 2.3 Schematic representation of 2-back working memory block structure

The 2-back results were calculated as the mean accuracy and reaction time. Moreover, the working memory index was also examined.

A working memory index called Dprime was tested the ability of the discriminant, how well individual participants distinguish between signal (target stimulus present or hit rate) and noise (non-target stimulus present or false alarm rate), as shown (**Figure 2.5**). The Dprime is assessed according to a previous study (Haatveit et al., 2010) and is defined as the given equation (2.9).

$$D_{\text{prime}} = Z_{\text{Hit}} - Z_{\text{FA}} \quad (2.9)$$

Where Z presents the transformation of hit rate (Hit) and false alarm rate (FA). Hit indicates the proportion of YES trials to which participants responded $\text{YES} = P(\text{"yes"} \mid \text{present signal})$ and FA reflects the proportion of NO trials to which subjects responded $\text{YES} = P(\text{"yes"} \mid \text{absent signal})$ as illustrated with signal detection theory (**Figure 2.4**). Therefore, H in the present study represents the proportion of YES (\rightarrow) = $P(\text{"yes"} \mid \text{matched 2 trials back})$ while F is the proportion of NO (\leftarrow) = $P(\text{"yes"} \mid \text{no matched 2 trials back})$.

The higher distance of Dprime represents the better discriminant ability (a higher hit rate and lower false alarm rate), as shown in the ROC curve (**Figure 2.6**)

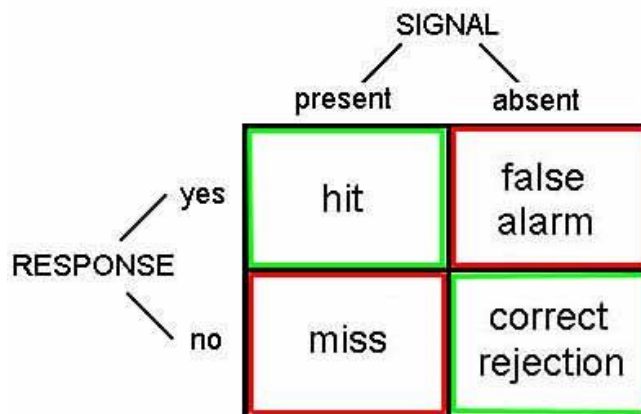


Figure 2.4 Signal detection theory shows the possible consequences of the responses to the present and absent signal (Ye & Van Raaij, 2004)

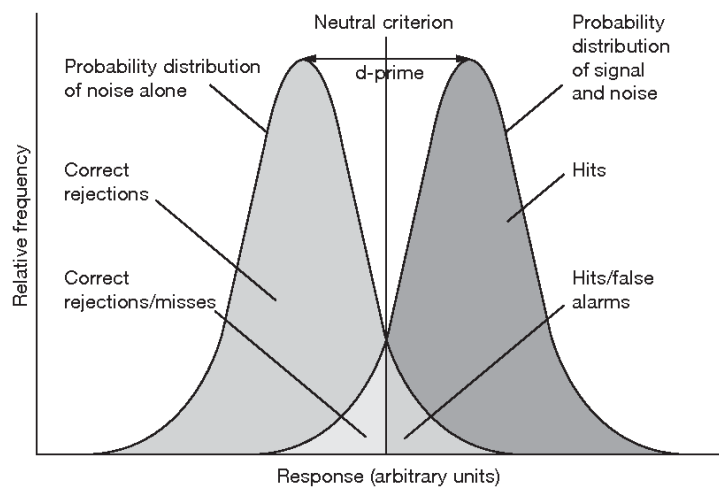


Figure 2.5 The distributions of response to a signal (present signal) and noise (absent signal) are separated by the distance of Dprime. (Oliver et al., 2008).

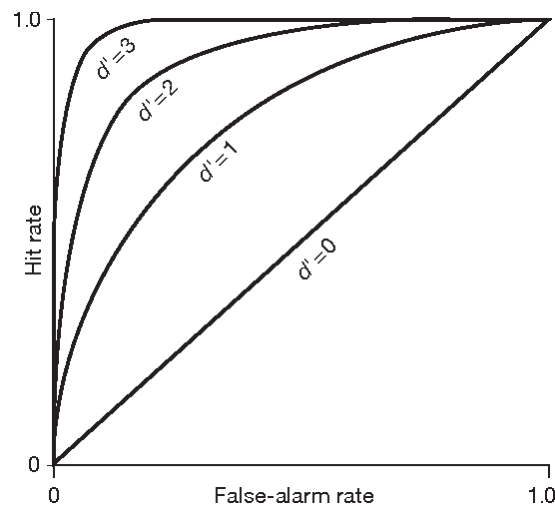


Figure 2.6 The ROC curve plots the hit rate against the false alarm rate on different d' (Dprime) values. The curve that approaches the upper left corner provides a higher Dprime value that reflects the greater accuracy (Oliver et al., 2008).

- **Kratom Dependence Scale (KDS)**

The LKU group was instructed to rate their Kratom dependence with 16-items of KDS scales based on the Diagnostic and Statistical Manual of Mental Disorders, Fourth Edition (DSM-VI). The KDS provided the levels of Kratom dependence into 3 levels: low (KDS score: 0-13), moderate (KDS score: 13-34), and high (KDS score: 35-48) levels. The reliability of the KDS was 0.97 with Cronbach's alpha coefficient (Saingam et al., 2014).

2.9 Statistical analysis

Prior to comparison in group differences, the data were checked for the normal distribution with the Kolmogorov-Smirnov normality test. As the data in this study was non-normal distribution with positive skewness, the log-transformation or non-parametric testing was applied. All parameters were assessed with the statistical tests in the interesting factors as follows:

- **Spearman's rank correlation:** non-parametric test for Pearson correlation
To evaluate the association between the interested factors (age, duration, and quantity of Kratom use) and biomarkers of physiological signals/working memory performance.
- **Partial rank correlation:** non-parametric test for Partial correlation
To test the association between the interested factors (age, duration and quantity of Kratom use), and biomarkers of physiological signals /working memory performance for controlling the covariate effects.
- **T -test:** comparing the means of two groups
To determine the Katom dependence score between LKU for those with VH and those with LTH group.
- **Two-way ANOVA:** comparing the mean differences between groups based on the effect of two independent variables
To examine the effect of groups (control vs. LKU) and alcohol drinking/smoking on the TAR level
- **Multivariate Analysis of Variance (MANOVA):** comparing means for multiple dependent variables across independent variables
To compare group differences (controls vs. LKU and, LKU those for very high dose consumption vs. those low to high doses) on multiple dependent variables in different domains, as given (**Table 2.2**).

Table 2.2 The proposed features and working memory performances for MANOVA testing

Domain	Features
EEG	TAR, PVF
Heart rate variability	RMSSD, SDSD, MeanNN, LFn,HFn, LFn/HFn, SD1,SD2, SD1/SD2
Working memory performance	correctness, error, reaction time Dprime,

The significance of MANOVA testing was followed-up with univariate ANOVAs to test the group difference on individual parameters. Then, the post-hoc test for pairwise multiple comparisons using the Bonferroni test was applied to correct the p -value.

Based on our preliminary study, the effect size and observed power were also evaluated for the given sample size. The effect size is the magnitude of the difference between groups which is an independent sample size. The effect size with $n2p$ is used in MANOVA testing and is interpreted as small effect = 0.01, medium effect = 0.06, large effect = 0.14 (Grissom & Kim, 2012).

All significant testing was set at $p < 0.05$.

2.10 Path analysis

Path analysis in LKU was used to determine the hypothesized causal relationships across certain factors, the proposed EEG features, and neurobehavioral testing based on the significant statistical results (**CHAPTER 3**). The possible model of path analysis was hypothesized as given (**Figure 2.9**). Age, duration, and the daily quantity of Kratom use were determined as the exogenous variables and among them showed the covariance of each other (Green double-head arrow). The mediate variable represented with TAR and PVF and Kratom dependence score was considered as an endogenous variable. Each gray single-headed arrow or path indicated the multiple regression. The overall path or the final model was evaluated the fitness of the model with structural equation modeling (SEM) using *lavaan* packaged in R programming. The model fitness was interpreted by the indicative fit index (Bollen, 1989; Browne, M. W., & Cudeck, 1992), as shown (**Table 2.3**).

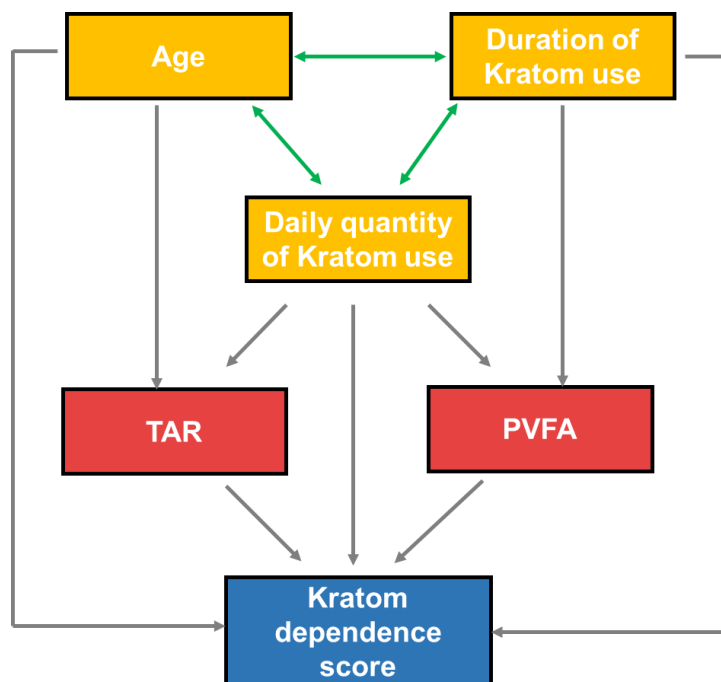


Figure 2.7 The expected model of path analysis in LKU. The Green double-head arrow indicates covariance of each other while the grey single-headed arrow represents the predicted path with multiple regression. The fitness of the overall path was examined by SEM.

Table 2.3 The indicators of model fitness and their recommended best fit value (Bollen, 1989; Browne, M. W., & Cudeck, 1992)

Indicative fit index	Recommended good fit value
Comparative fit index (CFI)	≥ 0.95
Tucker-Lewis index (TLI)	≥ 0.90
Root mean square error of approximation (RMSEA)	< 0.05
Standardized root means square residual (SRMR)	< 0.05

2.11 Classifications

The significant parameters in statistical analysis were proved with the classification methods using traditional machine learning algorithms, such as random forest (RF), support vector machine (SVM), *k*-nearest neighbors (*k*NN), and logistic regression (LR). The present study was performed 2 tasks of binary classifications based on the significantly statistical results (**CHAPTER 3**) as follows:

- 1) The classification between the control and LKU groups in age effect.
- 2) The classification of different doses of Kratom consumption.

- **Feature extraction**

Since the EEG signals are non-stationary in nature which inhibits the accuracy for classification, the statistical-based features were extracted from 5 non-overlap segmented EEG data instead of the entire processed data with a window size of 30 seconds per segmentation (**Figure 2.7**). Then, the individual and the combination of statistical-based features extraction were used to classify using the mentioned machine learning algorithms with a cross-validation method.

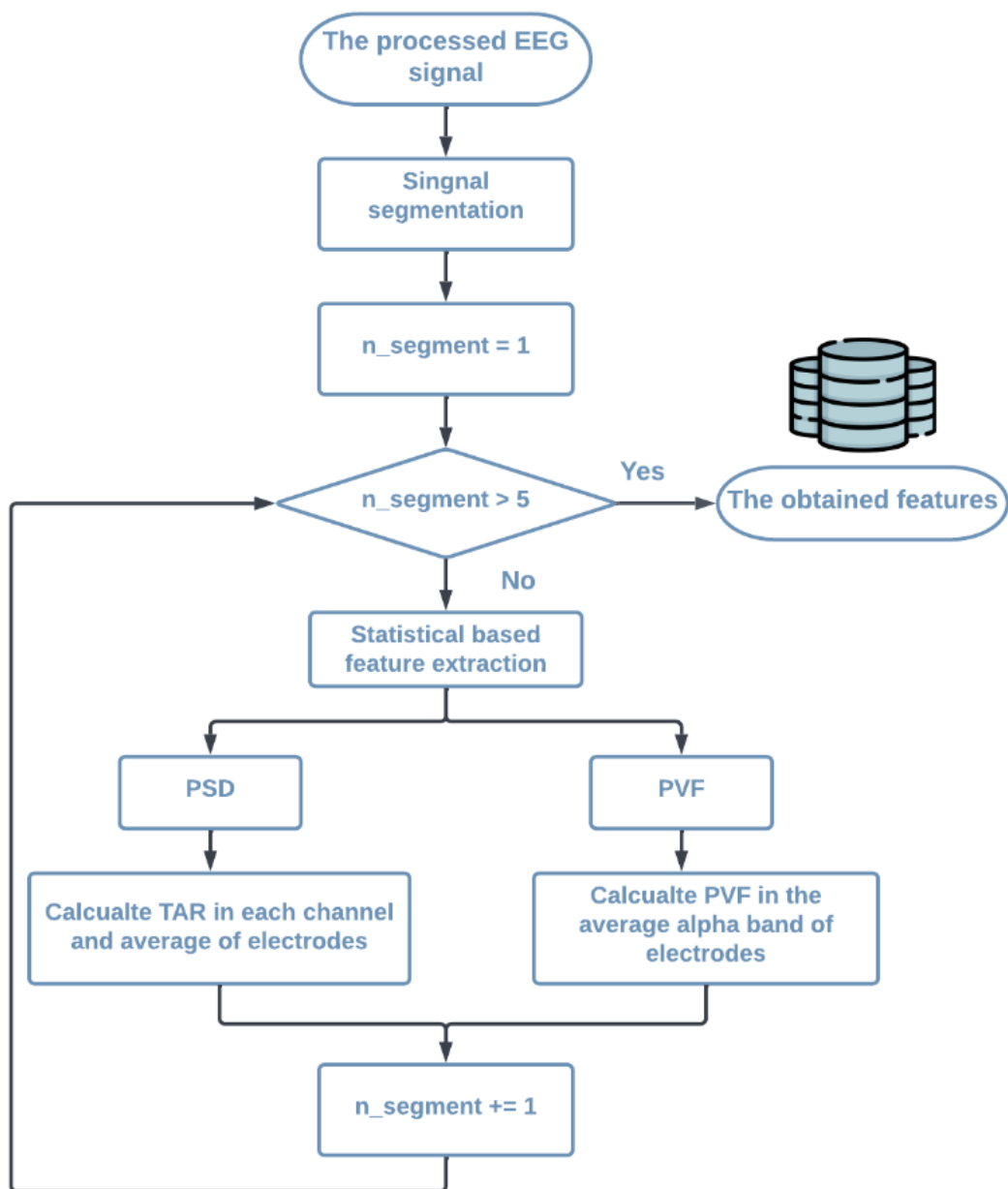


Figure 2.8 The procedure of feature extraction

- **Cross-validation and evaluation model**

The stratified K-fold (SKF) method was performed using scikit-learn. The SKF is a cross-validation method to divide the data into K folds in which each fold is comprised of an equal ratio of the amount data of each class in both training and testing datasets. The method is useful for unbalanced classes to reduce bias during accuracy verification (Coroiu, 2016). The present study used $K = 10$ in the outer loop and $K = 5$ in the inner loop. In the outer loop, the data was resampling in 10 iterations with each iteration consisting of 9 parts for the training set and one part for the testing set. Then, the hyperparameter tuning with the grid search method was performed in the inner loop to search for the optimal parameters that provided the highest accuracy. The training set was again partitioned into 4 parts for the training set and the one part for validating the data set with resampling of 5 iterations. The hyperparameters tuning in each recognized classification were adjusted (**Table 2.4**). Finally, the classification performances in the given equation (2.10 -2.14) were evaluated by the test set with optimal parameters in each iteration (**Figure 2.8**). Moreover, the area under the curve (AUC) was also computed from the area under the ROC curve that was widely used to gain the acceptance of the classifier model. All these classification performances were reported as the averaged percentage and standard error of the completed outer iterations. The procedure of cross-validation and evaluation models was performed separately based on the significantly statistical results (**CHAPTER 3**).

Table 2.4 Hyperparameter tuning

Classifiers	Parameter	Value
RF	number of estimators	10, 100, 150, 200
	max features	auto, sqrt, log2
	criterion	gini, entropy
	class weight	balance
SVM	kernel	linear, rbf, sigmoid
	Gamma	$10^{-2}, 10^{-3}, 10^{-4}, 10^{-5}$
	C	0.001, 0.01, 0.1, 10, 25, 50, 100, 1000
	class weight	balance
kNN	number of neighbors	3, 5, 7, 9
	weight	uniform, distance
	metric	euclidean, manhattan
LR	penalty	L1, L2
	C	0.001, 0.01, 0.1, 1, 10, 100, 1000
	solver	liblinear
	class weight	balance

$$Accuracy = \frac{TP + TN}{TP + FN + TN + FP} \quad (2.10)$$

$$F1 \text{ score} = \frac{2 * precision * sensitivity}{precision + sensitivity} \quad (2.11)$$

$$Sensitivity = \frac{TP}{TP + FN} \quad (2.12)$$

$$Specificity = \frac{TN}{TN + FP} \quad (2.13)$$

$$AUC = \frac{1}{2} \left(\frac{TP}{TP + FN} + \frac{TN}{TN + FP} \right) \quad (2.14)$$

Where TP and TN are true positive and true negative, respectively, FP and FN are false positive and false negative respectively. TP and TN represent the outcome where the models correctly predict the positive and negative classes, respectively while FP and FN represent the outcome where the models incorrectly predict the positive and negative classes.

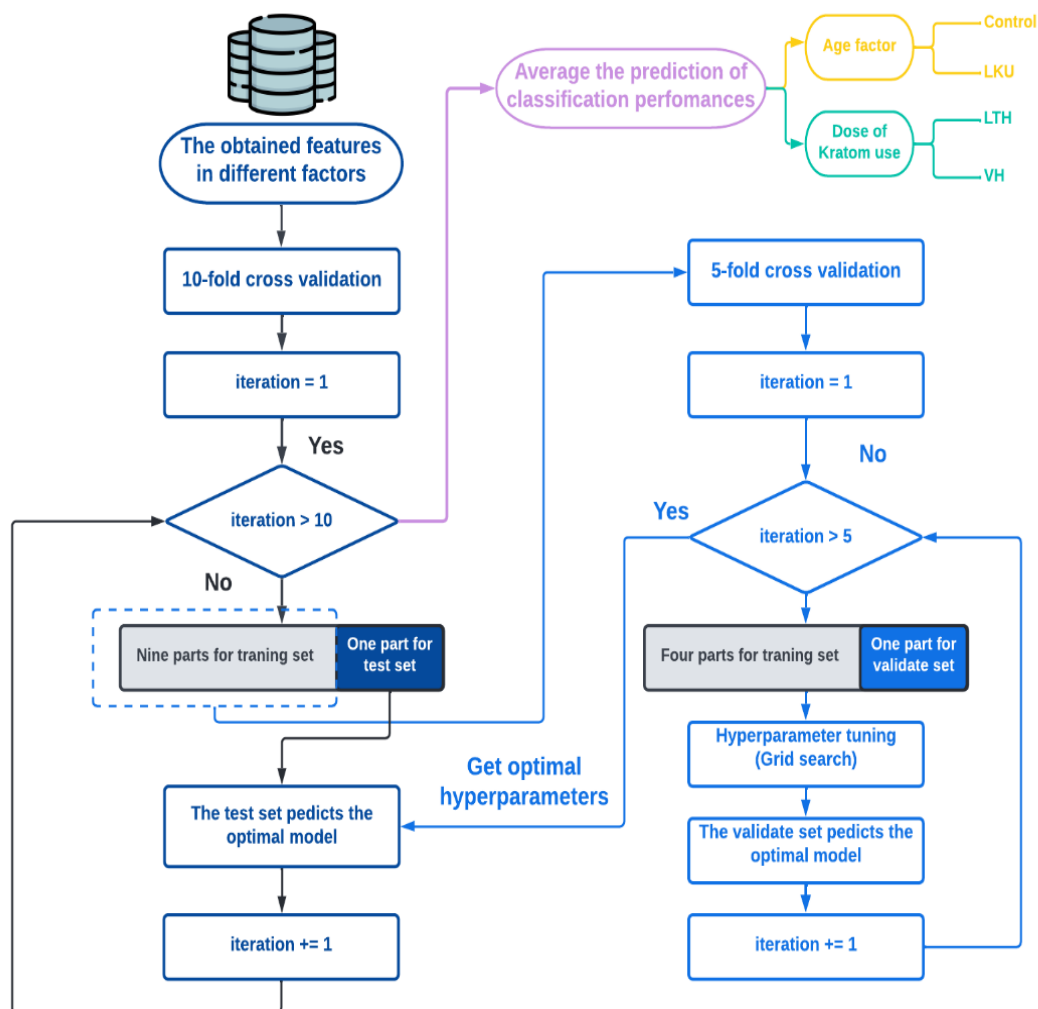


Figure 2.9 The procedure of cross-validation and evaluation models. VH and LTH represent LKU for those with very high doses and low to high doses, respectively.

CHAPTER 3

RESULTS

The results were described in three parts: 1) statistical analysis, 2) path analysis and 3) supervised machine learning method for binary classification, as shown in (Figure 3.1).

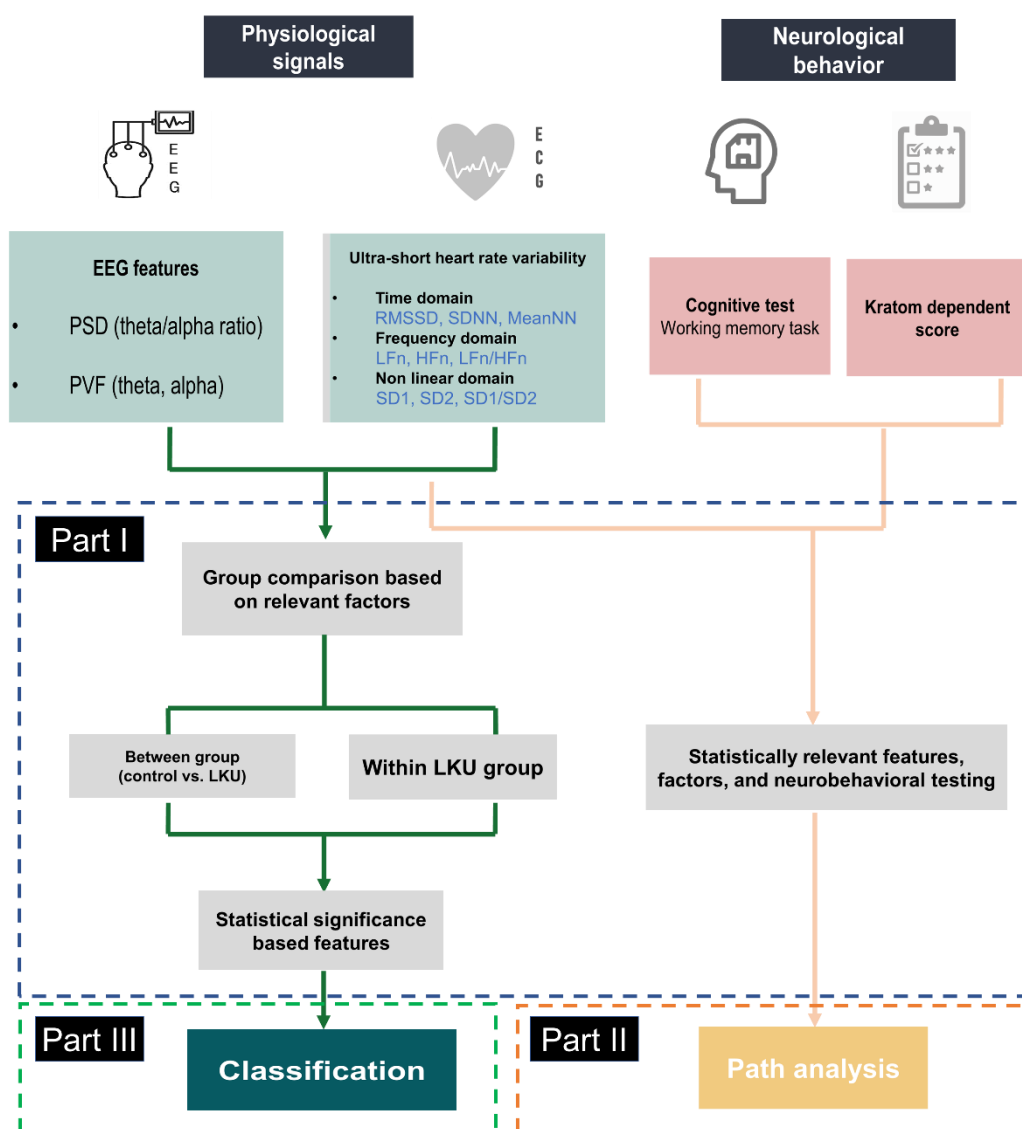


Figure 3.1 The overview of the results description in different parts.

3.1 Statistical analysis

3.1.1 Socio-demographic characteristics and kratom use history

The demographic characteristics were compared between groups, as summarized in (Table 3.1). The LKU group was significantly more prevalent in smoking and alcohol drinking than the control group. In addition, the information on kratom use history was shown in (Table 3.2).

Table 3.1 Participant's demographic characteristics

Factors	LKU (n= 28)	Controls (n = 24)	p-value
Age			
Total (mean ± SD)	52.41 ± 15.45 (n=28)	56.64± 10.70 (n=24)	0.251 ^a
≤ 50 (y)	46.44 ± 3.71 (n = 9)	40.08 ±9.18 (n=12)	0.060 ^a
> 50 (y)	61.47±9.44 (n=19)	64.75 ±9.11 (n=12)	0.348 ^a
Occupation			
Farmers n(%)	24 (85.71)	22 (91.66)	
Other n(%)	4 (14.29)	2 (8.33)	
			0.503 ^b
Smoking			
Non-smoking n(%)	9 (32.15)	17 (70.83)	
Smoking n(%)	19 (67.85)	7 (29.17)	
			0.005^b
Alcohol drinking			
Non-drinking	9 (32.15)	17 (70.83)	
Drinking	19 (67.85)	7 (29.17)	
			0.005^b

Note: ^a t-test, ^b chi square test

Table 3.2 Kratom use history

Factors	n(%)
Duration of Kratom use (y)	26.85 ± 11.11 (mean ± SD)
< 30 (y) n(%)	14 (50)
≥ 30 (y) n(%)	14 (50)
Daily Kratom consumption (leaves/day)	10.39 ± 7.20 (mean ± SD)
< 10 leaves/day n(%)	14 (50)
≥ 10 leaves/day n(%)	14 (50)
Dependent score	25.07 ± 96 (mean ± SD)
Low (0-13) n(%)	4 (14.28)
Moderate (13-34) n(%)	20 (71.44)
Hight (35-48) n(%)	4 (14.28)

3.1.2 The comparison of EEG power and their variability between the controls and LKU

The normalized PSD and PAF at both electrode position during eyes closed were computed to examine between-group differences. Both PSD (Figure 3.2A) and PVF (Figure 3.2B) in the LKU group were likely to increase in the frequency range of 4-7 Hz (theta) and decrease in 8-13 Hz (alpha), but not reach statistical significance compared to the control group. Thus, further experiments investigated these EEG features in the relevant factors to determine between-group differences.

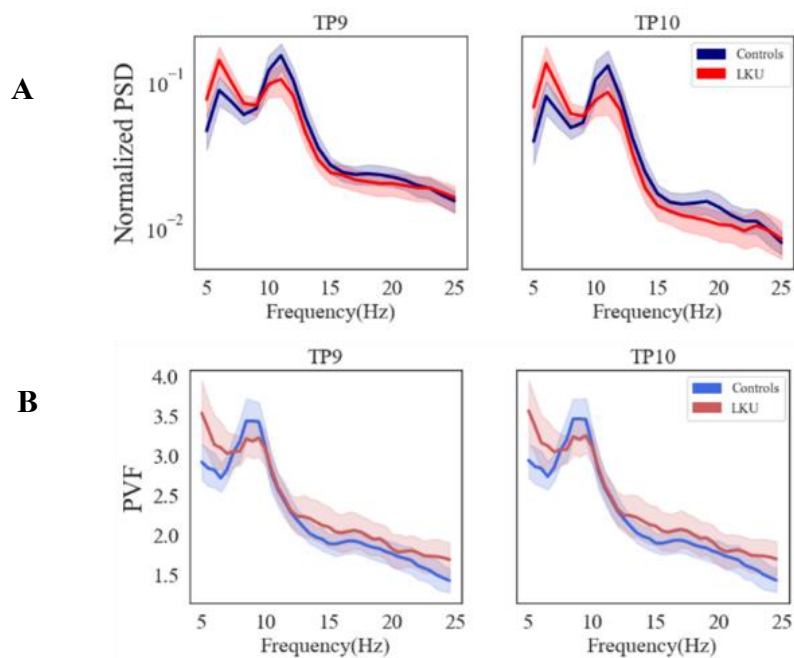


Figure 3.2 The comparison of PSD (A) and PVF (B) during resting-state (eyes-closed) between groups

3.1.3 The correlation between the proposed EEG features and age

The PSD and PVF were computed in sub-band frequencies (theta and alpha bands) and correlated with age. The spearman's rank showed that the PSD (**Figure 3.3A**) of that frequency bands had more tendency to correlate with age than PVF (**Figure 3.2B**) in both groups and more likely to be an opposite correlation between groups. Thus, the PSD of that frequency in various age ranges might be the most significant difference between groups.

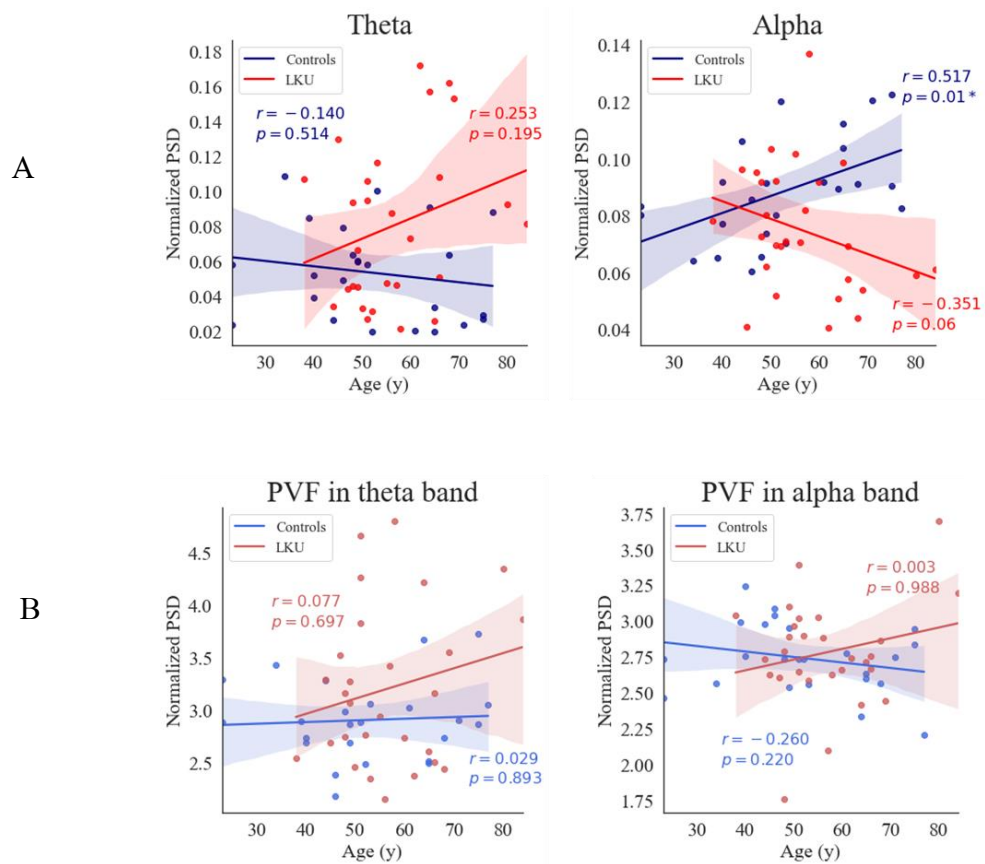


Figure 3.3 The correlation between PSD (A), PVF (B), and age in sub-frequency bands; theta and alpha

3.1.4 The comparison of TAR between groups in different age ranges

To better understand the PSD of that frequencies between-group in different age ranges (**Figure 3.4A**), we subdivided those age distributions based on the median age into ≤ 50 and > 50 years old. The PSD in specific frequency ranges theta to the alpha band at both electrodes, highlighted with gray band color, clearly showed a between-groups difference in the age range of > 50 years old.

Furthermore, the PSD of theta and alpha bands over 50 years old showed more adverse effects between them in both groups. Thus, the ratio between theta/alpha (TAR) across electrodes and their average was compared between groups using the MANOVA test (**Figure 3.4B**). The results showed that the multivariate effect of MANOVA were statistically significant between-group differences in age range > 50 years old [Wilks Lambda = 0.667, $F(3,27) = 4.497$, $p = 0.011$,

$n^2 p = 0.333$, observed power = 0.829]. The significant overall multivariate effect was followed by ANOVAs to test which individual EEG features provided the significant group difference (Table 3.3). All EEG features of TAR showed a significantly increased in the LKU compared to the control group. Their significant differences between groups were adjusted p -value by Bonferroni correction. The results suggested that the different TAR levels between groups might be involved in the age effect.

However, the factors of smoking and alcohol drinking were not discarded as the proportion between groups was a significant difference in that factor. A two-way ANOVA analysis was performed to test the main effect of groups and smoking/alcohol drinking on the TAR level. The results showed that both the main effects of group and smoking were significant differences (**Figure 3.5A**). For alcohol drinking, there was a significantly difference in the main effect of group and their interaction (group x alcohol drinking) (**Figure 3.5B**). The results indicated that the TAR level was also dependent on smoking and alcohol drinking.

Furthermore, we found that the increased TAR in LKU those with > 50 years old was significantly positively correlated with the quantity of Kratom use tested by spearman's rank correlation (**Figure 3.6**). Thus, the increased TAR in LKU over 50 years old, compared to the controls was age-related to the quantity of Kratom consumption. The quantity of Kratom consumption was also the major effect to change the TAR level in LKU.

Table 3.3 The ANOVAs results for the group comparison between control and LKU in the same age range > 50 years old on individual EEG features. TAR stands for the theta/alpha ratio. * and ** indicate $p < 0.05$ and $p < 0.01$, respectively.

Features	Control (n = 12)		LKU (n=19)		ANOVAs F(1,29)	p-value	Effect size (η^2_p)	Power
	M	SD	M	SD				
TAR TP9	-0.418	0.311	0.022	0.412	10.046	0.004**	0.257 (Large effect)	0.865
TAR TP10	-0.356	0.372	0.015	0.415	6.393	0.017*	0.181 (Large effect)	0.686
Average TAR	-0.382	0.340	0.024	0.410	8.155	0.008**	0.219 (Large effect)	0.788

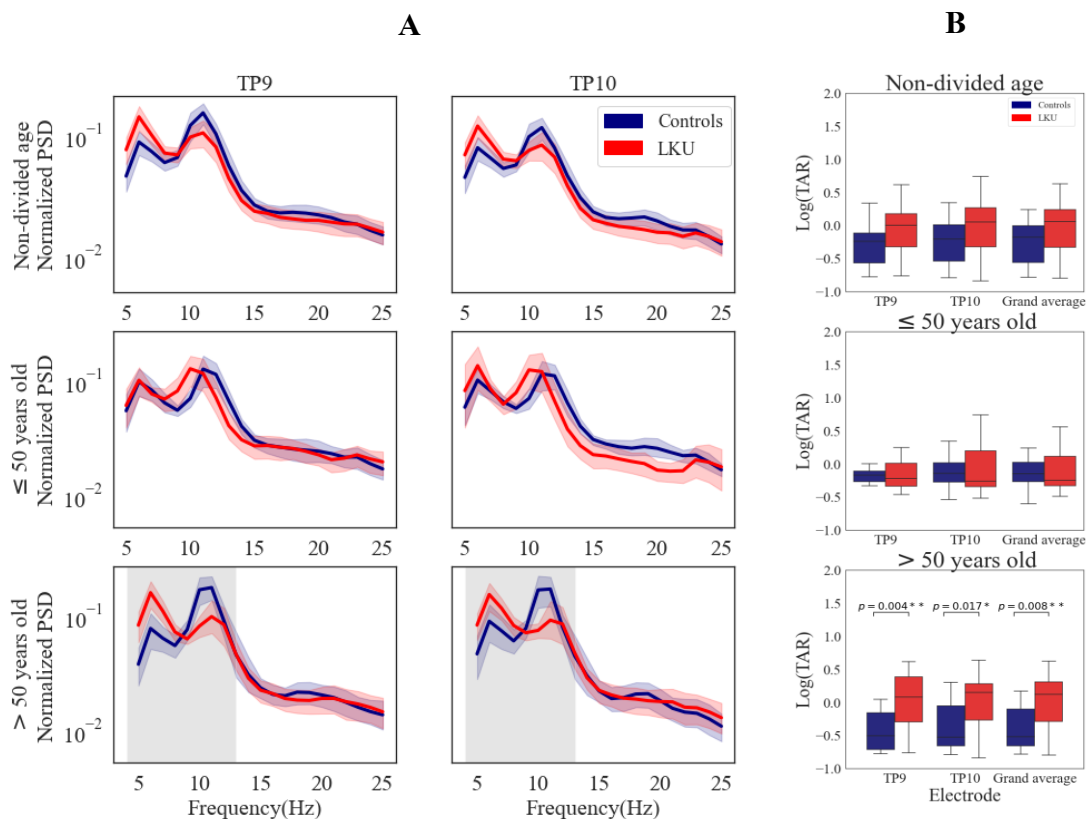


Figure 3.4 The broad PSD (A) and TAR (B) in the different age range between the control and LKU group. The comparison between groups for TAR levels in each electrode and their average was determined by the MANOVA test. The pairwise multiple comparisons were adjusted by Bonferroni correction. * $p < 0.05$, ** $p < 0.01$. Note: non-divided age; control (n =24) and LKU (n = 28), ≤ 50 years old; control (n =9) and LKU (n = 12), and > 50 years old; control (n =12) and LKU (n = 19).

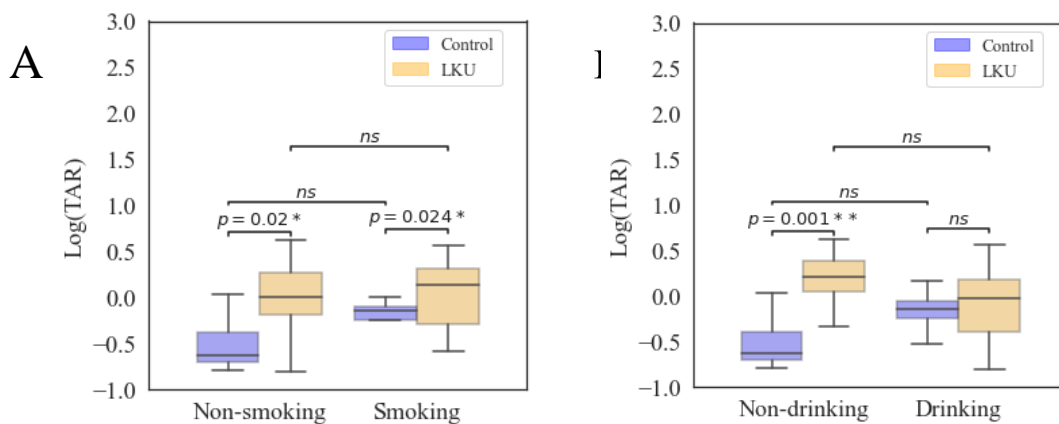


Figure 3.5 The effect of TAR levels on smoking (A) and alcohol drinking (B) between groups. The two-way ANOVA was conducted to examine the main effect of the group and the main effect of smoking/alcohol drinking. The significant pairwise comparisons were adjusted by Bonferroni correction. * $p < 0.05$, ** $p < 0.01$.

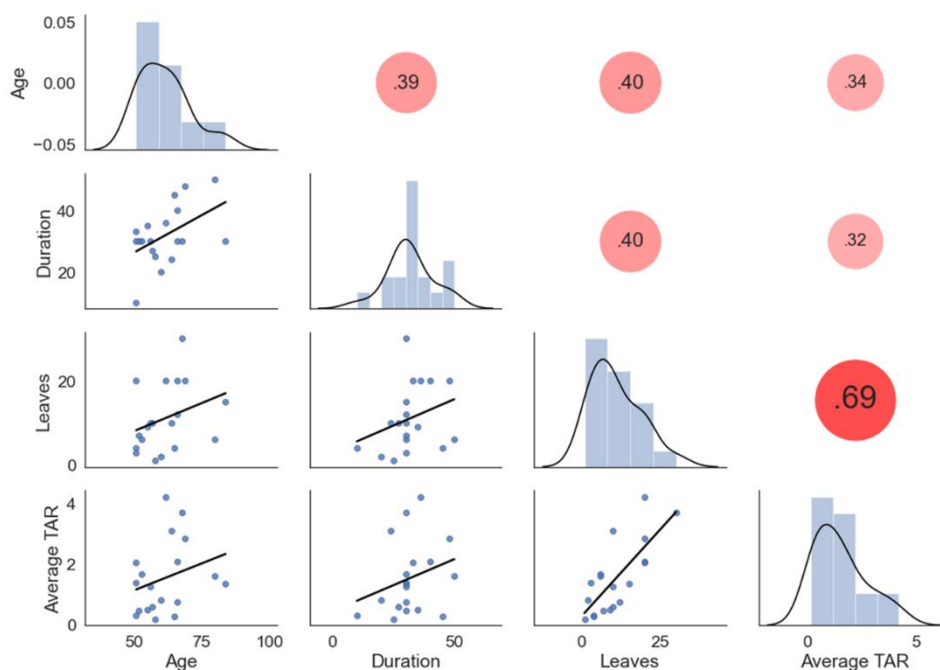


Figure 3.6 The correlation between average TAR and the relevant factors (quantity of Kratom leaves consumption, duration, and age) in LKU with those > 50 years old ($n = 12$), tested by spearman's rank correlation.

3.1.5 TAR and PVF were involved in the daily dose-dependent manner of kratom consumption.

Since the TAR level was highly related to the quantity of Kratom use, the TAR level was further observed in different daily doses. Based on a prior study (Prozialeck et al., 2012) and converting in the weight of Kratom leaves in Thai origin (Suwanlert, 1975). The dosages of Kratom intake were categorized into low to moderate doses (1-3 leaves/day), moderate to high doses (4–9 leaves/day), and very high doses (>10 leaves/day). The TAR levels (TP9, TP10, and their average) tended to be daily dose-dependent (**Figure 3.7A**) as well as PVF in theta and alpha bands (**Figure 3.7B**). To clearly compare between-group differences, we regrouped those who consumed kratom at low to high doses and very high doses for testing the levels of TAR and PVF in the alpha band. As a higher Kratom leaves consumption was observed in older adults and a longer time range of duration, the age, and duration of use were set as covariates in MANOVA testing to compare group differences across the proposed EEG features.

The results showed that the overall effect between groups were statistically significance [Wilks Lambda = 0.466, $F(5,20) = 4.582$, $p = 0.006$, $\eta^2_p = 0.534$, observed power = 0.918]. All introduced EEG features except PVF in the theta band were significant differences between groups tested by ANOVAs and provide a large effect size (**Table 3.4**). The TAR (across electrodes and their average) (**Figure 3.7C**) and PVF in the alpha band (**Figure 3.7D**) were significantly increased and decreased respectively, in a daily doses-dependent manner. The pairwise multiple comparisons from ANOVAs were tested by Bonferroni correction.

The results suggested that the changing of the proposed EEG features was in a dose-dependent manner.

Table 3.4 The ANOVAs results for the group comparison between LKU for those with LTH and those with VH on individual EEG features. TAR stands for the theta/alpha ratio. PVFT and PVFA stand for power variance function in theta and alpha bands. * and ** indicate $p < 0.05$ and $p < 0.01$, respectively.

Features	LTH (n = 14)		VH (n=14)		ANOVAs F(1,29)	p-value	Effect size (η^2_p)	Power
	M	SD	M	SD				
TAR TP9	-0.258	0.279	0.185	0.321	12.924	0.001**	0.335	0.932
TAR TP10	-0.226	0.355	0.199	0.356	8.334	0.008**	0.258	0.791
Average TAR	-0.239	0.318	0.203	0.328	10.957	0.003**	0.313	0.888
PVFT	0.503	0.109	0.486	0.089	0.592	0.449	0.024	0.115
PVFA	0.465	0.045	0.414	0.064	7.807	0.010*	0.245	0.765

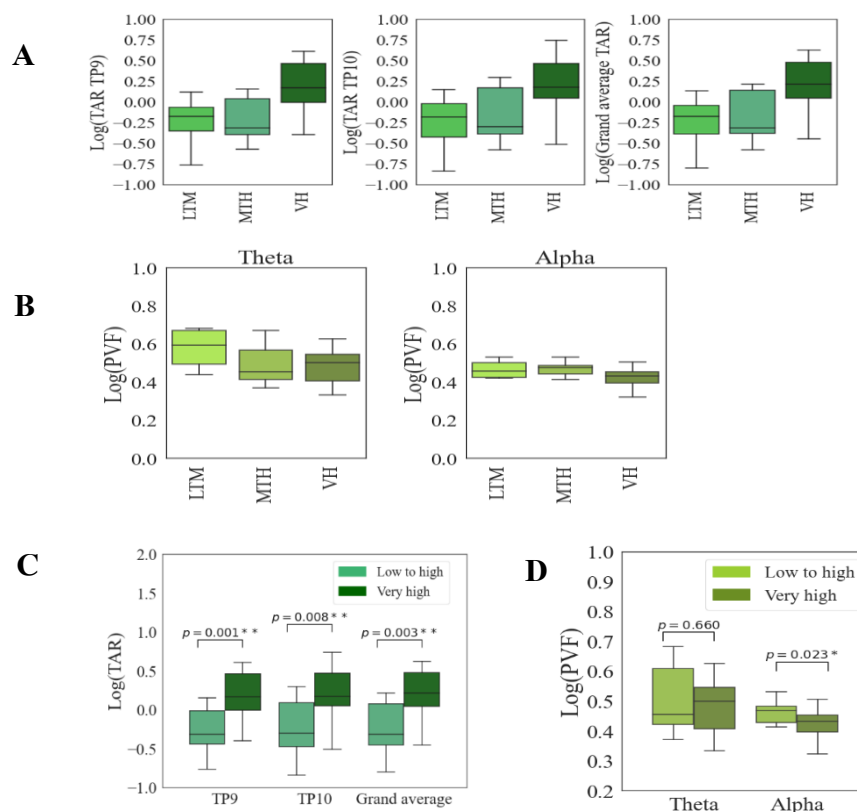


Figure 3.7 The effect of TAR (A) and PVF (B) in low to moderate doses (LTM), moderate to high doses (MTH), and very high (VH). The comparison between low to high doses (LTH); $n = 14$ and very high dose (VH); $n = 14$ for TAR (C) and PVF (D) in the alpha band was tested by MANOVA test. The pairwise multiple comparisons were adjusted by Bonferroni correction. * $p < 0.05$, ** $p < 0.01$.

3.1.6 The comparison of neurological behaviors in different doses of kratom use

Basically, the biological changes in the neuron activity were highly related to neurological behaviors. Therefore, the neurological behavior was examined to test whether it changes following the proposed EEG features. According to the previous results, the proposed EEG feature was directly associated with the daily kratom leaves consumption and showed a significant difference between LKU with LTH and VH. We compared the neurological behaviors with cognitive testing (working memory test) among the control, LTH, and VH groups (**Figure 3.8A**). Furthermore, Kratom dependent score in LKU with those who consumed different daily doses was also investigated.

The LKU those who consumed a very high dose had a tendency of lower performances in working memory tasks, compared to other groups. However, all parameters in the working memory test, such as % correctness, % error, reaction time, and Dprime in the cognitive test were not statistically significant differences among groups tested by MANOVA with age as a covariate due to age-related cognitive performance (**Figure 3.8A**). The comparison of false alarm rate and hit rate from working memory performance groups were plotted with ROC curves (**Figure 3.8A**). The ROC curves of all groups were in the range of better discriminant ability that the mean of ROC curves in each group was close.

In addition, LKU for those with VH was also likely to increase the Kratom dependent score compared to those with LTH, but the difference was not significance tested by the *t*-test (**Figure 3.8B**).

Collectively, the neurological behaviors in the LKU with different daily doses had a slight tendency of changing, which might correspond to the biological alteration with the proposed EEG.

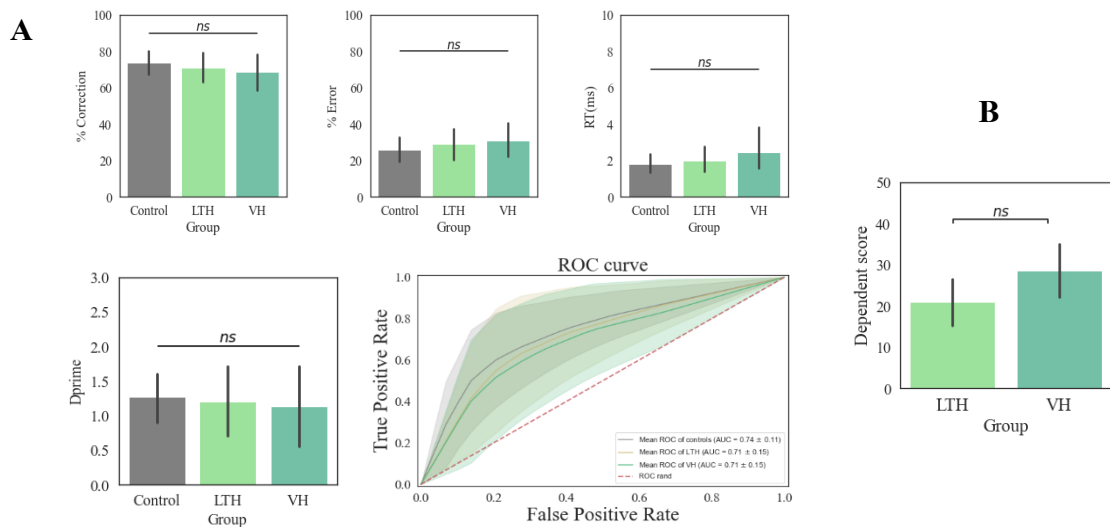


Figure 3.8 The neurological behaviors. The comparison among groups of the controls (n =12), LTH (n=12), and VH (n=12) in the working memory performance using MANOVA testing (**A**). Kratom dependent score rating in LKU those who consumed different daily doses tested by *t*-test independent (**B**). ns; non-significant difference.

3.1.7 The correlation between the proposed EEG and neurological behaviors

Since the neurological behaviors had a slight tendency of changing, the relationship between the neurological behaviors (working memory and Kratom dependent score rating) and the proposed EEG features in LKU responding to the doses of Kratom use were investigated (**Figure 3.9A**). From the statistical test with spearman's rank, Kratom dependent score was significantly correlated with age and the proposed EEG with PVF in the alpha band (**Figure 3.9B**). To control the confounding effect of age, the partial rank was performed. We found that the Kratom dependent score was significantly negatively correlated with the proposed EEG with PVF in the alpha band after the partial out age effect. The results indicated that the Kratom dependence was related to the proposed EEG especially the PVF in the alpha band.

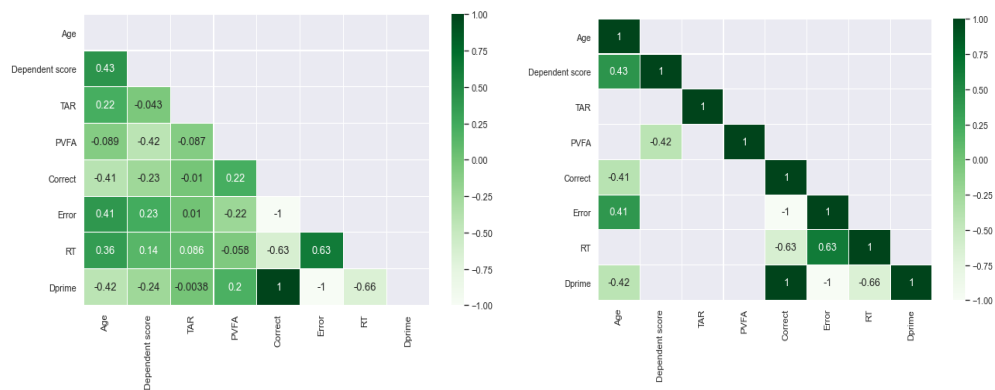


Figure 3.9 The correlation between the proposed EEG and neurological behaviors in cognitive tasks with working memory and Kratom dependent score rating using spearman's rank (A). The parameters provide statistically significant correlation (B).

3.1.8 The EEG features represented a more sensitive biomarker over than the HRV in LKU

The participants who had a history of cardiac disease were excluded. The final samples for HRV assessment were 38 (19 controls and 19 LKU). The characteristics of HRV in different domains were shown in the representative subjects (**Figure 3.10A**) and overall (**Figure 3.10B**) between groups. The LKU showed a lower LFn and higher HFn than the controls in the frequency domain while other domains showed a similar pattern between groups. The statistical multiple comparisons across HRV domains (RMSSD, SDNN, Mean_NN, LFn, HFn, LFn/HFn, SD1, SD2, SD1/SD2) between groups were tested by MANOVA with age and BMI as confounding effects or covariates because they were related to HRV parameters. The multivariate effect revealed no significant difference between groups as well as separated groups based on age (**Table 3.5**), and doses of Kratom use (**Table 3.6**) in corresponding groups comparison in the proposed EEG. Since the overall effects did not show statistically significant difference, the following ANOVAs in individual HRV indices did not be further conducted.

On the other hand, the multivariate test across the proposed EEG features provided a significant difference between groups based on the categorized age and doses of Kratom use equal to HRV samples. The results indicated that the EEG features produced a more sensitive

biomarker in LKU. Therefore, the proposed EEG features were the input features in the continued path analysis and classification tasks to prove the significant statistical test.

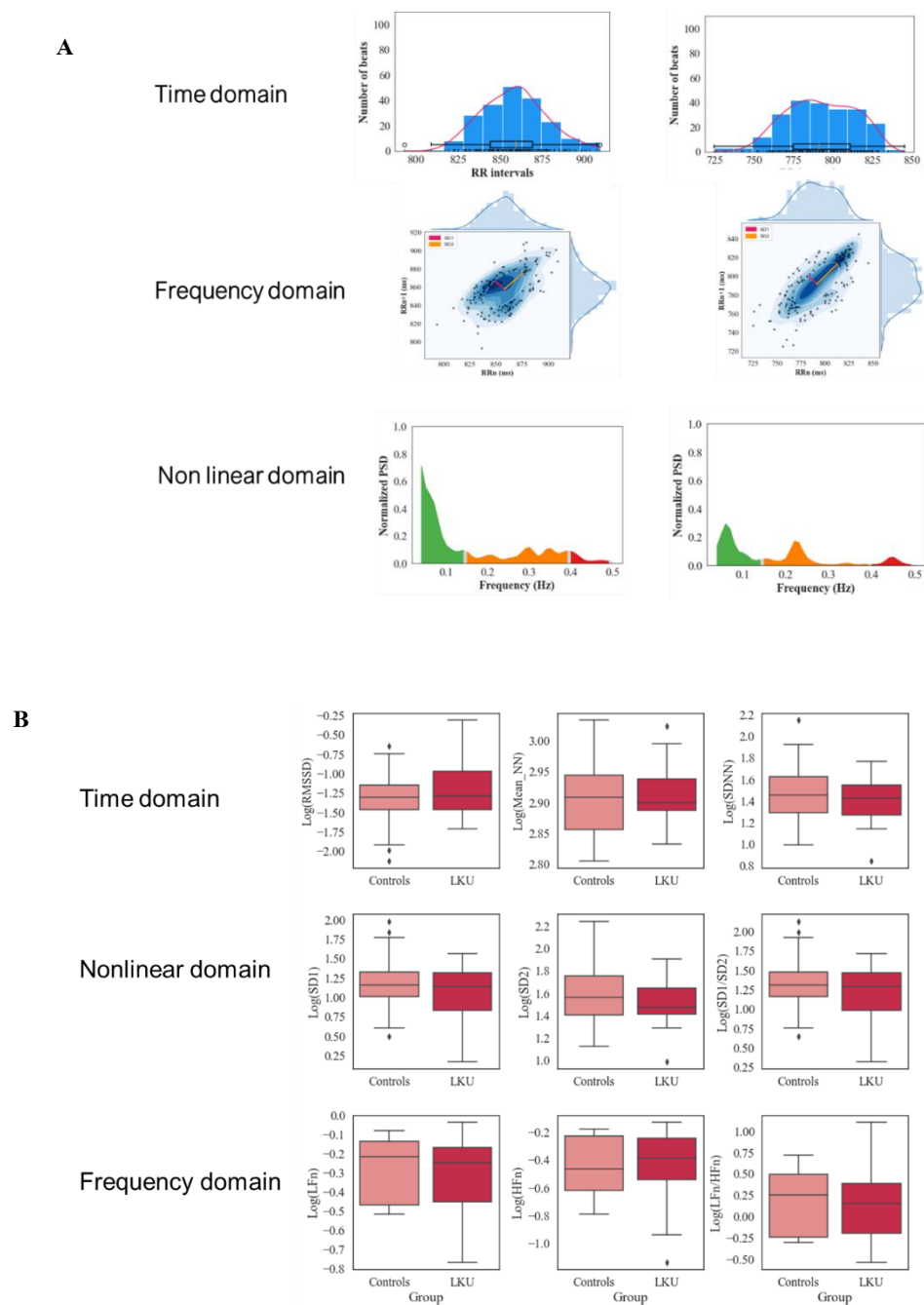


Figure 3.10 The comparison of ultra-short HRV in time, frequency, and non-linear domains between the control (n=19) and LKU group (n=19), illustrated by the representative subjects (A) and overall (B)

Table 3.5 The comparison between the control and LKU groups based on age (> 50 years old) across multiple features in domains of HRV and EEG tested by MANOVA

Domain	Control (n)	LKU (n)	Wilk's lambda	df, error	F-test	p-value
HRV	7	11	0.695	7, 9	0.563	0.769
EEG	7	11	0.524	3, 14	4.235	0.025*

Note: HRV features: RMSSD, SDNN, Mean_NN, LFn, HFn, LFn/HFn, SD1, SD2, SD1/SD2

EEG features: TAR [TP9], TAR [TP10], and averaged TAR. * $p < 0.05$.

Table 3.6 The comparison based on daily doses of Kratom use between the LKU those with low to high doses (LTH) and very high dose (VH) across multiple features in domains of HRV and EEG tested by MANOVA

Domain	LTH (n)	VH (n)	Wilk's lambda	df, error	F-test	p-value
HRV	9	10	0.574	7, 9	0.956	0.512
EEG	9	10	0.456	4,13	3.883	0.027*

Note: HRV features: RMSSD, SDNN, Mean_NN, LFn, HFn, LFn/HFn, SD1, SD2, SD1/SD2

EEG features: TAR [TP9], TAR [TP10], and averaged TAR, PVF in alpha band. * $p < 0.05$.

3.2 Path analysis

To characterize the causal relationship across the above EEG features, neurological behavior, and relevant factors in LKU, path analysis was conducted (**Figure 3.11**). We tested the hypothesis to prove the statistical analysis that the quantity of daily Kratom leaves consumption directly turned in the enhancement of TAR ($\beta = 0.110$, $SE = 0.038$, $p = 0.005$) and reduced the PVF in the alpha band ($\beta = -0.020$, $SE = 0.010$, $p = 0.044$), contributing to increasing in Kratom dependence score ($\beta = -13.373$, $SE = 4.828$, $p = 0.006$). The overall of model showed a good fit (Fit indices: $RMSEA < 0.05$ $SRMR < 0.05$, and $CFI > 0.90$, $TLI > 0.95$).

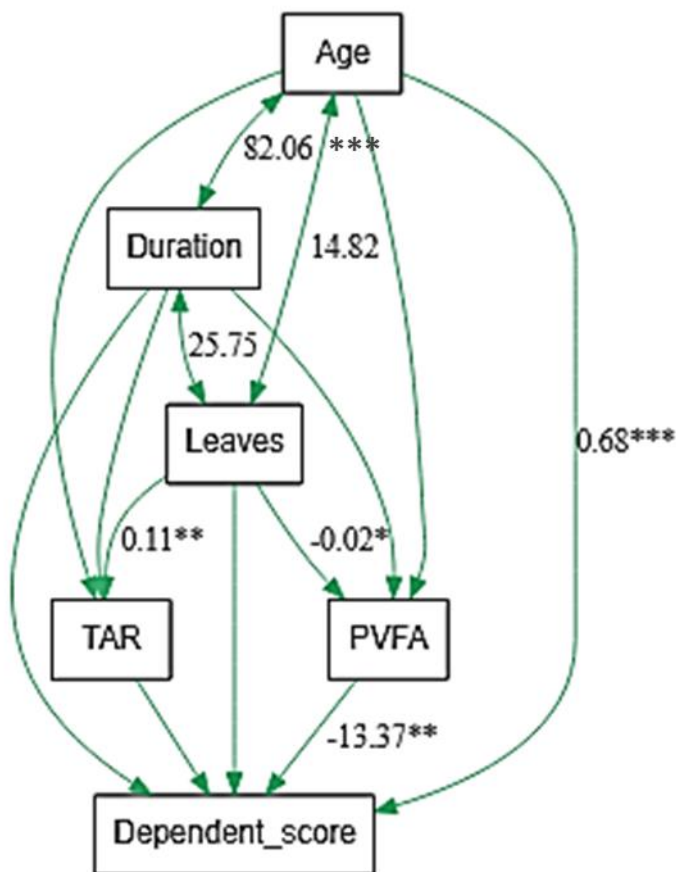


Figure 3.11 The illustration of path analysis for causal relationship in LKU ($n = 24$) among relevant factors (age, duration, and the daily Kratom leaves consumption), the proposed EEG features (TAR, PVFA) and neurological behaviors with Kratom dependent score rating.

3.3 Classification results

The statistical significance based on the proposed EEG features were as the input features to perform binary classification based on different age groups and doses of Kratom use as follows:

- **The classification between the control and LKU group in various age ranges**

The binary classification results between groups were separately performed in non-divided ages, ≤ 50 and > 50 years of age. The results of classification performances were summarized in (Table 3.7). The age range over 50 years old yielded higher classification performances more than non-divided age and ≤ 50 years of age. When we considered in each individual the proposed EEG feature, the averaged TAR achieved a higher classification output over their electrode positions classified by RF. To obtain more robust the classification performances, the feature combinations were acquired and produced the highest performance scores by using the SVM classifier with accuracy: $71.67\% \pm 7.05$, F1-score: $69.67\% \pm 9.51$, sensitivity: $70.00\% \pm 11.06$, specificity: $80.00\% \pm 11.06$.

The capability of SVM to separate the LKU over 50 years old from the control group using features combination was plotted in the ROC curve (Figure 3.12A) and confusion matrix (Figure 3.12B). The ROC curve showed the classification performance in each iteration of k-fold cross-validation and provided the mean area under the curve (AUC) with 0.74 ± 0.19 . The confusion matrix displayed the highest sensitivity of the LKU group whereas the control group was frequently misclassified.

Table 3.7 The classification results for LKU classifying from the controls in different age ranges, represented by the mean percentage \pm se of accuracy (Acc), F1-score (F1), sensitivity (Sens), and specificity (Spec). TAR stands for theta/alpha ratio.

Classifier	Non divided age (control n =24, LKU n=28)				≤ 50 (y) of age (control n =12, LKU n=9)				> 50 (y) of age (control n =12, LKU n=19)			
	Acc	F1	Sens	Spec	Acc	F1	Sens	Spec	Acc	F1	Sens	Spec
TAR TP9, TP10												
RF	56.67 \pm 7.64	57.29 \pm 10.56	63.33 \pm 12.62	61.67 \pm 10.26	51.67 \pm 7.64	23.33 \pm 12.22	30.00 \pm 15.28	70.00 \pm 13.33	68.83 \pm 8.43	65.67 \pm 8.40	70.00 \pm 11.06	50.00 \pm 14.91
SVM	44.00 \pm 5.62	33.38 \pm 8.46	35.00 \pm 10.08	58.33 \pm 11.98	45.00 \pm 5.00	6.67 \pm 6.67	10.00 \pm 10.00	75.00 \pm 13.44	58.33 \pm 10.90	48.33 \pm 14.15	45.00 \pm 13.84	85.00 \pm 10.67
knn	55.67 \pm 6.89	55.90 \pm 8.52	58.33 \pm 9.70	56.67 \pm 7.93	43.33 \pm 9.03	10.00 \pm 10.00	10.00 \pm 10.00	70.00 \pm 13.33	60.83 \pm 9.79	61.00 \pm 11.27	65.00 \pm 13.02	60.00 \pm 14.53
LR	64.00 \pm 6.36	67.21 \pm 6.36	75.00 \pm 9.04	51.67 \pm 13.25	48.33 \pm 7.64	11.67 \pm 7.88	20.00 \pm 13.33	70.00 \pm 15.28	55.00 \pm 8.62	54.67 \pm 10.16	55.00 \pm 11.67	60.00 \pm 14.53
Averaged TAR												
RF	55.33 \pm 6.89	50.88 \pm 9.28	53.33 \pm 12.37	65.00 \pm 10.96	51.67 \pm 13.02	43.33 \pm 14.95	50.00 \pm 16.67	50.00 \pm 14.91	64.17 \pm 9.30	69.00 \pm 9.08	75.00 \pm 11.18	50.00 \pm 14.91
SVM	44.00 \pm 4.47	24.00 \pm 10.10	53.00 \pm 13.56	70.00 \pm 8.89	46.67 \pm 11.86	10.00 \pm 10.00	10.00 \pm 10.00	70.00 \pm 15.28	51.67 \pm 5.24	53.33 \pm 6.48	50.00 \pm 7.45	60.00 \pm 14.53
knn	53.33 \pm 7.50	46.00 \pm 10.00	46.67 \pm 12.37	68.33 \pm 9.11	56.67 \pm 9.03	26.67 \pm 13.88	30.00 \pm 15.28	80.00 \pm 11.06	60.83 \pm 9.79	61.00 \pm 11.27	65.00 \pm 13.03	60.00 \pm 14.53
LR	56.00 \pm 7.50	54.07 \pm 10.68	63.33 \pm 13.56	51.67 \pm 9.77	65.00 \pm 10.67	30.00 \pm 15.28	30.00 \pm 15.38	90.00 \pm 10.00	51.67 \pm 7.22	54.00 \pm 9.65	60.00 \pm 12.47	40.00 \pm 14.53
Feature combination												
RF	57.67 \pm 5.67	58.21 \pm 7.63	63.33 \pm 10.48	58.33 \pm 10.61	53.33 \pm 9.23	20.00 \pm 13.33	20.00 \pm 13.33	80.00 \pm 11.06	60.83 \pm 8.43	65.67 \pm 8.40	70.00 \pm 11.06	50.00 \pm 14.91
SVM	46.00 \pm 4.99	39.00 \pm 9.30	46.67 \pm 13.3	53.33 \pm 12.12	40.00 \pm 10.00	6.67 \pm 6.67	10.00 \pm 10.00	60.00 \pm 16.33	71.67 \pm 7.05	69.67 \pm 9.51	70.00 \pm 11.06	80.00 \pm 11.06
knn	53.67 \pm 5.63	50.90 \pm 7.44	53.33 \pm 11.33	61.67 \pm 8.98	61.67 \pm 6.60	26.67 \pm 13.88	30.00 \pm 15.28	90.00 \pm 6.67	60.83 \pm 9.79	61.00 \pm 11.27	65.00 \pm 13.02	60.00 \pm 14.53
LR	60.00 \pm 3.94	64.93 \pm 3.55	71.67 \pm 7.05	48.33 \pm 13.25	65.00 \pm 10.67	30.00 \pm 15.28	30.00 \pm 15.28	90.00 \pm 10.00	48.33 \pm 8.77	45.00 \pm 10.84	45.00 \pm 11.67	65.00 \pm 15.00

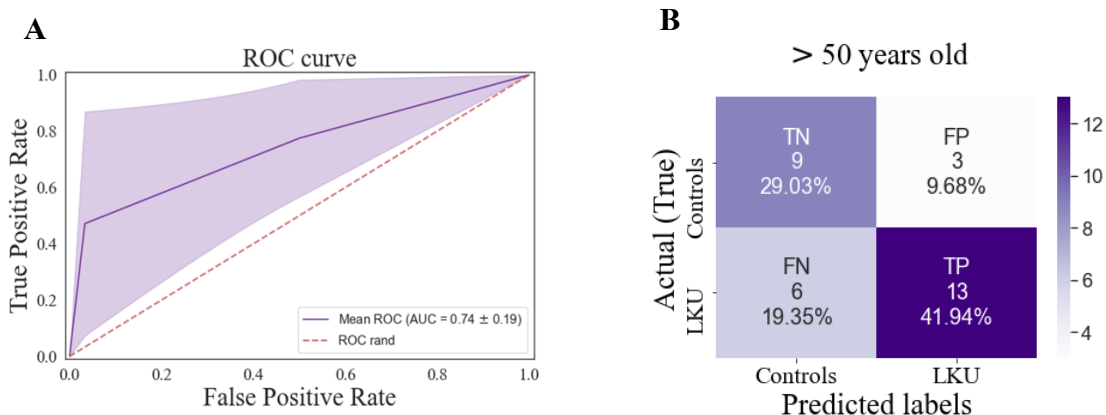


Figure 3.12 The ROC curve (A) and the confusion matrix (B) with SVM by using features combination to classify LKU (n = 12) from the controls (n = 19) in the age range of 50 years old.

- **The classification between the low to high doses and very high doses of Kratom consumption**

The differentiation between the low to high doses and very high doses of Kratom consumption was further classified (**Table 3.8**). Based on the individual EEG features, the averaged TAR yielded a better classification performance using the LR model over their electrodes position and PVF in the alpha band. The TAR features provided the better classification performances than PVF in the alpha band with the same model (LR), however, the classification scores in the SVM model were efficiently improved when used the feature combinations by including the feature of PVF in the alpha band with accuracy: 83.33% ± 10.24, F1-score: 84.67% ± 10.09, sensitivity: 90.00% ± 10.00, and specificity: 75% ± 13.44

ROC curve of the classification performance on LKU those with different doses yielded 0.81 ± 0.17 ACU obtained by SVM using features combination (**Figure 3.13A**). The SVM classifier showed the lower misclassification in both low to high doses and very high doses of Kratom consumption, represented by the lower false negative and positive prediction in the confusion matrix (**Figure 3.13B**).

Table 3.8 The classification results for LKU classifying between low to high doses (n=14) and very high dose consumption (n=14), represented by the mean percentage \pm se of accuracy (Acc), F1-score (F1), sensitivity (Sens), and specificity (Spec). TAR and PVFA stand for theta/alpha ratio and power variance function in the alpha band.

Classifier	Acc	F1	Sens	Spec
TAR TP9, TP10				
RF	66.67 \pm 9.94	58.00 \pm 13.37	65.00 \pm 15.00	65.00 \pm 13.02
SVM	58.33 \pm 9.70	46.33 \pm 13.47	50.00 \pm 14.91	65.00 \pm 15.00
knn	70.00 \pm 10.48	68.00 \pm 12.24	75.00 \pm 13.44	70.00 \pm 13.33
LR	73.33 \pm 9.69	74.67 \pm 9.68	85.00 \pm 10.67	65.00 \pm 13.02
Averaged TAR				
RF	75.00 \pm 5.69	64.67 \pm 11.72	70.00 \pm 13.33	80.00 \pm 11.06
SVM	70.00 \pm 7.37	58.00 \pm 13.37	60.00 \pm 14.53	80.00 \pm 13.33
knn	73.33 \pm 9.69	74.67 \pm 9.68	75.00 \pm 11.18	75.00 \pm 13.44
LR	81.67 \pm 6.31	71.33 \pm 12.65	75.00 \pm 13.44	85.00 \pm 10.67
PVFA				
RF	50.00 \pm 7.03	41.00 \pm 11.46	55.00 \pm 15.72	45.00 \pm 15.72
SVM	65.00 \pm 5.24	47.00 \pm 13.34	60.00 \pm 16.33	50.00 \pm 16.67
knn	45.00 \pm 8.62	38.33 \pm 11.40	45.00 \pm 13.84	50.00 \pm 14.91
LR	40.00 \pm 7.93	0.00 \pm 0.00	0.00 \pm 0.00	80.00 \pm 13.33
Feature combination				
RF	83.33 \pm 10.24	84.67 \pm 10.09	90.00 \pm 10	75.00 \pm 13.44
SVM	83.33 \pm 10.24	84.67 \pm 10.09	90.00 \pm 10	75.00 \pm 13.44
knn	70.00 \pm 10.48	68.00 \pm 12.24	70.00 \pm 13.33	75.00 \pm 13.44
LR	73.33 \pm 9.69	68.00 \pm 12.24	70.00 \pm 13.33	75.00 \pm 13.44

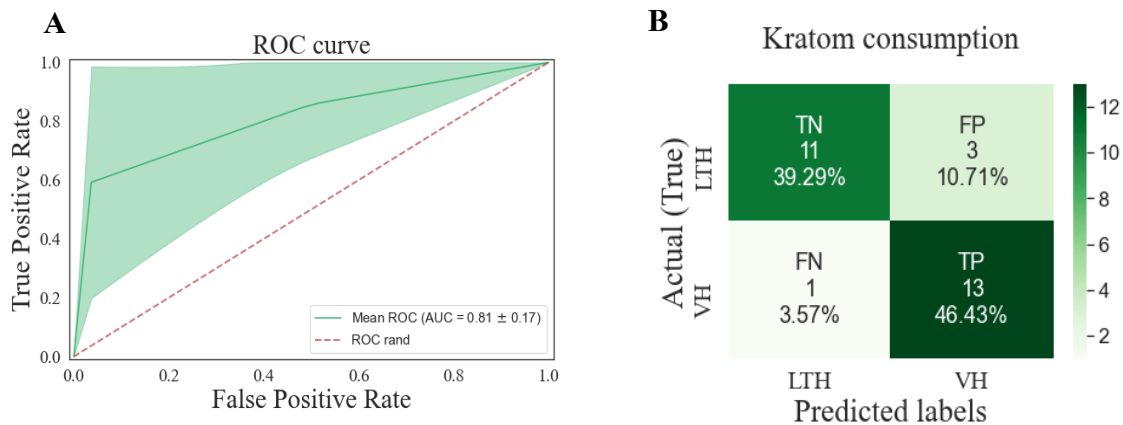


Figure 3.13 The ROC curve (A) and the confusion matrix (B) with SVM by using features combination to classify LKU those with VH (n = 14) from those with LTH (n = 14). Low to high doses (LTH); Very high dose (VH).

CHAPTER 4

DISCUSSIONS

In this study, we attempted to initiate the investigation of neurological biomarkers in LKU measured by EEG and HRV activity, compared to the controls. The neurological biomarkers in different factors, such as age, duration, quantity, and a daily dose of Kratom use were also examined. In addition, neurological behavior was investigated whether it is sensitive to changes in neurological biology. The statistically significant biomarkers were further proved with the path analysis and machine-learning classification.

The present findings were addressed according to our hypothesis that the proposed EEG features (TAR and PVF in the alpha band) showed a more sensitive biomarker over HRV in LKU. The TAR features (at both electrodes and their average) were a remarkably significant increase in LKU, compared to the control group in the same age range > 50 years of age. Furthermore, LKU those who consumed at very doses (≥ 10 leaves per day) significantly increased TAR and decreased PVF in the alpha band, compared to those with low to high doses (< 10 leaves per day). We found that the neurological behavior with the Kratom dependence score rating provided a tendency of change in different doses of Kratom use corresponding to the changing of EEG pattern, particularly in PVF in the alpha band, and produced a significantly negative correlation between both of them. The changing of the proposed EEG features was the direct effect of the quantity of Kratom use. Finally, the binary classifications were able to classify 1) the LKU from the control with the same age range > 50 years old, and 2) LKU who those consumed Kratom at a very high doses from those with low to high doses.

The physiological changes in response to long-term Kratom consumption were more sensitive to EEG activity than HRV measurement at the resting state by which the TAR and PVF in the alpha band were able to represent the EEG biomarker in LKU. It was feasibly that the target of opioids action is mainly represented in the brain (Farah et al., 2016). Mitragynine and its alkaloid such as 7-hydroxy mitragynine were able to passively cross the blood-brain barrier (BBB) interact with the efflux transporters P-glycoprotein (Manda et al., 2014). It has been also reported that chronic Kratom users might present an accumulation of mitragynine (the active

compound of Kratom) in the brain than plasma caused by the saturated protein-mediated efflux (Ya et al., 2021). In addition, HRV levels greatly fluctuated throughout the day and also responded differently among individuals, indicating the personal homeostasis (de Vries et al., 2022). According to the evidence, long-term kratom users may be more responsive to the changes in EEG features than HRV.

The proposed EEG feature of TAR (both electrodes and their average) was significantly increased in LKU compared to the control group in the same age range > 50 years. Our results suggested that the increased TAR level was the result of age-related to the quantity of Kratom consumption as older LKU favorably consumed a larger amount of kratom leaves daily which was the major effect associated with the TAR level. In the previous study, the TAR was commonly involved in age varying (Trammell et al., 2017), and also related to neurodegenerative disease with cognitive impairment in Parkinson's disease (Orso et al., 2020). However, the TAR level in LKU was not correlated with cognitive tasks tested by working memory performances. Our behavioral results were similar to a previous study in that regular Kratom users did not show working memory (D. Singh et al., 2019). However, other cognitive tests such as paired associates learning might be used. This task showed lower performance in regular kratom users with kratom tea form than non-kratom users (D. Singh et al., 2019). Our statistical results were addressed by the causal relationship in path analysis that age not directly affects TAR level considered by non-significant path coefficient between them. Thus, the different TAR levels between the control and LKU groups were the indirect effects of age-related to the quantity of Kratom leaves consumption. Moreover, the binary classification results also confirmed that the LKU group was kindly differentiated from the control group in the age range over 50 years old with the TAR features and were more robust when used their combination features, classified by the SVM model.

Since the TAR level was highly related to the quantity of Kratom use, this feature was also evaluated in different daily doses of Kratom use. The LKU those who consumed at very high doses showed an increase in the TAR and a decrease in PVF in alpha band levels, compared to those with low to high doses. The path analysis confirmed the statistical results that the changing in TAR and PVF in alpha band levels were a significant direct effect of the quantity of Kratom use. The results were supported by the classification task that the proposed EEG features with

their combinations using the SVM classifier yielded the highest classification result to separate the LKU who consumed at a very high dose from those who consumed at low to high doses. The outperformed SVM classifier in the present study was in line with various studies that SVM had better predictive power since it can penalize training loss by a loss function, providing robust overfitting protection (Yoon et al., 2011). Moreover, using the feature combination approach yielded a higher classification performance due to obtaining the strength of multiple complementary features (Hou et al., 2011).

As our study was initiated to detect the EEG-biomarker in LKU which still missing the empirical evidence in human research. The possible way to differentiate our results that were in the animal study. The EEG oscillation in LKU was different from rats after being administrated to the chronic mitragynine in dose-dependent exposure.

An animal study showed the EEG pattern changed independent neighboring frequency bands (increased delta and decreased alpha) that reflected delayed response between the dopaminergic and cholinergic activity caused by high dose of mitragynine exposure (Farah Wahida Suhaimi et al., 2021). In controversy, our results exhibited EEG pattern altered dependent neighboring frequency bands (increased theta and decreased alpha). The incongruent results could feasibly explain that LKU were exposed to synergistic compounds effect of the plant as a whole, and lower dose of daily use compared to an animal study.

Compared to a human study, the increased theta and decreased alpha band in LKU with a very high dose corresponded to the common EEG response in opioid users with increased theta and decreased alpha) (Phillips et al., 1994; Wang et al., 2016). The change in these frequencies in our results similar to that of opioid users may be a result of the very high doses of kratom consumption which exhibited opioid-like effects.

Furthermore, the LKU with very high dose consumption trended to have a higher Kratom dependence score than those with low to high doses. Our result is supported by a previous study that Kratom dependence depended on the quantity of Kratom use (D. Singh et al., 2017). Moreover, the Kratom dependence score in our study negatively correlated with the PVF in the alpha band but did not correlate with the TAR level. The result was also in line with path analysis that the Kratom dependence score was a negatively causal relationship between the PVF in the alpha band and was TAR-independent. Our results indicated that the tendency of higher Kratom

dependence in LKU with those at very high doses may be a more responsive response to the decreased PVF in the alpha band than TAR. The results were consistent with the previous study that PVF was more sensitive to detecting the changing in brain activity than the traditional PSD. Since the PVF sensitive to detect the amplitude increase of specific frequencies while PSD detected the constant of frequency (Ueda et al., 2016). The negative correlation between PVF in the alpha band and kratom dependence in our results may be the result of a change in dopamine-related alpha activity. Since the previous study reported that the alpha activity was associated with dopamine modulation (Farah et al., 2021), and the decreased dopamine level in the mesolimbic pathway was found during the drug dependence phase (Listos et al., 2019). The present preliminary results were found to encourage for further investigation that would propose features in other conditions, such as cue-induced craving, to confirm the present results.

The current pilot study was not without its limitations. One of them was 1) small sample size for HRV assessment and shorter HRV recording, 2) low-channel EEG recording for data collection, and 3) non-recruitment of short-term Kratom users. Thus, future research needs a larger sample size for HRV to confirm and extend HRV results and a standard length for short-term HRV analysis to obtain a more stable RR interval measurement. In addition, measuring EEG activity from the dozen channels with a medical-grade system would yield the other important EEG biomarkers. Finally, recruiting short-term Kratom users would benefit more from early phase detection.

CHAPTER 5

CONCLUSION

This study was the first investigation of the neurological biomarkers in LKU. The proposed EEG features (TAR and PVF) extracted from MUSE headband recording and ultra-short HRV assessment (3-minutes ECG recording) in LKU were compared to the controls. These neurological features were also investigated in certain factors: age, duration, the quantity of kratom use, and different doses. In addition, the neurological behaviors (WM and Kratom dependent score) were investigated as well. The statistical significance-based features were proved by 1) path analysis for evaluation of the causal relationship across relevant factors/neurological behaviors, and 2) machine-learning technique for binary classification. Our findings are the first to our knowledge to highlight as follows:

- 1) EEG activity was more sensitive to physiological changes in response to long-term kratom ingestion, by which the TAR and PVF in the alpha band were able to reflect the EEG biomarker in LKU.
- 2) The different TAR levels between the control and LKU groups in the age range > 50 years old was an indirect effect of age-related to the quantity of Kratom leaves consumption.
- 3) The increased TAR and decreased PVF in alpha were a direct effect of the quantity of kratom consumption and showed between group different doses.
- 4) The tendency of higher Kratom dependence in LKU with those at VH might be a response to the decreased PVF in alpha due to their negative association with each other.
- 5) The binary classification with SVM classifier outperformed to separate LKU those with LTH from those with VH by using features combination.

Taken together, our findings indicated that the TAR and PVF in the alpha band extracted from the portable EEG recording were affordable biomarkers for LKU determination.

CHAPTER 6

APPLICATIONS

The present proposed to utilize these features (TAR at TP9, TP10 and their average, including PVFA)-based SVM model to monitor LKU who consumed excessive kratom that might develop kratom dependence. However, this approach focused on the accuracy of the model prediction in dichotomous outcomes (0: LKU with low to high doses, 1: LKU with very high dose) that would not identify the level of risk of the high dose kratom consumption.

The finding cut-off point method is widely used for classification of the outcome in distributional counting: 0= “lower than cut-off point” and 1 = “greater than or equal to cut-off point” to diagnose the continuous outcome (the power of each sub-band frequency component). The optimal cut-off point cannot indicate tell us to know the risk level of high dose kratom consumption into three levels: low, moderate, and high risk.

Therefore, the present application with feature-based machine learning combined with the finding cut-off point method would have high potential to be applied in health innovation.

REFERENCES

- Abdullah, M. F. I. L. Bin, Singh, D., Narayanan, S., Rahim, A. A., & Vicknasingam, B. (2019). Socio-demographic Characteristics, Kratom Use and Quality of Life (QoL) of Regular Kratom (*Mitragyna speciosa* Korth.) Users. *Malaysian Journal of Medicine and Health Sciences*.
- Anand, A., & Hosanagar, A. (2022). The Addictive Potential and Challenges with Use of the “Herbal Supplement” Kratom: A Case Report and Literature Review. *Pain Medicine*, 23(1), 4–9.
- Bartels, R., Neumamm, L., Peçanha, T., & Carvalho, A. R. S. (2017). SinusCor: An advanced tool for heart rate variability analysis. *BioMedical Engineering Online*.
<https://doi.org/10.1186/s12938-017-0401-4>
- Biasiucci, A., Franceschiello, B., & Murray, M. M. (2019). Electroencephalography. In *Current Biology*. <https://doi.org/10.1016/j.cub.2018.11.052>
- Bollen, K. A. (1989). *Structural equations with latent variables*. Wiley.
- Browne, M. W., & Cudeck, R. (1992). Alternative ways of assessing model fit. *Sociological Methods & Research*, 21(2), 230–258.
- Cao, P., Ye, B., Yang, L., Lu, F., Fang, L., Cai, G., Su, Q., Ning, G., & Pan, Q. (2020). Preprocessing Unevenly Sampled RR Interval Signals to Enhance Estimation of Heart Rate Deceleration and Acceleration Capacities in Discriminating Chronic Heart Failure Patients from Healthy Controls. *Computational and Mathematical Methods in Medicine*.
<https://doi.org/10.1155/2020/9763826>
- Castaldo, R., Montesinos, L., Melillo, P., James, C., & Pecchia, L. (2019). Ultra-short term HRV features as surrogates of short term HRV: A case study on mental stress detection in real life. *BMC Medical Informatics and Decision Making*. <https://doi.org/10.1186/s12911-019-0742-y>
- Charoenratana, S., Anukul, C., & Aramrattana, A. (2021). Attitudes towards Kratom use, decriminalization and the development of a community-based Kratom control mechanism in Southern Thailand. *International Journal of Drug Policy*.
<https://doi.org/10.1016/j.drugpo.2021.103197>
- Chen, Y. S., Lu, W. A., Pagaduan, J. C., & Kuo, C. D. (2020). A novel smartphone app for the

- measurement of ultra-short-term and short-term heart rate variability: Validity and reliability study. *JMIR MHealth and UHealth*. <https://doi.org/10.2196/18761>
- Chittrakarn, S., Sawangjaroen, K., Prasetho, S., Janchawee, B., & Keawpradub, N. (2008). Inhibitory effects of kratom leaf extract (*Mitragyna speciosa* Korth.) on the rat gastrointestinal tract. *Journal of Ethnopharmacology*. <https://doi.org/10.1016/j.jep.2007.11.032>
- Coroiu, A. M. (2016). Tuning model parameters through a Genetic Algorithm approach. *Proceedings - 2016 IEEE 12th International Conference on Intelligent Computer Communication and Processing, ICCP 2016*. <https://doi.org/10.1109/ICCP.2016.7737135>
- Dadu, K. S., & Deka, P. C. (2016). *Applications of Wavelet Transform Technique in Hydrology—A Brief Review*. https://doi.org/10.1007/978-3-319-40195-9_19
- de Vries, H., Kamphuis, W., van der Schans, C., Sanderman, R., & Oldenhuis, H. (2022). Trends in Daily Heart Rate Variability Fluctuations Are Associated with Longitudinal Changes in Stress and Somatisation in Police Officers. *Healthcare (Switzerland)*. <https://doi.org/10.3390/healthcare10010144>
- Dedeo, M., & Garg, M. (2021). Early Detection of Pediatric Seizures in the High Gamma Band. *IEEE Access*. <https://doi.org/10.1109/ACCESS.2021.3087782>
- Delorme, A., & Makeig, S. (2004). EEGLAB: An open source toolbox for analysis of single-trial EEG dynamics including independent component analysis. *Journal of Neuroscience Methods*. <https://doi.org/10.1016/j.jneumeth.2003.10.009>
- Domnic, G., Narayanan, S., Mohana-Kumaran, N., & Singh, D. (2022). Kratom (*Mitragyna speciosa* Korth.) an overlooked medicinal plant in Malaysia. In *Journal of Substance Use*. <https://doi.org/10.1080/14659891.2021.1885515>
- Eastlack, S. C., Cornett, E. M., & Kaye, A. D. (2020). Kratom—Pharmacology, Clinical Implications, and Outlook: A Comprehensive Review. *Pain and Therapy*. <https://doi.org/10.1007/s40122-020-00151-x>
- Estévez, M., Machado, C., Leisman, G., Estévez-Hernández, T., Arias-Morales, A., Machado, A., & Montes-Brown, J. (2016). Spectral analysis of heart rate variability. *International Journal on Disability and Human Development*. <https://doi.org/10.1515/ijdhhd-2014-0025>
- Fahimi, G., Tabatabaei, S. M., Fahimi, E., & Rajebi, H. (2017). Index of theta/alpha ratio of the

- quantitative electroencephalogram in Alzheimer's disease: A case-control study. *Acta Medica Iranica*.
- Fan, Y., Chen, J., Shirkey, G., John, R., Wu, S. R., Park, H., & Shao, C. (2016). Applications of structural equation modeling (SEM) in ecological studies: an updated review. In *Ecological Processes*. <https://doi.org/10.1186/s13717-016-0063-3>
- Fraivan, L., Lweesy, K., Khasawneh, N., Wenz, H., & Dickhaus, H. (2012). Automated sleep stage identification system based on time-frequency analysis of a single EEG channel and random forest classifier. *Computer Methods and Programs in Biomedicine*. <https://doi.org/10.1016/j.cmpb.2011.11.005>
- Graves, J. M., Dilley, J. A., Terpak, L., Brooks-Russell, A., Whitehill, J. M., Klein, T. A., & Liebelt, E. (2021). Kratom exposures among older adults reported to US poison centers, 2014–2019. *Journal of the American Geriatrics Society*, *69*(8), 2176–2184.
- Grissom, R. J., & Kim, J. J. (2012). Effect sizes for research: Univariate and multivariate applications, second edition. In *Effect Sizes for Research: Univariate and Multivariate Applications, Second Edition*. <https://doi.org/10.4324/9780203803233>
- Haatveit, B. C., Sundet, K., Hugdahl, K., Ueland, T., Melle, I., & Andreassen, O. A. (2010). The validity of d prime as a working memory index: Results from the Bergen n-back task. *Journal of Clinical and Experimental Neuropsychology*, *32*(8), 871–880. <https://doi.org/10.1080/13803391003596421>
- Hanapi, N. A., Chear, N. J. Y., Azizi, J., & Yusof, S. R. (2021). Kratom Alkaloids: Interactions with Enzymes, Receptors, and Cellular Barriers. *Frontiers in Pharmacology*, *12*.
- Hasan, M. J., Kim, J., Kim, C. H., & Kim, J. M. (2020). Health state classification of a spherical tank using a hybrid bag of features and K-Nearest neighbor. *Applied Sciences (Switzerland)*. <https://doi.org/10.3390/app10072525>
- Hassan, Z., Bosch, O. G., Singh, D., Narayanan, S., Kasinather, B. V., Seifritz, E., Kornhuber, J., Quednow, B. B., & Müller, C. P. (2017). Novel psychoactive substances-recent progress on neuropharmacological mechanisms of action for selected drugs. In *Frontiers in Psychiatry*. <https://doi.org/10.3389/fpsy.2017.00152>
- Hassan, Z., Muzaimi, M., Navaratnam, V., Yusoff, N. H. M., Suhaimi, F. W., Vadivelu, R., Vicknasingam, B. K., Amato, D., von Hörsten, S., Ismail, N. I. W., Jayabalan, N., Hazim,

- A. I., Mansor, S. M., & Müller, C. P. (2013). From Kratom to mitragynine and its derivatives: Physiological and behavioural effects related to use, abuse, and addiction. *Neuroscience and Biobehavioral Reviews*, 37(2), 138–151.
<https://doi.org/10.1016/j.neubiorev.2012.11.012>
- Hassan, Z., Suhaimi, F. W., Ramanathan, S., Ling, K. H., Effendy, M. A., Müller, C. P., & Dringenberg, H. C. (2019). Mitragynine (Kratom) impairs spatial learning and hippocampal synaptic transmission in rats. *Journal of Psychopharmacology*.
<https://doi.org/10.1177/0269881119844186>
- Hayano, J. (2016). Introduction to heart rate variability. In *Clinical Assessment of the Autonomic Nervous System*. https://doi.org/10.1007/978-4-431-56012-8_7
- Ho, C. N., Fu, P. H., Chen, J. Y., Hung, K. C., Chang, J. H., Peng, C. K., & Yang, A. C. (2020). Heart rate variability and surgical pleth index under anesthesia in poor and normal sleepers. *Journal of Clinical Monitoring and Computing*. <https://doi.org/10.1007/s10877-019-00450-5>
- Hou, J., Zhang, B. P., Qi, N. M., & Yang, Y. (2011). Evaluating feature combination in object classification. *Lecture Notes in Computer Science (Including Subseries Lecture Notes in Artificial Intelligence and Lecture Notes in Bioinformatics)*. https://doi.org/10.1007/978-3-642-24031-7_60
- Ismail, N. I. W., Jayabalan, N., Mansor, S. M., Müller, C. P., & Muzaimi, M. (2017). Chronic mitragynine (kratom) enhances punishment resistance in natural reward seeking and impairs place learning in mice. *Addiction Biology*. <https://doi.org/10.1111/adb.12385>
- Jiang, T., Gradus, J. L., & Rosellini, A. J. (2020). Supervised Machine Learning: A Brief Primer. *Behavior Therapy*. <https://doi.org/10.1016/j.beth.2020.05.002>
- Kapp, F. G., Maurer, H. H., Auwärter, V., Winkelmann, M., & Hermanns-Clausen, M. (2011). Intrahepatic Cholestasis Following Abuse of Powdered Kratom (*Mitragyna speciosa*). *Journal of Medical Toxicology*, 7(3), 227–231. <https://doi.org/10.1007/s13181-011-0155-5>
- Karmakar, C. K., Khandoker, A. H., Gubbi, J., & Palaniswami, M. (2009). Complex correlation measure: a novel descriptor for Poincaré plot. *Biomedical Engineering Online*.
<https://doi.org/10.1186/1475-925X-8-17>
- Kinnunen, H., Rantanen, A., Kentt, T., & Koskim ki, H. (2020). Feasible assessment of recovery

- and cardiovascular health: Accuracy of nocturnal HR and HRV assessed via ring PPG in comparison to medical grade ECG. *Physiological Measurement*.
<https://doi.org/10.1088/1361-6579/ab840a>
- Krigolson, O. E., Williams, C. C., & Colino, F. L. (2017). Using portable EEG to assess human visual attention. *Lecture Notes in Computer Science (Including Subseries Lecture Notes in Artificial Intelligence and Lecture Notes in Bioinformatics)*. https://doi.org/10.1007/978-3-319-58628-1_5
- Krigolson, O. E., Williams, C. C., Norton, A., Hassall, C. D., & Colino, F. L. (2017). Choosing MUSE: Validation of a low-cost, portable EEG system for ERP research. *Frontiers in Neuroscience*. <https://doi.org/10.3389/fnins.2017.00109>
- Kruegel, A. C., & Grundmann, O. (2018). The medicinal chemistry and neuropharmacology of kratom: A preliminary discussion of a promising medicinal plant and analysis of its potential for abuse. In *Neuropharmacology*.
<https://doi.org/10.1016/j.neuropharm.2017.08.026>
- KUYUK, H. S. E. R. D. A. R. (2015). On the use of Stockwell transform in structural dynamic analysis. *Sadhana - Academy Proceedings in Engineering Sciences*.
<https://doi.org/10.1007/s12046-014-0301-2>
- LaRocco, J., Le, M. D., & Paeng, D. G. (2020). A Systemic Review of Available Low-Cost EEG Headsets Used for Drowsiness Detection. In *Frontiers in Neuroinformatics*.
<https://doi.org/10.3389/fninf.2020.553352>
- Larsen, I., Zhang, E., & Farahmand, P. (2022). Current Understanding of the Effects and Potential Clinical Utility of Kratom: A Review. *Journal of Psychiatric Practice*[®], 2, 92–97.
- Leong Abdullah, M. F. I., Tan, K. L., Narayanan, S., Yuvashnee, N., Chear, N. J. Y., Singh, D., Grundmann, O., & Henningfield, J. E. (2020). Is kratom (*Mitragyna speciosa* Korth.) use associated with ECG abnormalities? Electrocardiogram comparisons between regular kratom users and controls. *Clinical Toxicology*.
<https://doi.org/10.1080/15563650.2020.1812627>
- Lim, C. (2020). (2020). A study on stock trend determination in stock trend prediction. *Journal of The Korea Society of Computer and Information*, 25(12), 35–44.
- Listos, J., Łupina, M., Talarek, S., Mazur, A., Orzelska-Górka, J., & Kotlińska, J. (2019). The

- mechanisms involved in morphine addiction: An overview. In *International Journal of Molecular Sciences*. <https://doi.org/10.3390/ijms20174302>
- Makowski, D., Pham, T., Lau, Z. J., Brammer, J. C., Lespinasse, F., Pham, H., Schölzel, C., & Chen, S. H. A. (2021). NeuroKit2: A Python toolbox for neurophysiological signal processing. *Behavior Research Methods*. <https://doi.org/10.3758/s13428-020-01516-y>
- Manda, V. K., Avula, B., Ali, Z., Khan, I. A., Walker, L. A., & Khan, S. I. (2014). Evaluation of in vitro absorption, distribution, metabolism, and excretion (ADME) properties of mitragynine, 7-hydroxymitragynine, and mitraphylline. *Planta Medica*. <https://doi.org/10.1055/s-0034-1368444>
- Mansi, Silvia Angela, Ilaria Pigliautile, Camillo Porcaro, Anna Laura Pisello, and M. A. (2021). Application of wearable EEG sensors for indoor thermal comfort measurements. *ACTA IMEKO*, 10(4), 214–220.
- Matsumoto, K., Hatori, Y., Murayama, T., Tashima, K., Wongseripipatana, S., Misawa, K., ... & Horie, S. (2006). Involvement of μ -opioid receptors in antinociception and inhibition of gastrointestinal transit induced by 7-hydroxymitragynine, isolated from Thai herbal medicine *Mitragyna speciosa*. *European Journal of Pharmacology*, 549(1–3), 63–70.
- Matsumoto, K., Hatori, Y., Murayama, T., Tashima, K., Wongseripipatana, S., et al. (2006). Involvement of μ -opioid receptors in antinociception and inhibition of gastrointestinal transit induced by 7-hydroxymitragynine, isolated from Thai herbal medicine *Mitragyna speciosa*. *European Journal of Pharmacology*, 549(1–3), 63–70.
- Matsumoto, Kenjiro, Horie, S., Takayama, H., Ishikawa, H., Aimi, N., Ponglux, D., Murayama, T., & Watanabe, K. (2005). Antinociception, tolerance and withdrawal symptoms induced by 7-hydroxymitragynine, an alkaloid from the Thai medicinal herb *Mitragyna speciosa*. *Life Sciences*. <https://doi.org/10.1016/j.lfs.2004.10.086>
- Matsumoto, Kinzo, Mizowaki, M., Suchitra, T., Takayama, H., Sakai, S. I., Aimi, N., & Watanabe, H. (1996). Antinociceptive action of mitragynine in mice: Evidence for the involvement of supraspinal opioid receptors. *Life Sciences*. [https://doi.org/10.1016/0024-3205\(96\)00432-8](https://doi.org/10.1016/0024-3205(96)00432-8)
- Md Isa, N. E. Z., Amir, A., Ilyas, M. Z., & Razalli, M. S. (2017). The Performance Analysis of K-Nearest Neighbors (K-NN) Algorithm for Motor Imagery Classification Based on EEG

- Signal. *MATEC Web of Conferences*. <https://doi.org/10.1051/mateconf/201714001024>
- Meghdadi, A. H., Karic, M. S., McConnell, M., Rupp, G., Richard, C., Hamilton, J., Salat, D., & Berka, C. (2021). Resting state EEG biomarkers of cognitive decline associated with Alzheimer's disease and mild cognitive impairment. *PLoS ONE*. <https://doi.org/10.1371/journal.pone.0244180>
- Mehreen, A., Anwar, S. M., Haseeb, M., Majid, M., & Ullah, M. O. (2019). A Hybrid Scheme for Drowsiness Detection Using Wearable Sensors. *IEEE Sensors Journal*. <https://doi.org/10.1109/JSEN.2019.2904222>
- Mejía-Mejía, E., Budidha, K., Abay, T. Y., May, J. M., & Kyriacou, P. A. (2020). Heart Rate Variability (HRV) and Pulse Rate Variability (PRV) for the Assessment of Autonomic Responses. *Frontiers in Physiology*. <https://doi.org/10.3389/fphys.2020.00779>
- Mind monitor*. (n.d.). Retrieved April 23, 2022, from <https://mind-monitor.com/>
- Mol, M. B. A., Strous, M. T. A., van Osch, F. H. M., Jeroen Vogelaar, F., Barten, D. G., Farchi, M., Foudraïne, N. A., & Gidron, Y. (2021). Heart-rate-variability (HRV), predicts outcomes in COVID-19. *PLoS ONE*. <https://doi.org/10.1371/journal.pone.0258841>
- Munoz, M. L., Van Roon, A., Riese, H., Thio, C., Oostenbroek, E., Westrik, I., De Geus, E. J. C., Gansevoort, R., Lefrandt, J., Nolte, I. M., & Snieder, H. (2015). Validity of (Ultra-)Short recordings for heart rate variability measurements. *PLoS ONE*. <https://doi.org/10.1371/journal.pone.0138921>
- Muse*. (n.d.). Retrieved April 23, 2022, from <https://choosemuse.com/>
- Nanda, M. A., Seminar, K. B., Nandika, D., & Maddu, A. (2018). A comparison study of kernel functions in the support vector machine and its application for termite detection. *Information (Switzerland)*. <https://doi.org/10.3390/info9010005>
- Naranjo-Hernández, D., Roa, L. M., Reina-Tosina, J., Barbarov-Rostan, G., & Galdámez-Cruz, O. (2017). Smart Device for the Determination of Heart Rate Variability in Real Time. *Journal of Sensors*. <https://doi.org/10.1155/2017/8910470>
- Oliver, R., Bjoertomt, O., Greenwood, R., & Rothwell, J. (2008). "Noisy patients" - Can signal detection theory help? In *Nature Clinical Practice Neurology*. <https://doi.org/10.1038/ncpneuro0794>
- Orso, B., Arnaldi, D., Famà, F., Girtler, N., Brugnolo, A., Doglione, E., Filippi, L., Massa, F.,

- Peira, E., Bauckneht, M., Morbelli, S., Nobili, F., & Pardini, M. (2020). Anatomical and neurochemical bases of theory of mind in de novo Parkinson's Disease. *Cortex*.
<https://doi.org/10.1016/j.cortex.2020.06.012>
- Palma, J. A., Urrestarazu, E., Alegre, M., Pastor, M. A., Valencia, M., Artieda, J., & Iriarte, J. (2013). Cardiac autonomic impairment during sleep is linked with disease severity in Parkinson's disease. *Clinical Neurophysiology*. <https://doi.org/10.1016/j.clinph.2012.12.042>
- Pampiglione, G. (1980). Current Practice of Clinical Electroencephalography. *Journal of Neurology, Neurosurgery & Psychiatry*. <https://doi.org/10.1136/jnnp.43.6.559>
- Peirce, J. W. (2007). PsychoPy-Psychophysics software in Python. *Journal of Neuroscience Methods*, 162(1–2), 8–13. <https://doi.org/10.1016/j.jneumeth.2006.11.017>
- Petroff, O. A., Spencer, D. D., Goncharova, I. I., & Zaveri, H. P. (2016). A comparison of the power spectral density of scalp EEG and subjacent electrocorticograms. *Clinical Neurophysiology*. <https://doi.org/10.1016/j.clinph.2015.08.004>
- Phillips, R. L., Heming, R., & London, E. D. (1994). Morphine effects on the spontaneous electroencephalogram in polydrug abusers: Correlations with subjective self-reports. *Neuropsychopharmacology*. <https://doi.org/10.1038/npp.1994.19>
- Prozialeck, W. C., Jivan, J. K. and Andurkar, S. V. (2012). Pharmacology of kratom: an emerging botanical agent with stimulant, analgesic and opioid-like effects. *The Journal of the American Osteopathic Association*, 112(2), 792–799.
- Prozialeck, W. C., Jivan, J. K., & Andurkar, S. V. (2012). Pharmacology of Kratom: An emerging botanical agent with stimulant, analgesic and opioid-like effects. *Journal of the American Osteopathic Association*.
- Przegalinska, A., Ciechanowski, L., Magnuski, M., & Gloor, P. (2018). *Muse Headband: Measuring Tool or a Collaborative Gadget?* https://doi.org/10.1007/978-3-319-74295-3_8
- Psychopy*. (n.d.). Retrieved April 23, 2022, from <https://www.psychopy.org/>
- R programming*. (n.d.). Retrieved April 23, 2022, from <https://www.rstudio.com/>
- Ratti, E., Waninger, S., Berka, C., Ruffini, G., & Verma, A. (2017). Comparison of medical and consumer wireless EEG systems for use in clinical trials. *Frontiers in Human Neuroscience*, 11(August), 1–7. <https://doi.org/10.3389/fnhum.2017.00398>
- Rubin, J., Abreu, R., Ahern, S., Eldardiry, H., & Bobrow, D. G. (2016). Time, frequency &

complexity analysis for recognizing panic states from physiologic time-series.

PervasiveHealth: Pervasive Computing Technologies for Healthcare.

<https://doi.org/10.4108/eai.16-5-2016.2263292>

Ryali, S., Supekar, K., Abrams, D. A., & Menon, V. (2010). Sparse logistic regression for whole-brain classification of fMRI data. *NeuroImage*.

<https://doi.org/10.1016/j.neuroimage.2010.02.040>

Saidatul, A., Paulraj, M. P., Yaacob, S., & Yusnita, M. A. (2011). Analysis of EEG signals during relaxation and mental stress condition using AR modeling techniques. *Proceedings - 2011 IEEE International Conference on Control System, Computing and Engineering, ICCSCE 2011*.

<https://doi.org/10.1109/ICCSCE.2011.6190573>

Saidin, N. A., Holmes, E., Takayama, H., & Gooderham, N. J. (2015). The cellular toxicology of mitragynine, the dominant alkaloid of the narcotic-like herb, *Mitragyna speciosa* Korth.

Toxicology Research. <https://doi.org/10.1039/c5tx00113g>

Saingam, D., Assanangkornchai, S., Geater, A. F., & Lerkiatbundit, S. (2014). Validation of Krathom (*Mitragyna speciosa* Korth.) Dependence Scale (KDS): A dependence screen for internationally emerging psychoactive substance. *Substance Abuse*.

<https://doi.org/10.1080/08897077.2014.924464>

Sarang, P., & Telles, S. (2006). Effects of two yoga based relaxation techniques on Heart Rate Variability (HRV). *International Journal of Stress Management*.

<https://doi.org/10.1037/1072-5245.13.4.460>

Scikit-learn. (n.d.). Retrieved April 23, 2022, from <https://scikit-learn.org/stable/>

Scipy. (n.d.). Retrieved April 23, 2022, from <https://scipy.org/>

Shaffer, F., & Ginsberg, J. P. (2017). An Overview of Heart Rate Variability Metrics and Norms.

Frontiers in Public Health. <https://doi.org/10.3389/fpubh.2017.00258>

Simpson, D. S. A., & Oliver, P. L. (2020). Ros generation in microglia: Understanding oxidative stress and inflammation in neurodegenerative disease. In *Antioxidants*.

<https://doi.org/10.3390/antiox9080743>

Singh, A., Kukreti, R., Saso, L., & Kukreti, S. (2019). Oxidative stress: A key modulator in neurodegenerative diseases. In *Molecules*. <https://doi.org/10.3390/molecules24081583>

Singh, D., Chye, Y., Suo, C., Yücel, M., Grundmann, O., Ahmad, M. Z., Ho, E. T. W., Mansor,

- S. M., Yusof, S. R., McCurdy, C. R., Müller, C., Boyer, E. W., & Vicknasingam, B. (2018). Brain Magnetic Resonance Imaging of Regular Kratom (*Mitragyna speciosa* Korth.) Users: A preliminary study. *Malaysian Journal of Medicine and Health Sciences*.
- Singh, D., Narayanan, S., Müller, C. P., Swogger, M. T., Rahim, A. A., Leong Bin Abdullah, M. F. I., & Vicknasingam, B. K. (2018). Severity of Kratom (*Mitragyna speciosa* Korth.) Psychological Withdrawal Symptoms. *Journal of Psychoactive Drugs*.
<https://doi.org/10.1080/02791072.2018.1511879>
- Singh, D., Narayanan, S., Müller, C. P., Vicknasingam, B., Yücel, M., Ho, E. T. W., Hassan, Z., & Mansor, S. M. (2019). Long-Term Cognitive Effects of Kratom (*Mitragyna speciosa* Korth.) Use. *Journal of Psychoactive Drugs*, *51*(1), 19–27.
<https://doi.org/10.1080/02791072.2018.1555345>
- Singh, D., Narayanan, S., Vicknasingam, B., Corazza, O., Santacrose, R., & Roman-Urrestarazu, A. (2017). Changing trends in the use of kratom (*Mitragyna speciosa*) in Southeast Asia. *Human Psychopharmacology*. <https://doi.org/10.1002/hup.2582>
- Siuly, Li, Y., & Wen, P. (2014). Modified CC-LR algorithm with three diverse feature sets for motor imagery tasks classification in EEG based brain-computer interface. *Computer Methods and Programs in Biomedicine*. <https://doi.org/10.1016/j.cmpb.2013.12.020>
- Sobanski, P., Krajnik, M., Shaqura, M., Bloch-Boguslawska, E., Schäfer, M., & Mousa, S. A. (2014). The presence of mu-, delta-, and kappa-opioid receptors in human heart tissue. *Heart and Vessels*. <https://doi.org/10.1007/s00380-013-0456-5>
- Stieglitz, H. M., & Cotten, S. W. (2020). Kratom, a novel herbal opioid in a patient with benzodiazepine use disorder. In *Toxicology Cases for the Clinical and Forensic Laboratory*.
<https://doi.org/10.1016/b978-0-12-815846-3.00076-4>
- Streiner, D. L. (2005). Finding our way: An introduction to path analysis. In *Canadian Journal of Psychiatry*. <https://doi.org/10.1177/070674370505000207>
- Suhaimi, Farah W., Yusoff, N. H. M., Hassan, R., Mansor, S. M., Navaratnam, V., Müller, C. P., & Hassan, Z. (2016). Neurobiology of Kratom and its main alkaloid mitragynine. In *Brain Research Bulletin*. <https://doi.org/10.1016/j.brainresbull.2016.03.015>
- Suhaimi, Farah Wahida, Hassan, Z., Mansor, S. M., & Müller, C. P. (2021). The effects of chronic mitragynine (Kratom) exposure on the EEG in rats. *Neuroscience Letters*.

- <https://doi.org/10.1016/j.neulet.2021.135632>
- Sundling, C. M., Sukumar, N., Zhang, H., Embrechts, M. J., & Breneman, C. M. (2006). Wavelets in chemistry and cheminformatics. In *Reviews in Computational Chemistry*. <https://doi.org/10.1002/0471780367.ch5>
- Suwanlert, S. (1975). A study of kratom eaters in Thailand. *Bulletin on Narcotics*.
- Tanguay, P., & Drug Policy Consortium, I. (2012). Kratom in Thailand. *SSRN Electronic Journal*. <https://doi.org/10.2139/ssrn.1908849>
- Tayel, M., & AlSaba, E. (2015). Poincaré Plot for Heart Rate Variability. *International Journal of Medical, Health, Biomedical, Bioengineering and Pharmaceutical Engineering*.
- Teo, J., & Chia, J. (2019). Excitement classification of virtual reality stimuli using brain-computer interfacing and deep learning. *Journal of Computational and Theoretical Nanoscience*. <https://doi.org/10.1166/jctn.2019.7880>
- Trammell, J. P., MacRae, P. G., Davis, G., Bergstedt, D., & Anderson, A. E. (2017). The relationship of cognitive performance and the Theta-Alpha power ratio is age-dependent: An EEG study of short term memory and reasoning during task and resting-state in healthy young and old adults. *Frontiers in Aging Neuroscience*. <https://doi.org/10.3389/fnagi.2017.00364>
- Tsuchiya, S., Miyashita, S., Yamamoto, M., Horie, S., Sakai, S. I., Aimi, N., Takayama, H., & Watanabe, K. (2002). Effect of mitragynine, derived from Thai folk medicine, on gastric acid secretion through opioid receptor in anesthetized rats. *European Journal of Pharmacology*. [https://doi.org/10.1016/S0014-2999\(02\)01588-1](https://doi.org/10.1016/S0014-2999(02)01588-1)
- Übeyli, E. D., Cvetkovic, D., & Cosic, I. (2008). AR spectral analysis technique for human PPG, ECG and EEG signals. *Journal of Medical Systems*. <https://doi.org/10.1007/s10916-007-9123-7>
- Ueda, T., Musha, T., Asada, T., & Yagi, T. (2016). Classification Method for Mild Cognitive Impairment Based on Power Variability of EEG Using Only a Few Electrodes. *Electronics and Communications in Japan*. <https://doi.org/10.1002/ecj.11906>
- Ueda, T., Musha, T., & Yagi, T. (2010). Research on the characteristics of alzheimer's disease using EEG. *IEEJ Transactions on Electronics, Information and Systems*. <https://doi.org/10.1541/ieejieiss.130.1827>

- Ueda, T., Musha, T., & Yagi, T. (2013). Diagnosis method of mild cognitive impairment based on power variance of EEG. *Proceedings of the Annual International Conference of the IEEE Engineering in Medicine and Biology Society, EMBS*.
<https://doi.org/10.1109/EMBC.2013.6610920>
- Unoki, T., Grap, M. J., Sessler, C. N., Best, A. M., Wetzel, P., Hamilton, A., Mellott, K. G., & Munro, C. L. (2009). Autonomic nervous system function and depth of sedation in adults receiving mechanical ventilation. *American Journal of Critical Care*.
<https://doi.org/10.4037/ajcc2009509>
- Vanderlei, L. C. M., Pastre, C. M., Júnior, I. F. F., & de Godoy, M. F. (2010). Analysis of cardiac autonomic modulation in obese and eutrophic children. *Clinics*.
<https://doi.org/10.1590/S1807-59322010000800008>
- Vishwajeet, Singh, D., & Deepak, K. K. (2020). Investigation of heart rate variability with the help of welch periodogram in indian young adults based on body physique. In *Smart Healthcare for Disease Diagnosis and Prevention*. <https://doi.org/10.1016/B978-0-12-817913-0.00008-0>
- Wang, G. Y., Kydd, R. R., & Russell, B. R. (2016). Quantitative EEG and Low-Resolution Electromagnetic Tomography (LORETA) Imaging of Patients Undergoing Methadone Treatment for Opiate Addiction. *Clinical EEG and Neuroscience*.
<https://doi.org/10.1177/1550059415586705>
- Warner, M. L., Kaufman, N. C., & Grundmann, O. (2016). The pharmacology and toxicology of kratom: from traditional herb to drug of abuse. *International Journal of Legal Medicine*, *130*(1), 127–138. <https://doi.org/10.1007/s00414-015-1279-y>
- White, C. M. (2018). Pharmacologic and clinical assessment of kratom. In *American Journal of Health-System Pharmacy*. <https://doi.org/10.2146/ajhp161035>
- Ya, K., Methaneethorn, J., Tran, Q. B., Trakulsrichai, S., Wananukul, W., & Lohitnavy, M. (2021). Development of a Physiologically Based Pharmacokinetic Model of Mitragynine, Psychoactive Alkaloid in Kratom (*Mitragyna Speciosa* Korth.), In Rats and Humans. *Journal of Psychoactive Drugs*. <https://doi.org/10.1080/02791072.2020.1849877>
- Ye, G., & Van Raaij, W. F. (2004). Brand equity: Extending brand awareness and liking with signal detection theory. In *Journal of Marketing Communications*.

<https://doi.org/10.1080/13527260410001693794>

- Yoon, H., Jun, S. C., Hyun, Y., Bae, G. O., & Lee, K. K. (2011). A comparative study of artificial neural networks and support vector machines for predicting groundwater levels in a coastal aquifer. *Journal of Hydrology*. <https://doi.org/10.1016/j.jhydrol.2010.11.002>
- Yucelbas, C., Ozsen, S., Gunes, S., & Yosunkaya, S. (2013). Effect of some power spectral density estimation methods on automatic sleep stage scoring using artificial neural networks. *Proceedings of the IADIS International Conference Intelligent Systems and Agents 2013, ISA 2013, Proceedings of the IADIS European Conference on Data Mining 2013, ECDM 2013*.
- Yusoff, N. H., Suhaimi, F. W., Vadivelu, R. K., Hassan, Z., Rümmler, A., et al. (2016). Abuse potential and adverse cognitive effects of mitragynine (kratom)No Title. *Addiction Biology*, *21*(1), 98–110.
- Yusoff, N. H. M., Mansor, S. M., Müller, C. P., & Hassan, Z. (2017). Opioid receptors mediate the acquisition, but not the expression of mitragynine-induced conditioned place preference in rats. *Behavioural Brain Research*, *332*(March), 1–6.
<https://doi.org/10.1016/j.bbr.2017.05.059>

Appendix A Original Article

Consumer-Grade Brain Measuring Sensor in People with Long-Term Kratom Consumption.

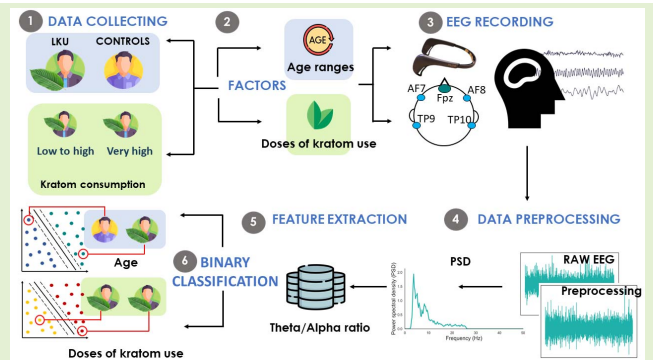
(Published in IEEE Sensors Journal)

Consumer-Grade Brain Measuring Sensor in People With Long-Term Kratom Consumption

Wanumaidah Saengmolee, Rattanaphon Chaisaen^{ID}, Graduate Student Member, IEEE, Phairot Autthasan^{ID}, Graduate Student Member, IEEE, Chutimon Rungsilp, Nusaib Sa-ih, Dania Cheaha, Ekkasit Kumarnsit, and Theerawit Wilaiprasitporn^{ID}, Member, IEEE

Abstract—Neurophysiological characteristics of long-term Kratom users have been challenged for identification due to the lack of evidence. Long-term and high Kratom consumption caused concern, particularly in older adults. Thus, the study aims to explore EEG biomarkers in long-term Kratom users (LKU) based on consumer-grade EEG systems. The fifty-two participants were collected EEG using MUSE portable system during resting-state to examine EEG biomarkers with the proposed features: theta/alpha ratio and power variance function (PVF) in theta and alpha bands. The statistical analysis was further carried out to test the existent difference between controls and LKU in various age ranges (≤ 50 and > 50 years of age) and different doses of Kratom consumption (low to high doses and very high dose). Subsequently, the statistical-based EEG biomarkers were extracted and performed classification among four classifiers (Random forest, Support vector machine, K -Nearest Neighbor, and Logistic regression). As a result, the TAR ratio was remarkably different between groups over 50 years of age. Furthermore, TAR and PVF in the alpha band were dominant in those who consumed Kratom at a very high dose and was classified well by support vector machine using the features combination (accuracy at $83.33\% \pm 10.24$, sensitivity at $90.00\% \pm 10.00$, specificity at $75.00\% \pm 13.44$). Our preliminary results concluded that the proposed EEG features were an important EEG biomarker for LKU with a large effect size. This finding led us to the promising aspect of applying machine learning-based EEG biomarkers to screen the overdose of Kratom consumption in the future.

Index Terms—Kratom consumption, consumer grade EEG, theta/alpha ratio, power function variance, brain.



I. INTRODUCTION

KRATOM or *Myragyna speciosa* (Korth.) is an indigenous tropical plant in Southeast Asia [1]. Thai older

Manuscript received January 10, 2022; accepted January 24, 2022. Date of publication January 27, 2022; date of current version March 14, 2022. This work was supported by the Graduate School Dissertation Funding for Thesis and Revenue Budget Fund, and Educational Institutions Scholarship for Outstanding Grade Point Average (GPA) from Prince of Songkla University, Thailand. The associate editor coordinating the review of this article and approving it for publication was Prof. Subhas C. Mukhopadhyay. (Corresponding author: Theerawit Wilaiprasitporn.)

This work involved human subjects or animals in its research. Approval of all ethical and experimental procedures and protocols was granted by the Ethics Committee of Prince of Songkla University, Thailand, under Application No. HSc-HREC-63-017-1-1, and performed in line with the Declaration of Helsinki.

Wanumaidah Saengmolee, Nusaib Sa-ih, and Ekkasit Kumarnsit are with the Physiological Program, Division of Health and Applied Sciences, and the Biosignal Research Center for Health, Faculty of Science, Prince of Songkla University, Hat Yai, Songkhla 90110, Thailand.

Rattanaphon Chaisaen, Phairot Autthasan, Chutimon Rungsilp, and Theerawit Wilaiprasitporn are with the Bio-Inspired Robotics and Neural Engineering (BRAIN) Laboratory, School of Information Science and Technology (IST), Vidyasirimedhi Institute of Science and Technology (VISTEC), Rayong 21210, Thailand (e-mail: theerawit.w@vistec.ac.th).

Dania Cheaha is with the Biology Program, Division of Biological Science, and the Biosignal Research Center for Health, Faculty of Science, Prince of Songkla University, Hat Yai, Songkhla 90110, Thailand.

Digital Object Identifier 10.1109/JSEN.2022.3147207

people in a rural area prevalently ingested Kratom leaves in traditional contexts to relieve their pain and increase their energy for hard work [2]. Even though long-term Kratom users (LKU) had recently raised the concern about the development of physical dependency [3], it appeared to be less severe than opioid dependence. The most often self-reported dependent/withdrawal effects trended to be dose-dependent which Kratom users were motivated to Kratom consuming at a high dose rather than a low dose to relieve their withdrawal symptoms [4]. Prolong and high intake of Kratom were expected to have neurotoxicity in the long-term outcomes, particularly in older adults. Chronic exposure of Kratom was a greater risk in the older adults due to age-related change in pharmacokinetics [5]. These changes might increase the sensitivity to the central nervous system (CNS) effect regarding the age-related failure of regulatory processes [6]. However, there was no significant evidence indicating the change in the brain activity of traditional Kratom use. Therefore, it needed to explore factor-related-biomarkers leading to the detection of Kratom consumption risk to prevent the brain abnormality later.

The conventional method for detecting the effect of long-term Kratom consumption on brain activity widely uses behavioral and cognitive testing [7]. However, it could not

detect intrinsic brain abnormalities. EEG technique is sensitive to diagnose possible dysfunction of the brain early before pathology advances to behavioral impairments emerge [8]–[10]. Resting-state EEG has been investigated for spontaneous brain activity and produced the dominant alpha-band frequency. The reduction of alpha power was expressed in normal aging [11] and age-related neurological disorder [12]. Interestingly, chronic exposure to high-dose substance use, such as alcohol, promoted the accelerated aging of the brain as a result of the reactive oxygen species (ROS) accumulating [13]. The increased ROS production induced neuronal damage [14], eventually contributing to neurodegenerative diseases [15]. Theta/alpha ratio (TAR) was a hallmark in neurodegenerative diseases such as Parkinson’s Disease (PD). The Mini-Mental State Examination (MMSE) in PD patients was correlated with the cholinergic deafferentation marker (the posterior Theta/Alpha ratio) [16]. Accordingly, EEG characteristics of neurodegenerative disorder might be the possible surrogate markers in long-term and excessive Kratom consumption. Besides TAR, there was a feature that performed well even using a few electrodes. A power variance function (PVF), the variability of EEG power at each frequency, was indicated as an index for the classification of neurodegenerative disorders such as mild cognitive impairment [17].

The quantitative EEG measure was typically recorded by a routine clinical EEG device which has the limitation in a long-time consuming to require skin abrasion, and impedance optimization [18]. As a result, wearable EEG technology that focused EEG acquisition in a more comfortable method than standard systems had widespread commercial use. The recent study had developed EEG-consumer grade for advantages of emotional assessment [19], [20]. However, using EEG consumer-grade to measure natural substance dependence such as Kratom has never been reported in recent review articles [21], [22]. MUSE headband [23] is one of the low-cost consumer-grade EEG devices, easy to set up and less time-consuming. Suppose the EEG signal acquired using MUSE has enough sensitivity to identify LKU. In that case, this low-cost and comfortable device might be substituted for the high cost of medical assessment.

Thus, the aim of this study was to investigate EEG biomarkers based-the proposed features in LKU in different factors, such as age and the doses of Kratom consumption, using MUSE portable device. The appropriate EEG biomarkers were further used as input data to perform binary classification. We hypothesized that EEG biomarkers would differentiate LKU from controls with increasing age and would classify the Kratom consumption in different doses.

The future applications of machine learning-based EEG biomarkers might potentially predict which Kratom users are at risk of excessive Kratom consumption that might possibly develop brain abnormality in long-term outcomes. Our three principal contributions are presented as follows:

- We were the first group that proposed the novel investigation of EEG-biomarker in LKU with the power variance function (PVF) feature and common EEG feature (theta/alpha ratio; TAR) using MUSE portable device.

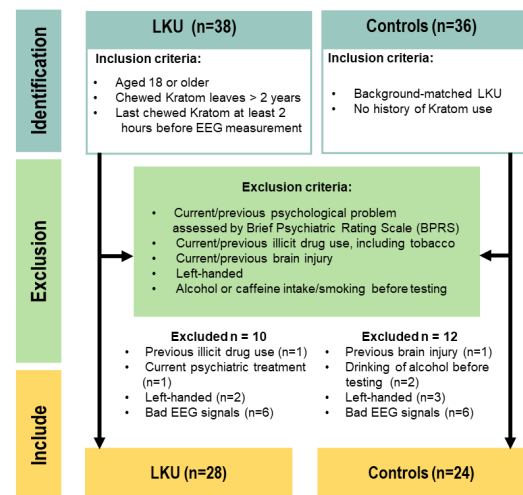


Fig. 1. Participants recruitment and inclusion/ exclusion criteria in the study. **Note:** we included LKU those who consumed Kratom \geq two years due to Kratom-related unpleasant side effects [26] and who last consumed Kratom at least 2-hours before experimenting for escaping the direct effect of Kratom ingestion [27].

- The proposed features were examined in different factors, such as age and the doses of Kratom use.
- The statistical-based proposed EEG features were performed binary classification in the relevant factors using the evaluation of the traditional algorithms.

The remainder of the present study is organized as follows: the experiment setups, including participant recruitment, EEG recording, and preprocessing following the classification methods, are described in Section II. Then, the results and discussion are presented in Section III. Finally, the conclusion is illustrated in Section IV.

II. METHODS AND MATERIALS

Participants were recruited and divided into two groups: controls and long-term kratom users (LKU). First, the participants were subjected to record EEG. After that, the collected EEG data were statistically analyzed and further performed machine learning. The overview of the present study is displayed in Figure 2. The details of this section are described in the following subsections.

A. Participants

A total of 74 volunteers: 36 normal male participants and male 38 LKU were collected from Ban Nasarn district, Surat Thani province, and Natavee district, Songkhla province located in southern Thailand. The experimental data acquisition was performed according to the Declaration of Helsinki and was approved by the Ethics Committee of Prince of Songkla University, Thailand (HSc-HREC-63-017-1-1). All participants were obtained verbal consent. The final of 52 participants met inclusion criteria, composed of 28 LKU and 24 controls as shown in Figure 1. Demographic information for each participant group is available in Table I. There were no females among the participants in this study. Despite our

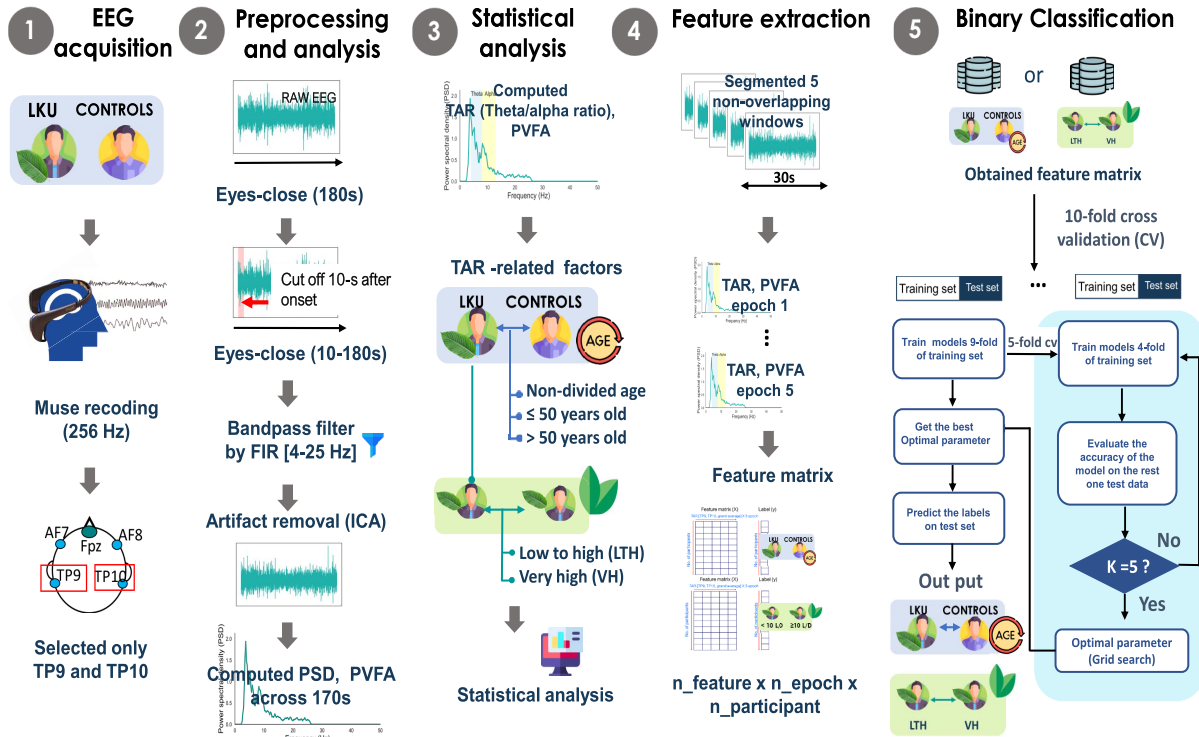


Fig. 2. An overview of the present study. TAR and PVFA are theta/alpha ratio and power variance function in the alpha band, respectively.

TABLE I
DEMOGRAPHIC AND KRATOM USE HISTORY

Variable	Category	LKU(n=28)	Controls (n=24)	p-value
Sex	Male	28	24	-
	Female	-	-	-
Age group	Total	52.41 ± 15.45 (n = 28)	56.64 ± 10.70 (n = 24)	0.251 ^a
	≤ 50 years old	46.44 ± 3.71 (n = 9)	40.08 ± 9.18 (n = 12)	0.06 ^a
	> 50 years old	61.473 ± 9.44 (n = 19)	64.75 ± 9.11 (n = 12)	0.348 ^a
Duration of Kratom use	Total	26.85 ± 11.11 (n = 28)	-	-
	< 30 years	18.21 ± 6.48 (n = 14)	-	-
	≥ 30 years	35.50 ± 7.31 (n = 14)	-	-
Kratom chewing (leaves/day)	Total	10.39 ± 7.20 (n = 28)	-	-
	< 10 leaves/day	4.78 ± 2.25 (n = 14)	-	-
	≥ 10 leaves/day	16.00 ± 5.90 (n = 14)	-	-

Note: ^a t-test

efforts to recruit female kratom users, they were hesitant to participate due to Thai culture's social discrimination. Furthermore, they infrequently consumed kratom and different purposes use from males [24], [25].

B. EEG Recording, Preprocessing, and Analysis

Continuous EEG data during eyes-closed for 3 minutes were collected at 256 Hz sampling rate using MUSE headband sensor through Mind Monitor graphical user interface [28]. MUSE consisted of one for a reference point (Fz) and four for recording brain wave activity (TP9, AF7, AF8, and TP10).

Raw EEG data from AF7 and AF8 electrodes (located prefrontal region) were not performed EEG analysis as the placement was near the ocular region provided an ocular muscle interference examined by positive and negative deflection waveform. Thus, only the temporal electrodes (TP9 and TP10) were decided to use for quantitative EEG measures with

power spectrum density and power variance function. Since eye movement-related artifacts were predominantly observed at a time interval of 10 s after the onset, the EEG signals were selected from 10–180s (43517 sampling points, given the 256 Hz sampling frequency rate). The recorded EEG signal was band-pass filtered between 4–25 Hz, using Finite Impulse Response (FIR). Subsequently, Independent Component Analysis (ICA) using *run_ica* function in EEGLAB toolbox (version 2019.1) [29] was further used to detect and remove artifacts [30].

1) *Power Spectrum Density (PSD)*: The entire processed EEG data were averaged across time to compute PSD at each electrode for each participant. The PSD was estimated by using *spectopo* function implemented in the EEGLAB toolbox using *pwelch* function (welch periodogram) from MATLAB, which applied a hamming window [31]. As *spectopo* computed the logarithm of PSD given in Equation (1), the PSD values were computed eliminating logarithms as shown in Equation (2) and normalized to total power in the considered broadband (4–25 Hz). Therefore, the original dataset consisted of 44 observed variables in the columns (22 frequencies x 2 electrodes) and 52 participants in the rows. The average PSD was further measured in different frequency bands; theta (4–7 Hz) and alpha (8–13 Hz) bands. Finally, the TAR was calculated in Equation (3) in each electrode, including their average from both electrodes.

$$X = 10 \times \log(PSD) \quad (1)$$

$$PSD = e^{X/10} \quad (2)$$

$$TAR = \frac{\text{theta power}}{\text{alpha power}} \quad (3)$$

2) *Power Variance Function (PVF)*: The processed EEG data were also computed the PVF at each frequency in temporal electrodes (TP9 and TP10). The PVF is defined as follows:

$$\sigma_i^2 = E \left[(P_i(f, t) - E[P_i(f, t)])^2 \right] \quad (4)$$

$$PVF(f) = \log \sigma_i^2(f) \quad (5)$$

$E[x]$ is the averaged value at temporal location of x , where f , i and t are the frequency, electrode, and time, respectively. $P_i(f, t)$ represents the power variance of electrode i and is calculated using Gabor wavelets to execute wavelet transformation from previous study [32]. The dispersion $\sigma_i^2(f)$ is further computed to activate the temporal variance of $\sigma_i^2(f)$, as given in Equation (4). To prevent the asymmetrical distribution of $\sigma_i^2(f)$, PVF is quantified by the natural log transformation of $\sigma_i^2(f)$, as shown in Equation (5). After acquiring the PVF of all frequencies, the theta and alpha frequency bands are averaged across electrodes.

C. Statistical Analysis

Before conducting the statistical difference between groups, the EEG feature distribution was evaluated an assumptions of normality by Kolmogorov-Smirnov (KS) test. The EEG features were significantly non-normal distribution with positively skewed data. Thus, the appropriated log transformation or non-parametric test was conducted. The EEG features related factors were tested with statistical analyses as following bullets:

- Spearman's rank correlation (non-parametric correlation) was applied to examine the correlation between TAR and the age
- Partial rank correlations (non-parametric Partial correlation) were applied to examine the correlation between TAR and the quantity of Kratom consumption for controlling the confounding age effect.
- A multivariate analysis of variance (MANOVA) using Wilk's Lambda was tested for multiple EEG feature comparisons between groups in relevant factors, as shown in Figure 3. The significant Wilk's Lambda was followed by univariate analyses of variance (ANOVAs) and post-hoc test with Bonferroni correction.

Based on our preliminary study, we reported effect size and observed power to detect the sensitivity analysis of the given sample size. The η_p^2 as an indicator of effect size which independent sample size and was interpreted as small effect = 0.01, medium effect = 0.06, large effect = 0.14 [33].

The significant level was defined at $p < 0.05$ for all statistical tests.

D. Classification and Performance Evaluation

As the EEG-biomarkers revealed a significant group difference in in Section III-A.2 and in Section III-A.3, the significant EEG biomarkers were extracted to perform machine learning for group classification divided into two tasks following:

- The binary classification task on EEG features was separately constructed based on the different age ranges (non-divided age ranges, ≤ 50 and > 50 years of age) with the ability to discriminate LKU from controls.

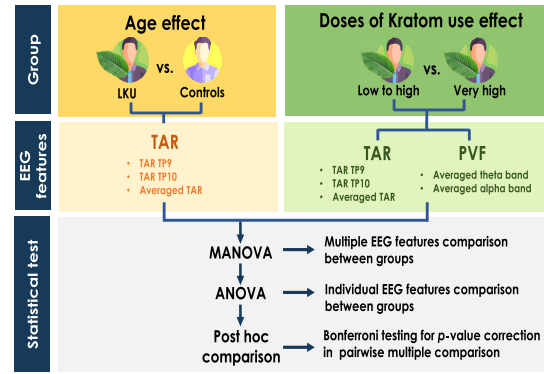


Fig. 3. The statistical testing in different factors between groups.

- The binary classification task was also conducted to identify EEG biomarkers in LKU who ingested Kratom in different doses (low to high doses vs. very high dose).

1) *Feature Extraction*: The entire processed EEG signals were further segmented into five non-overlapping epochs. Each epoch contained the 30s per each. The features were extracted according to the statistical significance in the relevant factors, as shown in Section III-B.1 and Section III-B.2. Therefore, the processed EEG data were formed in dimensions of $n_EEG_features \times n_epochs \times n_participants$ based on the following factors:

Age:

- Non-divided age ranges: ($3 \times 5 \times 52$)
- group of ≤ 50 years of age: ($3 \times 5 \times 21$)
- group of > 50 years of age: ($3 \times 5 \times 31$)

The doses of Kratom use:

- Low to high doses vs. very high dose: ($4 \times 5 \times 28$)

2) *Classifiers*: Four different conventional machine learning algorithms were used to perform classification. The details of all considered classifiers are described below:

1) Random Forest (RF) is used for classification based on multiple decision trees. During the training phase, each decision tree was randomly generated from an individual internal node. This used the split features through a separate bootstrap sample of entire features. Final prediction, the classification output among the tree was used to examine the overall classification by considering a majority voting of the ensemble trees [34].

2) Support vector machine (SVM) is used to classify the data with linear inseparability in the original space by mapping the predictors onto a new high-dimensional space. The main objective of data fitting for SVM is to separate the most significant margin distance between the nearest points of each class using a kernel function that splits the classes through constructing a hyperplane within the predictor space [35].

3) *K*-Nearest Neighbors (*k*NN) is the most straightforward distance-based supervised machine learning classification technique. It is determined by the number of k samples that are nearest neighbors. The distance between nearby objects was calculated to categorize the test data. The test set was then classified by a majority vote of the training set's *k*NN [36].

TABLE II
HYPERPARAMETER OF DIFFERENT MODELS EVALUATED

Model classification	Parameter	Value
RF	n_estimator max_feature criterion class_weight	10, 100, 150, 200 auto, sqrt, log2 gini, entropy balance
SVM	kernel gamma C class_weight	linear, rbf, sigmoid $10^{-2}, 10^{-3}, 10^{-4}, 10^{-5}$ 0.001, 0.01, 0.1, 10, 25, 50, 100, 1000 balance
kNN	n_neighbors weight metric	3, 5, 7, 9 uniform, distance euclidean, manhattan
LR	penalty c solver class_weight	l1,l2 np.logspace(-3,3,7) liblinear balance

4) Logistic regression (LR) is used for classification based on the probability that evaluates the relationship between the dependent and independent variables using the logistic or sigmoid function to map the predicted output value between 0 to 1. During the training phase, the LR model is estimated by maximum likelihood regression coefficients (weights). Classification output is classified by selecting the label with the greater probability that provided test sample of interest belongs to class 1 [37].

3) *Performance Evaluation Method*: Since the dataset contained unequal class proportions, stratified k -fold cross-validation using Scikit-learn [38] was conducted. This approach was employed to ensure that each fold represented the equal proportion of each class in the training dataset [39]. The subject-independent classification was implemented with the nested stratified 10-fold cross-validation in the outer loop. One fold was used for a testing set, and the remaining fold was left as a training set. The grid search method with stratified 5-folds cross-validation in the inner loop was applied on the training set to find out the optimal hyperparameter of models that yielded the highest accuracy. The hyperparameter tuning each classifier is shown in Table II. Finally, the testing set was used to predict the classification model with optimal hyperparameters in each fold of the outer loop and reported by the percentage and standard error. To evaluate the performance of the classification model, the accuracy, precision, F1-score, sensitivity, and specificity of that classification were computed.

III. RESULTS AND DISCUSSION

A. Statistical Results

1) *The Correlation Between TAR and Age Effect*: The PSD of long-term Kratom users (LKU) and controls during eyes-closed were computed across the frequency range 4 to 25 Hz in both electrode positions (TP9, TP10). The frequency range 4-13 Hz emphasized with the grey band color reflected that the LKU trended to be different from controls, as shown in the Figure 4(a).

The different frequencies in Theta (4-7 Hz) and Alpha (8-13 Hz) bands were averaged from both electrode sites then performed MANOVA analysis to assess group

differences across these features. The MANOVA test showed significantly overall effect between groups [Wilks Lambda = 0.879, $F(2,49) = 3.378$, $p = 0.042$, $\eta_p^2 = 0.121$, observed power = 0.610]. The significant multivariate test was followed by ANOVAs to examine the differences between group in individual frequency bands. Compared to controls, the LKU significantly increased theta power [$F(1,50) = 5.432$, $p = 0.024$, $\eta_p^2 = 0.098$, observed power = 0.628] and decreased alpha power [$F(1,50) = 6.731$, $p = 0.012$, $\eta_p^2 = 0.119$, observed power = 0.721]. Bonferroni correction was then used to adjust the significant p -value as shown in Figure 4(b).

We further focused on TAR between the group. The TAR was found a biomarker in age-related disorder [12]. Thus, the correlation between the averaged TAR and age was tested by Spearman's rank correlation in each group. From the statistical test, the averaged TAR was not significantly correlated with the age in both groups as shown in Figure 4(c). However, the LKU found a tendency for increased TAR as age increases, while TAR was reversely correlated in the control group. As PVF in the theta and alpha bands from both temporal electrodes showed no significant difference between group and no tendency of correlation with age in both groups.

The result suggested that age might be affecting the TAR level in LKU. To better understand the age-related change, the further experiment was designed to separate both groups into two subgroups based on a median value of those age distributions: ≤ 50 and > 50 years of age.

2) *TAR Potentially Indicated Between-Group Difference When Age Increased*: The PSD of specific frequency [4-13 Hz] was clearly different between groups of > 50 years of age in both electrode positions emphasized with grey band color as illustrated in Figure 5(a).

Subsequently, TAR across electrodes and their average were executed MANOVA testing for multiple EEG feature comparisons between groups in separated age ranges. The results showed a significant multivariate effect between groups in age range of > 50 years of age [Wilks Lambda = 0.667, $F(3,27) = 4.497$, $p = 0.011$, $\eta_p^2 = 0.333$, observed power = 0.829]. The ANOVA analysis was further conducted for each EEG feature between groups presented in Table III. All EEG features were a significant difference between groups and provided large effects. The significant differences were adjusted with Bonferroni correction as shown in Figure 5(b). Furthermore, the TAR in the LKU over 50 years of age was also significantly positively correlated with the quantity of Kratom consumption as shown in Figure 5(c).

As the group of non-divided age and ≤ 50 years of age did not show significance in multivariate effect, we did not test further the results for ANOVAs.

Our results indicated that enhanced TAR with age increasing was an important EEG biomarker and had a large effect on LKU compared to controls. LKU for those more than 50 years of age may be possibly involved in age-related neurodegeneration since the increased TAR was also found in Alzheimer's disease [12]. So far as we know, the investigation of age-related EEG-biomarker in LKU had never been explored. As a result, we suggested that a future study simultaneously

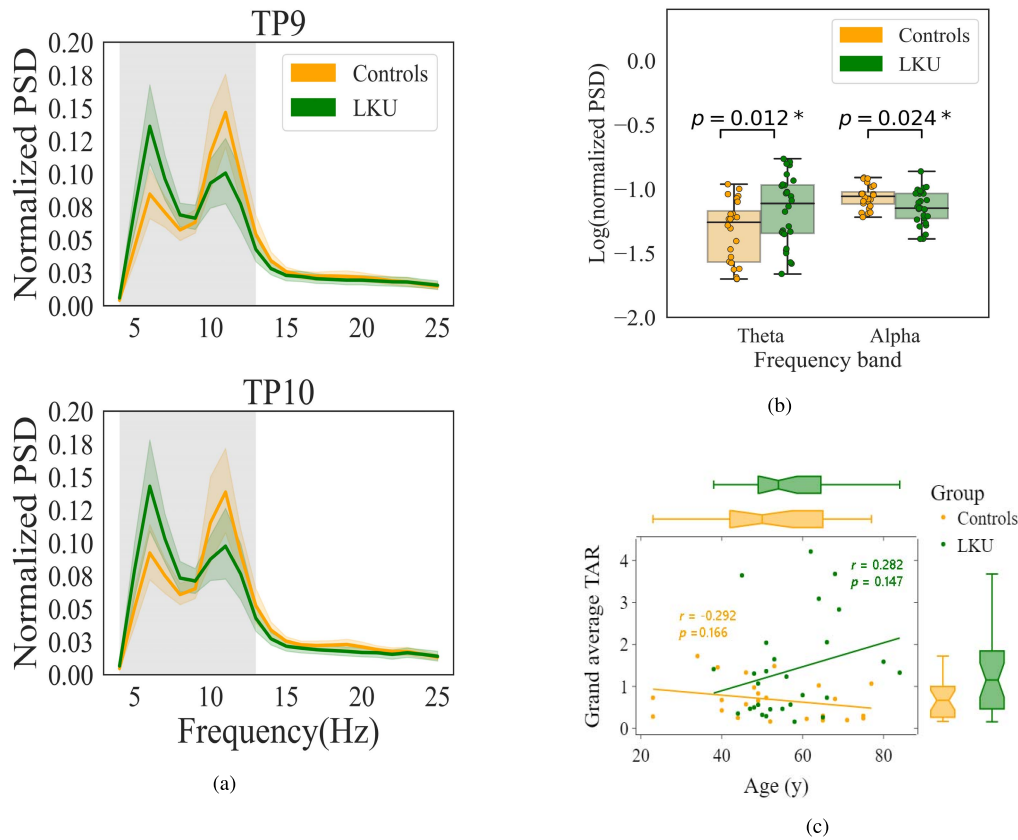


Fig. 4. The PSD across the frequency range of 4-25 Hz during eyes-closed. (a) The PSD power in the specific frequency range 4-13 Hz highlighted gray band color both TP9 and TP10 trends to be different between groups, (b) MANOVA tests the difference of grand average theta and alpha band between groups following ANOVAs and adjusts p -value with Bonferroni Test. (c) The correlation between the grand average TAR and the age in both groups is evaluated by Spearman's rank correlation. LKU ($n = 28$), controls ($n = 24$), $*p < 0.05$ versus control group.

TABLE III
THE RESULTS FOR ANOVAS ON INDIVIDUAL EEG FEATURES BETWEEN GROUPS (CONTROLS VS. LKU) OVER 50 OF THE AGE. TAR REPRESENTS THETA/ALPHA RATIO

Feature	Controls (n=12)		LKU (n=19)		ANOVA $F(1,29)$	p -value	Effect size (η_p^2)	Observed power
	Mean	SD	Mean	SD				
TAR [TP9]	-0.418	0.311	0.022	0.412	10.046	0.004	0.257 (Large effect)	0.865
TAR [TP10]	-0.356	0.372	0.015	0.415	6.393	0.017	0.181 (Large effect)	0.686
Grand averaged TAR	-0.382	0.340	0.024	0.410	8.155	0.008	0.219 (Large effect)	0.788

TABLE IV
THE RESULTS FOR ANOVAS ON INDIVIDUAL EEG FEATURES OF LKU WHO CONSUMED KRATOM IN DIFFERENT DOSES (LOW TO HIGH DOSES VS. VERY HIGH DOSE). TAR, PVFT AND PVFA REPRESENT THETA/ALPHA RATIO AND POWER VARIANCE FUNCTION IN SEPARATED FREQUENCY BANDS; THETA AND ALPHA BANDS, RESPECTIVELY

Feature	LTH (n=14)		VH (n=14)		ANOVA $F(1,24)$	p -value	Effect size (η_p^2)	Observed power
	Mean	SD	Mean	SD				
TAR [TP9]	-0.258	0.279	0.185	0.321	12.924	0.001	0.350 (Large effect)	0.932
TAR [TP10]	-0.226	0.355	0.199	0.356	8.334	0.008	0.258 (Large effect)	0.791
Grand averaged TAR	-0.239	0.318	0.203	0.328	10.957	0.003	0.313 (Large effect)	0.888
PVFT	0.503	0.109	0.486	0.089	0.592	0.449	0.024 (Small effect)	0.115
PVFA	0.465	0.045	0.414	0.064	7.807	0.010	0.245 (Large effect)	0.765

investigate the neurobehavioral testing and EEG assessment since neurological behaviors are highly relevant to changes in neuronal oscillation.

Moreover, we found that change in TAR resulted from the combined effects of age and the quantity of Kratom consumption factors. Thus, we are interested in the effect of different quantities of Kratom consumption in the next experiment.

3) *TAR and PVF Were Doses-Dependent Manner*: Prolonged Kratom users were typically found in older adults [40] and also observed in those who consumed a large Kratom quantity [41]. Thus, the different doses of Kratom consumption were investigated with the proposed EEG-biomarkers. The doses of Kratom consumption in this study were divided into low to moderate doses (1-3 leaves/day), moderate to high doses (4-9 leaves/day), and very high dose (≥ 10 leaves/day)

according to the previous study [42] and in relative to the weight of Kratom leaves in Thai origin [43]. We found that both TAR and PVF in the alpha bands tended to be the dose-dependent effect as given in Figure 6(a) and (b). As the proposed features show no significant difference among those who consumed Kratom in different doses, LKU had regrouped to be those who consumed at low to high doses compared to the very high dose.

The MANOVA showed a significant multivariate effect between groups after adjusting age and duration of consumption [Wilks Lambda = 0.466, $F(5,20) = 4.582$, $p = 0.006$, $\eta_p^2 = 0.534$, observed power = 0.918]. The difference between groups on individual EEG features was reported with ANOVAs

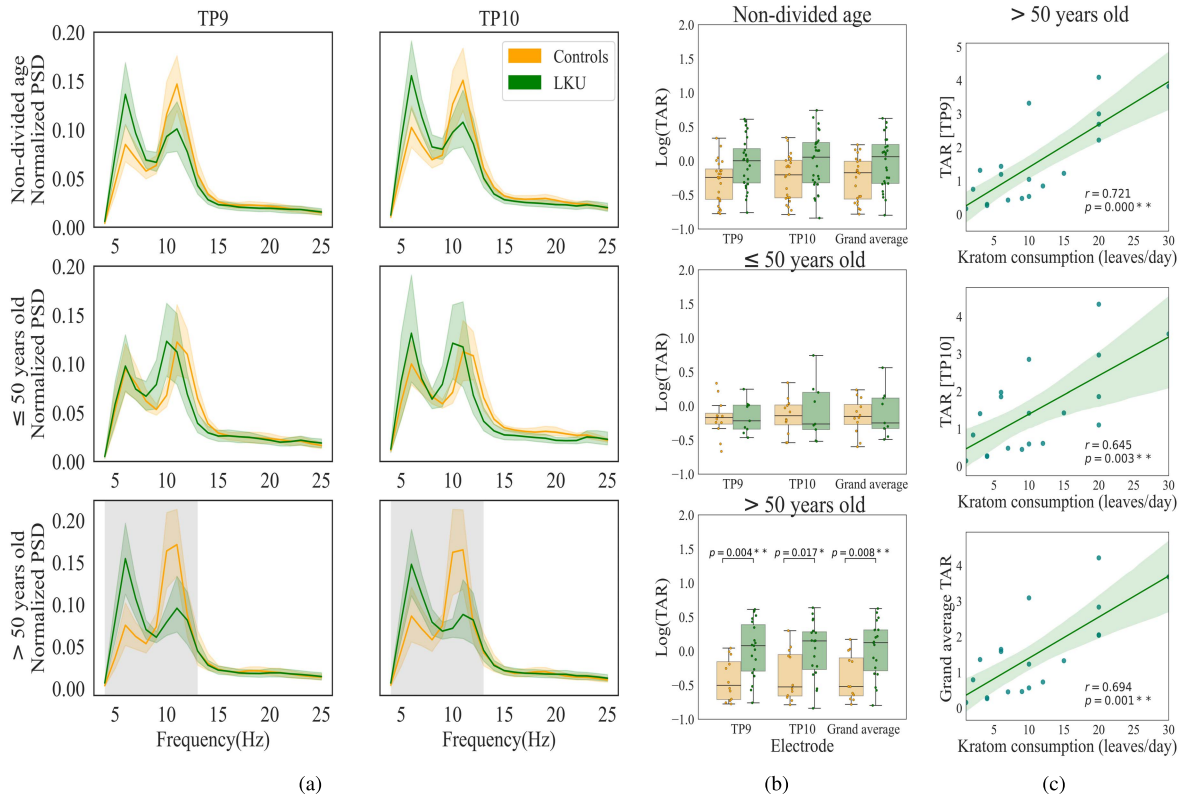


Fig. 5. The pattern of PSD power during eyes closed in different age ranges. The frequency range of 4-13 Hz in both electrode positions is clearly different between LKU and the controls highlighted in the gray-band color in the age range of > 50 years (a). The significant p-value for TAR between groups in the age range of > 50 years was adjusted with a Bonferroni test after MANOVA analysis (b). The correlation between TAR and the quantity of Kratom consumption in LKU over 50 years of age was tested by Partial rank correlation for controlling the age effect. **Note:** non-divided age range (LKU = 28, controls n = 24), ≤ 50 years of age (LKU n = 9, controls n = 12), > 50 years of age (LKU n = 19, controls n = 12), ** $p < 0.01$ versus control group, Significant correlation ** $p < 0.01$.

TABLE V

THE SUMMARY OF RESULTS FOR CLASSIFICATION BETWEEN LKU AND CONTROLS GROUPED BY AGE RANGES USING VARIOUS TRADITIONAL MACHINE LEARNING ALGORITHMS (RF, SVM, kNN, AND LR) REPORTED AS THE PERCENTAGE OF ACCURACY ± SE, F1-SCORE ± SE, SENSITIVITY ± SE, AND SPECIFICITY ± SE). TAR REPRESENTS THE THETA/ALPHA RATIO

Feature	Classifier	Non-divided age (controls n=24, LKU n=28)				≤ 50 years old (controls n=12, LKU n=9)				> 50 years old (controls n=12, LKU n=19)			
		Accuracy	F1-score	Sensitivity	Specificity	Accuracy	F1-score	Sensitivity	Specificity	Accuracy	F1-score	Sensitivity	Specificity
TAR[TP9], TAR[TP10]	RF	59.67 ± 7.64	57.29 ± 10.56	63.33 ± 12.62	61.67 ± 10.26	51.67 ± 7.64	23.33 ± 12.22	30.00 ± 15.28	70.00 ± 13.33	60.83 ± 8.43	65.67 ± 8.40	70.00 ± 11.06	50.00 ± 14.91
	SVM	44.00 ± 5.62	33.38 ± 8.46	35.00 ± 10.08	58.33 ± 11.98	45.00 ± 5.00	6.67 ± 6.67	10.00 ± 10.00	75.00 ± 13.44	58.33 ± 10.90	48.33 ± 14.15	45.00 ± 13.84	85.00 ± 10.67
	kNN	55.67 ± 6.89	55.90 ± 8.52	58.33 ± 9.70	56.67 ± 7.93	43.33 ± 9.03	10.00 ± 10.00	10.00 ± 10.00	70.00 ± 13.33	60.83 ± 9.79	61.00 ± 11.27	65.00 ± 13.02	60.00 ± 14.53
	LR	64.00 ± 6.36	67.21 ± 6.36	75.00 ± 9.04	51.67 ± 13.25	48.33 ± 7.64	11.67 ± 7.88	20.00 ± 13.33	70.00 ± 15.28	55.00 ± 8.62	54.67 ± 10.16	65.00 ± 11.67	60.00 ± 14.53
Grand averaged TAR	RF	55.33 ± 6.89	50.88 ± 9.28	53.33 ± 12.37	65.00 ± 10.96	51.67 ± 13.02	43.33 ± 14.95	50.00 ± 16.67	50.00 ± 14.91	64.17 ± 9.30	69.00 ± 9.08	75.00 ± 11.18	50.00 ± 14.91
	SVM	44.00 ± 4.47	24.00 ± 10.10	30.00 ± 13.56	70.00 ± 8.89	46.67 ± 11.86	10.00 ± 10.00	10.00 ± 10.00	70.00 ± 15.28	51.67 ± 5.24	53.33 ± 6.48	50.00 ± 7.45	60.00 ± 14.53
	kNN	53.33 ± 7.50	46.00 ± 10.00	46.67 ± 12.37	68.33 ± 9.11	56.67 ± 9.03	26.67 ± 13.88	30.00 ± 15.28	80.00 ± 11.06	60.83 ± 9.79	61.00 ± 11.27	65.00 ± 13.02	60.00 ± 14.53
	LR	56.00 ± 7.50	54.07 ± 10.68	63.33 ± 13.56	51.67 ± 9.77	65.00 ± 10.67	30.00 ± 15.28	30.00 ± 15.28	90.00 ± 10.00	51.67 ± 7.22	54.00 ± 9.65	60.00 ± 12.47	40.00 ± 14.53
Feature combination	RF	57.67 ± 5.67	58.21 ± 7.63	63.33 ± 10.48	58.33 ± 10.61	53.33 ± 9.23	20.00 ± 13.33	20.00 ± 13.33	80.00 ± 11.06	60.83 ± 8.43	65.67 ± 8.40	70.00 ± 11.06	50.00 ± 14.91
	SVM	46.00 ± 4.99	39.00 ± 9.30	46.67 ± 13.33	53.33 ± 12.12	40.00 ± 10.00	6.67 ± 6.67	10.00 ± 10.00	60.00 ± 16.33	71.67 ± 7.05	69.67 ± 9.51	70.00 ± 11.06	80.00 ± 11.06
	kNN	53.67 ± 5.63	50.90 ± 7.44	53.33 ± 11.33	61.67 ± 8.98	61.67 ± 6.60	26.67 ± 13.88	30.00 ± 15.28	90.00 ± 6.67	60.83 ± 9.79	61.00 ± 11.27	65.00 ± 13.02	60.00 ± 14.53
	LR	60.00 ± 3.94	64.93 ± 3.55	71.67 ± 7.05	48.33 ± 13.25	65.00 ± 10.67	30.00 ± 15.28	30.00 ± 15.28	90.00 ± 10.00	48.33 ± 8.77	45.00 ± 10.84	45.00 ± 11.67	65.00 ± 15.00

in Table IV. All proposed EEG features showed a significant difference and provided a large effect size in a dose-dependent manner except for PVF in the theta band. The significant p -value was adjusted with Bonferroni correction as shown in Figure 6(c) and (d). The results suggested that the levels of TAR and PVF (the average alpha band) were dependent on the doses of Kratom use.

We attempted to initially assess EEG-biomarker in long-term and high dose of Kratom consumption in a human study, which had never been studied in prior research. However, if we compared our results to chronic mitragynine (Kratom) exposure in an animal study, the EEG pattern

in LKU showed frequency bands response different from the finding in rats [44]. Nonetheless, we could not totally explain our result with the animal results as LKU were exposed to other external factors and consumed in different doses.

In addition, PVF in the alpha band was decreased in those who consumed Kratom at a very high dose. In the previous study, the reduced PVF in theta-alpha bands was also observed in mild cognitive disorder [17]. However, we could not imply that LKU would be promoting that pathology. Based on our preliminary results, it may be the research question for further studies.

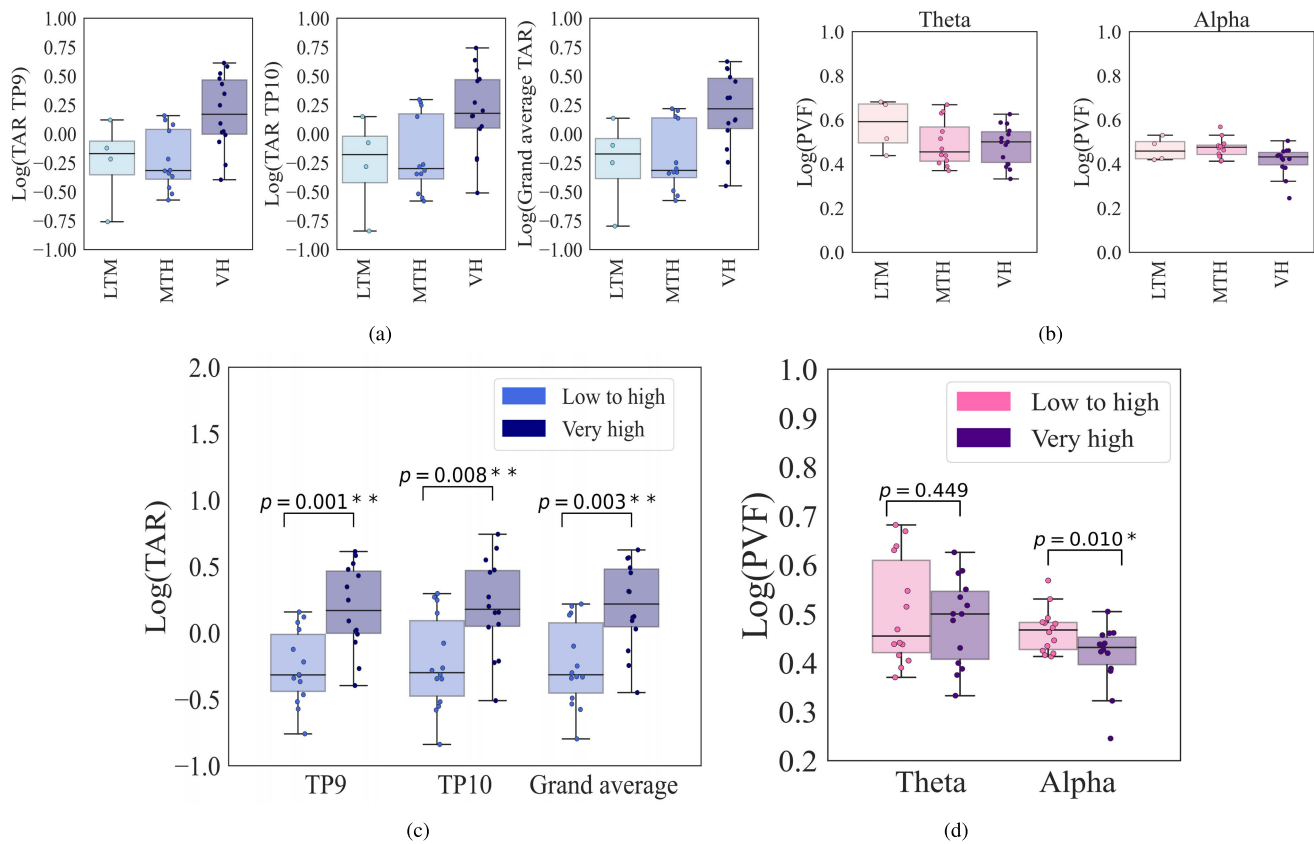


Fig. 6. The effect of Kratom consumption in different doses on TAR (a) and PVF in the theta and alpha bands (b). The significant differences of TAR (c) and PVF (d) between those who consumed at low to high doses and those who consumed at a very high dose were tested by MANOVA with duration and age as covariates followed by p -value adjustment with Bonferroni correction. ** p -value < 0.01, * p -value < 0.05. **Note:** low to moderate doses (LTM) ($n = 4$), moderate to high doses (MTH) ($n = 10$), low to high doses (LTH) ($n = 14$), and very high (VH) dose ($n = 14$).

TABLE VI

THE SUMMARY OF RESULTS FOR CLASSIFICATION THE LKU BASED ON THE DOSES OF KRATOM USE (LOW TO HIGH DOSES (LTH) VS. VERY HIGH DOSE (VH)) REPORTED AS THE PERCENTAGE OF ACCURACY \pm SE, F1-SCORE \pm SE, SENSITIVITY \pm SE, AND SPECIFICITY \pm SE). TAR AND PVFA REPRESENT THETA/ALPHA RATIO AND POWER VARIANCE FUNCTION OF ALPHA BANDS, RESPECTIVELY

Feature	Classifier	Accuracy	F1-score	Sensitivity	Specificity
TAR [TP9], TAR [TP10]	RF	66.67 \pm 9.94	58.00 \pm 13.37	65.00 \pm 15.00	65.00 \pm 13.02
	SVM	58.33 \pm 9.70	46.33 \pm 13.47	50.00 \pm 14.91	65.00 \pm 15.00
	kNN	70.00 \pm 10.48	68.00 \pm 12.24	75.00 \pm 13.44	70.00 \pm 13.33
	LR	73.33 \pm 9.69	74.67 \pm 9.68	85.00 \pm 10.67	65.00 \pm 13.02
Grand averaged TAR	RF	75.00 \pm 5.69	64.67 \pm 11.72	70.00 \pm 13.33	80.00 \pm 11.06
	SVM	70.00 \pm 7.37	58.00 \pm 13.37	60.00 \pm 14.53	80.00 \pm 13.33
	kNN	73.33 \pm 9.69	74.67 \pm 9.68	75.00 \pm 11.18	75.00 \pm 13.44
	LR	81.67 \pm 6.31	71.33 \pm 12.65	75.00 \pm 13.44	85.00 \pm 10.67
PVFA	RF	50.00 \pm 7.03	41.00 \pm 11.46	55.00 \pm 15.72	45.00 \pm 15.72
	SVM	65.00 \pm 5.24	47.00 \pm 13.34	60.00 \pm 16.33	50.00 \pm 16.67
	kNN	45.00 \pm 8.62	38.33 \pm 11.40	45.00 \pm 13.84	50.00 \pm 14.91
	LR	40.00 \pm 7.93	0.00 \pm 0.00	0.00 \pm 0.00	80.00 \pm 13.33
Feature combination	RF	83.33 \pm 10.24	84.67 \pm 10.09	90.00 \pm 10.00	75.00 \pm 13.44
	SVM	83.33 \pm 10.24	84.67 \pm 10.09	90.00 \pm 10.00	75.00 \pm 13.44
	kNN	70.00 \pm 10.48	68.00 \pm 12.24	70.00 \pm 13.33	75.00 \pm 13.44
	LR	73.33 \pm 9.69	68.00 \pm 12.24	70.00 \pm 13.33	75.00 \pm 13.44

LTH ($n = 14$); VH ($n = 14$)

B. Classification Results

1) The Classification Between LKU and Controls in Different Age Ranges:

The classification results between LKU and controls in different age ranges were summarized in Table V. The best age range for distinguishing between LKU and controls was over 50 years. If we only considered individual

EEG features, the averaged TAR produced a higher classification performance than the TAR at both electrode sites using RF classifier. The feature combinations achieved the highest performance score classified by SVM with Accuracy: 71.67% \pm 7.05, F1-score: 69.67% \pm 9.51, Sensitivity: 70.00% \pm 11.06, Specificity: 80.00% \pm 11.06. According to the classification result, it was consistent with the statistical analysis as described in Section III-A.2.

The confusion matrix of the SVM model in an over 50 years of age scenario is shown in Figure 7(a). It was observed that SVM provided the highest recall of the LKU class. However, the model was frequently misclassified in the control class.

Therefore, the combinations of the features were appropriate for discriminating LKU from the controls over 50 years of age with the SVM model.

2) The Classification Based on the Different Doses of Kratom Consumption:

If we focused on the individual feature, the averaged TAR and their average outperformed PVF in the alpha band using the LR model to classify those who consumed Kratom at different doses (low to high doses vs. very high dose). As a classification result, it was also supported by statistical significance in Section III-A.3 that all TAR features provided a larger significant p -value than the feature of PVF in the alpha band. However, the SVM classifier improved the classification efficiencies when using feature combination by including the feature of PVF in the alpha band. The mentioned

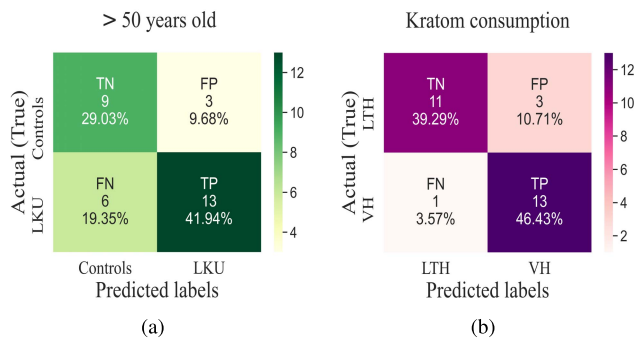


Fig. 7. The classification performances of SVM using feature combination for differentiation between LKU and controls over 50 years of age (a), and between LKU those who consumed Kratom at low to high doses and those who consumed at a very high dose (b).

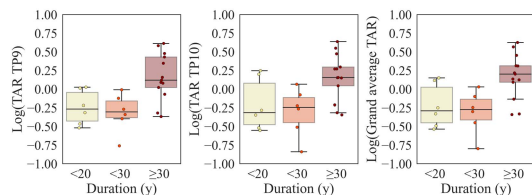


Fig. 8. The effect of the duration of Kratom consumption on TAR in the small ranges. **Note:** the duration of Kratom consumption < 20 years ($n = 6$), < 30 years ($n = 6$), and ≥ 30 years ($n = 13$).

classifier yielded the best performance with the percentage of accuracy, F1-score, sensitivity, and specificity as $83.33\% \pm 10.24$, $84.67\% \pm 10.09$, $90.00\% \pm 10.00$, and $75\% \pm 13.44$, respectively as represented in Table VI.

The visualization of the capability of the SVM classifier is represented by the confusion matrix, as given in Figure 7(b). It was noticed that the SVM classifier produced a lower misclassification in both low to high doses and very high dose.

C. Research Challenge

Although the short-term duration of Kratom consumption did not scope in this study, we showed the possibility of TAR to be an indirect detector for screening in the early stages, as given in Figure 8.

IV. CONCLUSION

The present study aimed to investigate resting-state EEG-biomarkers with the proposed features in LKU, which had never been explored, by using an EEG portable device. Furthermore, the proposed EEG features were examined in different factors, such as age and doses of Kratom consumption. The statistical-based features extractions were then performed separated binary classification in the relevant factors. Our findings highlighted that the proposed feature combinations (TAR TP9, TAR TP10, and their average) provided the acceptable classification score for differentiation of LKU from the controls in the age range of > 50 years using an SVM classifier. Interestingly, the proposed feature combinations using the mentioned classifier achieved the highest classification score for identifying those who consumed Kratom in different doses

by the additional feature of PVF in the alpha band. Therefore, it is feasible that the feature-based machine learning approach can be applied to monitor LKU who consumed Kratom excessively.

There are a few limitations to this study. First, short-term Kratom users were not recruited in this study. Second, the collected data were obtained from low-channel EEG recordings. Third, the given classification method is not complex enough.

To improve the limitations, the future study intends to recruit short-term Kratom users that would be more beneficial for early phase detection. In addition, utilizing EEG signals derived from multi-channels with medical-grade would provide the other essential EEG biomarkers. Finally, an advanced method such as deep learning can be further applied for a more robust classification performance of EEG signals.

REFERENCES

- [1] P. Tanguay, "Kratom in Thailand," *Legislative Reform Drug Policies*, vol. 13, pp. 1–16, Apr. 2011.
- [2] S. Likhitsathian *et al.*, "Polydrug use among kratom users: Findings from the 2011 Thailand national household survey," *J. Substance Use*, vol. 23, no. 4, pp. 384–389, Jul. 2018.
- [3] S. C. Eastlack, E. M. Cornett, and A. D. Kaye, "Kratom—Pharmacology, clinical implications, and outlook: A comprehensive review," *Pain Therapy*, vol. 9, no. 1, pp. 55–69, Jun. 2020.
- [4] C. Veltri and O. Grundmann, "Current perspectives on the impact of kratom use," *Substance Abuse Rehabil.*, vol. 10, p. 23, Jan. 2019.
- [5] J. M. Graves *et al.*, "Kratom exposures among older adults reported to U.S. poison centers, 2014–2019," *J. Amer. Geriatrics Soc.*, vol. 69, no. 8, pp. 2176–2184, Aug. 2021.
- [6] I. C. M. Verheggen *et al.*, "Increase in blood–brain barrier leakage in healthy, older adults," *GeroScience*, vol. 42, no. 4, pp. 1183–1193, Aug. 2020.
- [7] D. Singh *et al.*, "Long-term cognitive effects of kratom (*Mitragyna speciosa* Korth.) use," *J. Psychoactive Drugs*, vol. 51, no. 1, pp. 19–27, Jan. 2019.
- [8] M. S. Safi and S. M. M. Safi, "Early detection of Alzheimer's disease from EEG signals using Hjorth parameters," *Biomed. Signal Process. Control*, vol. 65, Mar. 2021, Art. no. 102338.
- [9] J. A. de la O Serna, M. R. A. Paternina, A. Zamora-Mendez, R. K. Tripathy, and R. B. Pachori, "EEG-rhythm specific Taylor–Fourier filter bank implemented with O-splines for the detection of epilepsy using EEG signals," *IEEE Sensors J.*, vol. 20, no. 12, pp. 6542–6551, Jun. 2020.
- [10] S. K. Khare, V. Bajaj, and U. R. Acharya, "PDCNNNet: An automatic framework for the detection of Parkinson's disease using EEG signals," *IEEE Sensors J.*, vol. 21, no. 15, pp. 17017–17024, Aug. 2021.
- [11] B. Scally, M. R. Burke, D. Bunce, and J.-F. Delvenne, "Resting-state EEG power and connectivity are associated with alpha peak frequency slowing in healthy aging," *Neurobiol. Aging*, vol. 71, pp. 149–155, Nov. 2018.
- [12] A. H. Meghdadi *et al.*, "Resting state EEG biomarkers of cognitive decline associated with Alzheimer's disease and mild cognitive impairment," *PLoS ONE*, vol. 16, no. 2, Feb. 2021, Art. no. e0244180.
- [13] D. Tomasi *et al.*, "Accelerated aging of the amygdala in alcohol use disorders: Relevance to the dark side of addiction," *Cerebral Cortex*, vol. 31, no. 7, pp. 3254–3265, Jun. 2021.
- [14] R. Stefanatos and A. Sanz, "The role of mitochondrial ROS in the aging brain," *FEBS Lett.*, vol. 592, no. 5, pp. 743–758, Mar. 2018.
- [15] D. Gohel and R. Singh, "Mitohormesis; potential implications in neurodegenerative diseases," *Mitochondrion*, vol. 56, pp. 40–46, Jan. 2021.
- [16] B. Orso *et al.*, "Anatomical and neurochemical bases of theory of mind in de novo Parkinson's disease," *Cortex*, vol. 130, pp. 401–412, Sep. 2020.
- [17] T. Ueda, T. Musha, T. Asada, and T. Yagi, "Classification method for mild cognitive impairment based on power variability of EEG using only a few electrodes," *Electron. Commun. Jpn.*, vol. 99, no. 11, pp. 107–114, Nov. 2016.

- [18] M. O'Sullivan, A. Temko, A. Bocchino, C. O'Mahony, G. Boylan, and E. Popovici, "Analysis of a low-cost EEG monitoring system and dry electrodes toward clinical use in the neonatal ICU," *Sensors*, vol. 19, no. 11, p. 2637, Jun. 2019.
- [19] A. Arsalan, M. Majid, A. R. Butt, and S. M. Anwar, "Classification of perceived mental stress using a commercially available EEG headband," *IEEE J. Biomed. Health Informat.*, vol. 23, no. 6, pp. 2257–2264, Nov. 2019.
- [20] P. Lakhan *et al.*, "Consumer grade brain sensing for emotion recognition," *IEEE Sensors J.*, vol. 19, no. 21, pp. 9896–9907, Nov. 2019.
- [21] P. Sawangjai, S. Hompoonsup, P. Leelaarporn, S. Kongwudhikunakorn, and T. Wilaiprasitporn, "Consumer grade EEG measuring sensors as research tools: A review," *IEEE Sensors J.*, vol. 20, no. 8, pp. 3996–4024, Apr. 2020.
- [22] P. Leelaarporn *et al.*, "Sensor-driven achieving of smart living: A review," *IEEE Sensors J.*, vol. 21, no. 9, pp. 10369–10391, May 2021.
- [23] *Muse*. Accessed: Sep. 28, 2021. [Online]. Available: <https://choosemuse.com/>
- [24] S. Assanangkornchai, A. Muekthong, N. Sam-Angsri, and U. Pattanasattayawong, "The use of *mitragynine speciosa* ('kratom'), an addictive plant, in Thailand," *Substance Use Misuse*, vol. 42, no. 14, pp. 2145–2157, 2007.
- [25] D. Singh, S. Narayanan, and B. Vicknasingam, "Traditional and non-traditional uses of Mitragynine (kratom): A survey of the literature," *Brain Res. Bull.*, vol. 126, pp. 41–46, Sep. 2016.
- [26] D. Singh *et al.*, "Evaluating the hematological and clinical-chemistry parameters of kratom (*Mitragyna speciosa*) users in Malaysia," *J. Ethnopharmacol.*, vol. 214, pp. 197–206, Mar. 2018.
- [27] J. Diep, D. T. Chin, S. Gupta, F. Syed, M. Xiong, and J. Cheng, "Kratom, an emerging drug of abuse: A case report of overdose and management of withdrawal," *A&A Pract.*, vol. 10, no. 8, pp. 192–194, 2018.
- [28] J. Clutterbuck. *Mind Monitor*. Accessed: Sep. 28, 2021. [Online]. Available: <https://mind588monitor.com/FAQ.php>
- [29] A. Delorme and S. Makeig, "EEGLAB: An open source toolbox for analysis of single-trial EEG dynamics including independent component analysis," *J. Neurosci. Methods*, vol. 134, no. 1, pp. 9–21, Mar. 2004.
- [30] R. Chaisaen *et al.*, "Decoding EEG rhythms during action observation, motor imagery, and execution for standing and sitting," *IEEE Sensors J.*, vol. 20, no. 22, pp. 13776–13786, Nov. 2020.
- [31] M. Dedeo and M. Garg, "Early detection of pediatric seizures in the high gamma band," *IEEE Access*, vol. 9, pp. 85209–85216, 2021.
- [32] T. Ueda, T. Musha, and T. Yagi, "Research of the characteristics of Alzheimer's disease using EEG," in *Proc. Annu. Int. Conf. IEEE Eng. Med. Biol. Soc.*, Sep. 2009, pp. 4998–5001.
- [33] R. J. Grissom and J. J. Kim, *Effect Sizes for Research: Univariate and Multivariate Applications*. Evanston, IL, USA: Routledge, 2012.
- [34] L. Breiman, "Random forests," *Mach. Learn.*, vol. 45, no. 1, pp. 5–32, 2001.
- [35] V. Kecman, "Support vector machines: An introduction," in *support Vector Machines: Theory and Applications*. Berlin, Germany: Springer, 2009, pp. 1–47.
- [36] A. Mucherino, P. J. Papajorgji, and P. M. Pardalos, "K-nearest neighbor classification," in *Data Mining in Agriculture*. New York, NY, USA: Springer, 2009, pp. 83–106.
- [37] F. E. Harrell, Jr., "Ordinal logistic regression," in *Regression Modeling Strategies*. Cham, Switzerland: Springer, 2015, pp. 311–325.
- [38] F. Pedregosa *et al.*, "Scikit-learn: Machine learning in Python," *J. Mach. Learn. Res.*, vol. 12, pp. 2825–2830, Oct. 2011.
- [39] A. M. Coroiu, "Tuning model parameters through a genetic algorithm approach," in *Proc. IEEE 12th Int. Conf. Intell. Comput. Commun. Process. (ICCP)*, Sep. 2016, pp. 135–140.
- [40] S. Charoenratana, C. Anukul, and A. Aramrattana, "Attitudes towards kratom use, decriminalization and the development of a community-based kratom control mechanism in southern Thailand," *Int. J. Drug Policy*, vol. 95, Sep. 2021, Art. no. 103197.
- [41] D. Singh *et al.*, "Severity of kratom (*Mitragyna speciosa* Korth.) psychological withdrawal symptoms," *J. Psychoactive Drugs*, vol. 50, no. 5, pp. 445–450, Oct. 2018.
- [42] W. C. Prozialeck, J. K. Jivan, and S. V. Andurkar, "Pharmacology of kratom: An emerging botanical agent with stimulant, analgesic and opioid-like effects," *J. Osteopathic Med.*, vol. 112, no. 12, pp. 792–799, 2012.
- [43] S. Suwanlert, "A study of kratom eaters in Thailand," *Bull Narc.*, vol. 27, no. 3, pp. 21–27, 1975.
- [44] F. W. Suhaimi, Z. Hassan, S. M. Mansor, and C. P. Müller, "The effects of chronic mitragynine (Kratom) exposure on the EEG in rats," *Neurosci. Lett.*, vol. 745, Feb. 2021, Art. no. 135632.

Appendix B

The Human Ethic Committee



**Health Science Human Research Ethics Committee,
Prince of Songkla University**

This document is a record of review and approval/acceptance of health science study protocol that;

HSc-HREC	63-017-1-1		
Protocol Title	Physiological response in participants who consume Krathom daily		
Principal Investigator	Assoc. Prof. Dr. Ekkasit Kumarnsit	Affiliation	Faculty of Science PSU
Co-investigator	Prof. Dr. Sawitri Assanangkonchai	Affiliation	Faculty of Medicine PSU
	Asst Prof Dr. Dania Cheaha	Affiliation	Faculty of Science PSU
	Miss Wanumaidah Saengmolee	Affiliation	Faculty of Science PSU
	Miss Nusaib Sa-id	Affiliation	Faculty of Science PSU
	Mr.Nopporn Tantirangsee	Affiliation	SongKhla Rajanagarindra Psychiatric Hospital
	Mr.Thanurat Phutachart	Affiliation	Thanyarak Songkhla Hospital
	Dr.Darika Saingam	Affiliation	Faculty of Medicine PSU
Approved documents:			
1. Submission Form for Health Science Study			No. 2 Date 1/10/2020
2. Study Protocol			No. 2 Date 1/10/2020
3. Information Sheet			No. 2 Date 1/10/2020
4. Case Record/ Data Collection Forms			No. 2 Date 1/10/2020
5. Subject recruitment materials (document, video clip, leaflet, etc.) Forms			No. 2 Date 1/10/2020
6. Curriculum Vitae of all Investigators			

have/has been reviewed and approved by the Health Science Human Research Ethics Committee, Prince of Songkla University in full compliance with International Guidelines for human research subject protection based on Declaration of Helsinki and the International Conference on Harmonization in Good Clinical Practice (ICH-GCP).

This review is documented in the meeting minutes of the meeting 5/2021 agenda 5.2.4 on 23/08/2021

Please submit the progress report every 6 months.

Renewal must be submitted at least 30 days prior to expired date.

(For a case report, please submit a final report after study completion and no progress report is needed)


(Asst.Prof.Dr.Somchai Sriwiryajan)

Chairman of Health Science Human Research Ethics Committee,
Prince of Songkla University

Date of Approval: 4/08/2021

Date of Expiration: 3/08/2022

VITAE

Name Wanumaidah Saengmolee
Student ID 5910230036
Educational Attainment

Degree	Name of Institution	Year of Graduation
Bachelor of Thai Traditional Medicine	Prince of Songkla university	2016

Scholarship Awards during Enrolment

- Graduate School Dissertation Funding for Thesis and Revenue Budget Fund
- Educational Institutions Scholarship for Outstanding GPA

List of Publication and Proceeding

Publications:

- 1) Saengmolee, Wanumaidah, Rattanaphon Chaisaen, Phairot Autthasan, Chutimon Rungsilp, Nusaib Sa-ih, Dania Cheaha, Ekkasit Kumarnsit, and Theerawit Wilaiprasitporn. "Consumer-Grade Brain Measuring Sensor in People with Long-Term Kratom Consumption." *IEEE Sensors Journal* (2022).
- 2) Exploring of Cardiac Autonomic Activity with Heart Rate Variability in Long-Term Kratom (*Mitragyna speciosa* Korth.) Users: A Preliminary Study (Revising)

Proceeding:

Saengmolee W., Cheaha D., Sa-ih N., and Kumarnsit E. The effect of long-term and heavy use of kratom (*Mitragyna speciosa*) on EEG pattern and decision-making in Thai labors. The 48th Annual Scientific Meeting of Proceedings and Abstracts the Physiological Society of Thailand 2021. July 14-16. (First prize winner poster research presentation award doctoral level)